Università degli Studi di Milano
Department of Mathematics "Federigo Enriques"
Doctoral Course in Mathematical Sciences
Ph.D. in Mathematics

Predator-prey models: bifurcations, cross diffusion and Turing instability

Cinzia Soresina

Advisor: Prof. Giovanni Naldi
Co-advisors: Prof.ssa Maria Groppi
Prof. Laurent Desvillettes
Coordinator: Prof. Vieri Mastropietro

MAT/07, XXIX cycle, 2016

Ph.D. Thesis

Advisors:

Prof. Giovanni Naldi

Department of Mathematics "Federigo Enriques"
Università degli Studi di Milano

Prof.ssa Maria Groppi

Department of Mathematics and Computer Sciences
Università degli Studi di Parma

Prof. Laurent Desvillettes

Institut de Mathématiques de Jussieu - Paris Rive Gauche (IMJ-PRG)
Université Paris Diderot

Department of Mathematics "Federigo Enriques"
Via Cesare Saldini 50,
20133 Milano, Italy

Acknowledgments

I thank my advisor Giovanni Naldi, who gave me hints and ideas during these years. A special mention goes to Maria Groppi, for her meaningful assistance, tireless guidance and infinite patience. I thank Laurent Desvillettes for our hard working time in Paris on this interesting topic. I thank Giuseppe Buffoni, whose help, knowledge and advice have been priceless. I am grateful to the unknown referees for their careful revision and constructive comments. I would like also to thank Paola Causin, who has shown me "how to teach". Lastly, I thank my office mate and friend Elena Bonacini: we shared not only an office in these years.

Summary

Predator-prey models, homogeneous in space or with spatial diffusion, play a central role in this thesis. Indeed, from a mathematical view point, we investigate stability in systems of ordinary differential equations and of partial differential equations of parabolic type.

First, we deal with a predator-prey model, described by a system of two ODEs, in which a *strong Allee effect* on the prey growth and a *predator-dependent* trophic function are taken into account. The main strength of this part is that these functions are not specified by analytical expressions, but only characterized by some biologically meaningful properties determining their shapes. On the basis of these properties we are able to perform the stability analysis of the system, using the predation efficiency and a measure of the predator interference as bifurcation parameters. The system admits codimension-two bifurcations points, such as a Bogdanov-Takens and a cusp point; it is worthwhile to notice that they are independent of the particular expression of the model functions. The numerical investigation is further carried on choosing for the model equations some analytical expressions well known in literature, which satisfied the assumed properties, and using Matcont, a continuation Matlab toolbox. This investigation, in addition, has shown the presence of global bifurcations that determine the disappearance of limit cycles through the formation of homoclinic and heteroclinic orbits involving some equilibrium points. Moreover, we have detected a further codimension-two bifurcation point, a Generalized-Hopf. Together with the cusp and the Bogdanov-Takens bifurcation points, these three types of codimension-two bifurcations are the only admissible by a planar system of ordinary differential equations.

The second part of this thesis focuses on the study of two predator-prey models with diffusion that justify, in a suitable limit, two classical types of functional responses in the reaction part and present a cross-diffusion term. In detail, two trophic levels are considered, preys and predators which are further divided into *searching predators* and *handling predators*. The former are predators active in the predation process, the latter are resting individuals. Then, we start from a system of three partial differential equations, with a standard linear diffusion in terms of Laplacian, and with a Lotka-Volterra reaction term. Through a *quasi steady-state approximation* we end up with a system of two PDEs with prey and total predator densities as unknowns, in which an Holling-type II functional response appears together with a cross-diffusion term in the predator equation. It is proved that this class of predator-prey models can not give rise to Turing instability. Then we modify the starting model

inserting a competition among predators. With this change we end up after a *quasi steady-state approximation* with a system of two PDEs for prey and total predator densities, characterized by a Beddington-DeAngelis-type functional response and a cross-diffusion term in the predator equation. We look for conditions on the parameters values which lead to Turing instability and we compare these Turing instability regions with the ones obtained when the cross-diffusion term is substituted by a linear diffusion.

Riassunto

Questa tesi riguarda modelli differenziali preda-predatore, trattati inizialmente nel caso spazialmente omogeneo e successivamente considerando la diffusione spaziale. Dal punto di vista matematico pertanto vengono considerati sistemi di equazioni differenziali ordinarie e di equazioni differenziali alle derivate parziali di tipo parabolico.

In particolare, nella prima parte viene studiato un modello preda-predatore spazialmente omogeneo, retto da due equazioni differenziali ordinarie, in cui sono presi in considerazione un *effetto Allee forte* nella crescita delle prede e una risposta funzionale *predatore dipendente*. Il punto di forza dello studio risiede nel fatto che le funzioni che descrivono questi processi non hanno un'espressione esplicita, ma sono caratterizzate solo da alcune proprietà comuni a funzioni specifiche utilizzate in letteratura. Tali proprietà sono sufficienti per effettuare l'analisi qualitativa del sistema, con riguardo all'esistenza degli equilibri e alle loro proprietà di stabilità mediante i criteri di Lyapunov, utilizzando due parametri di biforcazione che caratterizzano il processo di predazione. Il modello presenta dei punti di biforcazione di codimensione 2 quali una biforcazione Bogdanov-Takens e una di tipo cuspide, non legati alla particolare realizzazione scelta per le funzioni del modello. Lo studio é stato proseguito numericamente fissando un'espressione per la funzione di crescita delle prede e per la funzione trofica che soddisfano le proprietà considerate e utilizzando il software di continuazione Matcont per Matlab. Tale studio ha mostrato l'ulteriore presenza di biforcazioni globali che determinano la sparizione dei cicli limite, mediante la formazione di orbite omocline ed eterocline. Inoltre é stato individuato una biforcazione di Hopf generalizzata, un altro punto di biforcazione di codimensione 2. Le biforcazioni di codimensione 2 individuate sono tutte e sole quelle ammesse da un sistema a due equazioni differenziali.

La seconda parte della tesi verte invece sullo studio di due sistemi preda-predatore con diffusione in cui vengono dedotte in un opportuno limite due tipi di risposte funzionali classiche come termine reattivo e un termine diffusivo non lineare. In dettaglio, vengono considerati due livelli trofici, le prede e i predatori. Questi ultimi sono suddivisi in due classi, *searching predators* e *handling predators*: i primi sono i predatori effettivamente impegnati nella predazione, mentre i secondi non sono attivi in tale processo. Ne deriva un sistema composto da tre equazioni differenziali alle derivate parziali, in cui la diffusione é modellizzata in modo classico, mediante un termine lineare in forma di Laplaciano e l'interazione tra prede e predatori é inizialmente del tipo Lotka-Volterra. Mediante una approssimazione *quasi steady-state* é possibile ridurre il sistema di partenza, ottenendo un sistema di due PDE,

una per le prede e una per la totalità dei predatori, in cui la risposta funzionale é del tipo Holling-II, in particolare preda-dipendente, e che presenta una non-linearità nel termine di diffusione. Questa classe di modelli non dà luogo a instabilità di Turing. Viene quindi considerata nel modello a tre equazioni una competizione tra i predatori che permette di ricavare, mediante un'approssimazione *quasi steady-state*, un sistema preda-predatore con risposta funzionale del tipo Beddington-DeAngelis nel termine di reazione e ancora una non-linearità nel termine di diffusione. Vengono quindi ricavate condizioni sui parametri che permettono di avere instabilità di Turing e confrontati i risultati sia nel caso di diffusione lineare che in quello non-lineare.

Contents

Introduction 1

Preliminaries 5
Bifurcation of equilibria in continuous-time dynamical systems 5
One-parameter bifurcations 6
Two-parameter bifurcations 10
Diffusion driven instability 18
Turing instability analysis 19
Turing instability analysis with cross-diffusion 23

Part I Dynamics of predator-prey models with a strong Allee effect on the prey and predator-dependent trophic functions

1 Introduction 29

2 The prey-predator model and the equilibrium stability analysis . . 37
2.1 Basic assumptions and model equations 37
2.2 Attractive invariant set 40
2.3 Non-coexistence equilibria and their stability properties 43
2.4 Coexistence equilibria 45
2.4.1 Shape of $\phi(x, h)$ 46
2.4.2 Solutions to $\phi(x, h) = p/p_0$ 48
2.5 Stability properties of coexistence equilibrium states 54
2.5.1 State E_{*1}: the case of $r_x \geq r_0$ 57
2.5.2 State E_{*1}: the case of $r_x < r_0$ 60
2.5.3 State E_{*3} 61

3 Numerical study 67
3.1 Behaviours of the system 67

4 Concluding remarks 75

Appendix 81
A Details on some parameters 81
B The cusp bifurcation point 83
C List of main symbols 84

Part II About reaction-diffusion predator-prey systems involving the Holling-type II and the Beddington-DeAngelis functional responses

5 Introduction 89

6 A justification of classical functional responses 95
6.1 The derivation of the Holling-type II functional response 95
6.1.1 Adimensionalization 97
6.2 The derivation of the Beddington-DeAngelis-like functional response . . 98
6.2.1 Adimensionalization 101
6.3 Rigorous results of convergence 102
6.3.1 Proof of Theorem. 6.3.1 105
6.3.2 Proof of Proposition 6.3.1 107
6.3.3 Proof of Theorem. 6.3.2 108

7 The Turing Instability analysis 113
7.1 The Holling-type II 113
7.1.1 Homogeneous equilibrium states 113
7.1.2 Turing Instability analysis 115
7.2 The Beddington-DeAngelis 116
7.2.1 Homogeneous equilibrium states 117
7.2.2 Turing Instability with linear diffusion terms 121
7.2.3 Turing Instability with cross-diffusion 122
7.2.4 Turing instability regions: linear vs cross diffusion 124

8 Concluding remarks 135

Appendix 139
A Very-weak formulation 139

References

List of Figures

0.1 Cusp bifurcation point 14
0.2 Bautin bifurcation point 16
0.3 Bogdanov-Takens bifurcation point 18

1.1 Typical shapes of prey growth functions with a strong Allee effect 33

2.1 Positively invariant and attractive set 41
2.2 Shape of the function $\psi(x)$ 47
2.3 Trend of $\phi(x,h)$ for $x \in (\epsilon, 1)$ and different values of h 49
2.4 Solutions to $\phi(x,h) = p/p_0$ 50
2.5 Equilibrium surface in the (h,p,x) space 52
2.6 Existence regions of coexistence equilibrium states in the (h,p) plane . 53
2.7 Qualitatively trend of x_{*j} versus p for different values of h 54
2.8 Stability regions of $E_{*1}(h,p)$ in the (h,p) plane $(r_x \geq r_0)$ 60
2.9 Stability regions of $E_{*1}(h,p)$ in the (h,p) plane $(r_x < r_0)$ 62
2.10 Instability regions of $E_{*3}(h,p)$ in the (h,p) 64

3.1 Local and global bifurcation curves 70
3.2 Limit cycles behaviours versus p 71
3.3 Phase portraits for $h_0 < h < h_1$ and different p 72
3.4 Local and global bifurcation curves for $h > h_R$ $(r_x < r_0)$ 73
3.5 Phase diagram close to the Bogdanov-Takens bifurcation 73

7.1 Turing Instability regions for linear and cross-diffusion 133

List of Tables

2.1 Number of solutions $\xi_j(h)$ to equation $\psi(x) = 1/h$ 47
2.2 Summary of existence of solutions to $\Phi(x, h) = p/p_0$ 51
2.3 Summary of stability properties of equilibrium states 65

Introduction

Predator-prey models, homogeneous in space or with spatial diffusion, play a central role in this thesis. Indeed, by a mathematical view point, we investigate stability in systems of ordinary differential equations and of partial differential equations of parabolic type.

First, we deal with a predator-prey model,described by a system of two ODEs, in which a *strong Allee effect* on the prey growth and a *predator-dependent* trophic function are taken into account. The strong Allee effect models undercrowding phenomena and is represented by a prey growth function which becomes negative for sufficiently small values of prey biomass. To simulate the Allee effect, different formulations of the prey growth rate, in the absence of predators, have been proposed in the literature. Many authors [20, 42, 61, 46, 94, 98, 106] use for instance a multiplicative factor to the logistic term, which introduce another critical value for the prey biomass, less than the carrying capacity. Concerning the trophic function, which describes the predator functional response to prey abundance ([92, p. 80]), it was introduced in predator-prey models to take into account the saturation limiting the predation process. Different formulations have been proposed in the literature, see for instance Gutierrez et al. [50], Beddington, DeAngelis and co-authors [1, 14, 29, 88]. In this thesis these functions are not specified by analytical expressions, but only characterized by some biologically meaningful properties determining their shapes. One of the main achievements of this thesis is that, on the basis of these properties only, the stability analysis of the system has been performed, using the predation efficiency and a measure of the predator interference as bifurcation parameters. The system admits codimension-two bifurcations points, such as a Bogdanov-Takens and a cusp point. It is worthwhile to notice that they are independent of the particular expression of the model functions. The numerical investigation is further carried on choosing for the model equations some analytical expressions well known in the lit-

erature, which satisfied the assumed properties, and using Matcont, a continuation Matlab toolbox. This investigation, in addition, has shown the presence of global bifurcations that determine the disappearance of limit cycles through the formation of homoclinic and heteroclinic orbits involving some equilibrium points. Moreover, we have detected a further codimension-two bifurcation point, a Generalized-Hopf. Together with the cusp and the Bogdanov-Takens bifurcation points, these three types of codimension-two bifurcations are the only admissible by a planar system of ordinary differential equations.

The second part of this thesis focuses on the study of two "microscopic" (in terms of time scales) predator-prey models with diffusion that justify, in a suitable limit, two classical types of functional responses in the reaction part and present a cross-diffusion term. In detail, two trophic levels are considered, prey and predators which are further divided into *searching predators* and *handling predators*. The former are predators active in the predation process, the latter are resting individuals. Then, we start from a system of three partial differential equations, with a standard linear diffusion in terms of Laplacian, and with a Lotka-Volterra reaction term. Through a *quasi steady-state approximation* we end up with a system of two PDEs with prey and total predator densities as unknowns, in which an Holling-type II functional response appears together with a cross-diffusion term in the predator equation. Then we modify the starting model inserting a competition among predators. With this change we end up after a *quasi steady-state approximation* with a system of two PDEs for prey and total predator densities, characterized by a Beddington-DeAngelis-like functional response and a cross-diffusion term in the predator equation. We present also rigorous result of convergence of the solutions of these system towards the solution of the reaction-cross diffusion system. We are also interested in the Turing instability analysis of these systems. For the first case, it is known that predator-prey models with a prey-dependent trophic function in the reaction part and standard (linear) diffusion can not give rise to Turing instability [10]. Even with the cross-diffusion model, no patterns seem to appear under a (biologically reasonable) assumption on the diffusion coefficients. For the second case, in which the functional response is a Beddington-DeAngelis-like, we look for conditions on the parameters values which lead to Turing instability and we compare these Turing Instability regions with the ones obtained when the cross-diffusion term is substituted by a linear diffusion.

The thesis is organized as follow. We first introduce some basic concept on bifurcation theory and diffusion-driven instability, used in the sequel. Part I contains the study of the general predator-prey model with a strong Allee effect in the prey growth and predator-dependent trophic function. In detail, the basic assumptions and the ordinary differential equations describing the local dynamics of a predator-prey sys-

tem are presented, then the stability properties of the non-coexistence equilibrium states are summarized and an existence and stability analysis of the coexistence equilibrium states is performed, assuming two bifurcation parameters. Finally, results of numerical simulations, obtained for some concrete realization of the model functions, are presented to illustrate the behaviours of the system.

Part II presents the justification of the Holling-type II and a Beddington-DeAngelis type functional response in the context of reaction-diffusion systems, starting from a system of three partial differential equations for prey, searching predator and handling predator. From this approach also a cross-diffusion term arises in the predator equations, instead of a standard (linear) diffusion. Then the Turing instability analysis of these system is presented.

Where we go from here

The study of the general model of Part I suggests further improvements. First, a deeper analysis of codimension-two bifurcation points is very challenging: we would try to reduce the system on the center manifold in order to better characterize this points. A possible future work, related also to the second part of this thesis, is the extension of present results to the case of spatial diffusion: adding a linear diffusion in the equations of this system, we could obtain general conditions for Turing Instability for this class of predator-prey models.

Concerning the Part II, there are several further research directions. From the numerical point of view, pattern simulations will complete the theoretical study. Furthermore, the definition of an appropriate numerical scheme for the integration of the cross-diffusion term is still an open question. As a consequence, a comparison between the outcomes of the derived model and the classical one will be useful to understand the role of the Beddington-DeAngelis-type functional response. From the modeling point of view, starting from a more complex "microscopic" model [41, 56] could lead to a different cross-diffusion term. Finally, the sub-classification of cross-diffusion with respect to their properties of enhancing diffusion-driven instability could be useful and interesting.

The final pages of this thesis present the publications coauthored by the candidate and the list of talks and posters presented at conferences and Summer Schools.

Preliminaries

This chapter introduces some basic concept of bifurcation theory and Turing instability used in this thesis. First, we define some type of bifurcations of finite dimensional continuous-time dynamical systems, depending on one or two parameters. We follow the notation of the Kuznetsov's book [66]. Then, the main concepts of diffusion-driven instability in reaction-diffusion systems are summarized [73, 78], in the case of standard (linear) diffusion. Then, an extension of this theory to the case of cross-diffusion is reported [39, 64, 99]: also in this case we determine the bifurcation threshold as usual by a linear stability analysis.

Bifurcation of equilibria in continuous-time dynamical systems

Consider a continuos-time parameter-dependent dynamical system

$$\dot{x} = f(x, \alpha)$$

where $x \in \mathbb{R}^n$ is the vector of the phase variables, $\alpha \in \mathbb{R}^m$ is a parameter, and f is smooth with respect to both x and α.

Varying the parameter, the phase portrait also varies. The appearance of a non-equivalent topological phase portrait under variation of parameter is called a *bifurcation*. Thus, a bifurcation is a change of the topological structure of the system as its parameters pass through bifurcation (critical) values.

Bifurcations which can be detected looking at the phase portraits of the system in a small neighborhood of the equilibrium point are called *local bifurcations* or bifurcations of equilibria. There are also bifurcations that cannot be detected by looking at

small neighborhoods of equilibrium points. Such bifurcations are called *global*. However, there are global bifurcations in which certain local bifurcations are involved. In such cases, looking at the local bifurcation provides only partial information on the behaviour of the system.

Let $\alpha = \alpha_0$ and consider a maximal connected parameter set (called a *stratum*) containing α_0 and composed by those points for which the system has a phase portrait that is topologically equivalent to that at α_0. Taking all such strata in the parameter space $\mathbb{R}^m$, we obtain the *parametric portrait* of the system. The parametric portrait together with its characteristic phase portraits constitute a *bifurcation diagram*. In the simplest cases, the parametric portrait is composed by a finite number of regions in $\mathbb{R}^m$. Inside each region the phase portrait is topologically equivalent. These regions are separated by bifurcation boundaries, which are smooth submanifolds in $\mathbb{R}^m$ (i.e., curves, surfaces). The boundaries can intersect, or meet. These intersections subdivide the boundaries into subregions, and so on. A *bifurcation boundary* is defined by specifying a phase object (equilibrium, cycle, etc.) and some bifurcation conditions determining the type of its bifurcation. When a boundary is crossed, the bifurcation occurs.

The *codimension* of a bifurcation is the difference between the dimension of the parameter space and the dimension of the corresponding bifurcation boundary. Equivalently, but rather informally, the codimension is the number of independent conditions determining the bifurcation. This is the most practical definition of the codimension since it makes clear that the codimension of a certain bifurcation is the same in all generic systems depending on a sufficient number of parameters.

One-parameter bifurcations

Consider a one-parameter continuous-time dynamical system

$$\dot{x} = f(x, \alpha), \quad x \in \mathbb{R}^n, \ \alpha \in \mathbb{R},$$

where f is smooth with respect to both x and α. Let $x = x_*$ be a non-hyperbolic equilibrium[1] in the system for $\alpha = \alpha_*$. There are, generically, only two ways in which the hyperbolicity condition can be violated. Either a simple real eigenvalue approaches zero and we have $\lambda_1 = 0$, or a pair of simple complex eigenvalues reaches the imaginary axis and we have $\lambda_{1,2} = \pm i\omega_0, \ \omega_0 > 0$ for some value of the parameter. The occurrence of the zero eigenvalue is relevant to a transcritical or to a fold bifurcation, whereas the occurrence of a pair of pure imaginary eigenvalues leads to a Hopf bifurcation.

[1] An equilibrium is called *hyperbolic* if there are no eigenvalues of the Jacobian matrix of the system evaluated at the equilibrium with zero real part.

Transcritical bifurcation

The topological normal form of a generic one-dimensional dynamical system depending on one parameter having a *transcritical* bifurcation is the following

$$\dot{x} = f(x, \alpha) = \alpha x - x^2, \quad x \in \mathbb{R},\ \alpha \in \mathbb{R}.$$

This system has two equilibria $x_1 = 0,\ x_2(\alpha) = \alpha$. For the former, $\lambda = f_x(x_1, \alpha) = -\alpha$ which implies that the equilibrium is stable when $\alpha > 0$ and unstable when $\alpha < 0$; for the latter $\lambda = f_x(x_2, \alpha) = \alpha$, so that it is stable when $\alpha < 0$ and unstable when $\alpha > 0$. For $\alpha = 0$, we have $x_1 = x_2 = 0$, namely the equilibria collide, $\lambda = 0$ and the equilibria exchange their stability at the bifurcation point.

Fold bifurcation

In non-symmetric systems, the occurrence of a zero eigenvalue is related only to a fold bifurcation. The topological normal form of a generic one-dimensional system having a *fold* (or *tangent* or *saddle-node*) bifurcation is the following. Consider the one-dimensional dynamical system depending on one parameter

$$\dot{x} = f(x, \alpha) = \alpha + x^2, \quad x \in \mathbb{R}.$$

At $\alpha_* = 0$ this system has a nonhyperbolic equilibrium $x_* = 0$ with $\lambda = f_x(0, 0) = 0$. For $\alpha < 0$ there are two equilibria in the system:

$$x_{1,2}(\alpha) = \pm\sqrt{-\alpha},$$

the negative one of which is stable, while the positive one is unstable. For $\alpha > 0$ there are no equilibria in the system. When α crosses zero from negative to positive values, the two equilibria (stable and unstable) "collide", forming at $\alpha = 0$ an equilibrium with $\lambda = 0$, and disappear. In the (α, x)-plane, the equation $f(x, \alpha) = 0$ defines an equilibrium manifold, which is simply the parabola $\alpha = -x^2$.

Consider now the generic two-dimensional system

$$\dot{x} = f(x, \alpha), \quad x = (x_1, x_2)^T \in \mathbb{R}^2,\ \alpha \in \mathbb{R},$$

with a smooth function f, which has at $\alpha = 0$ the equilibrium $x = 0$ with one eigenvalue $\lambda = 0$. The Jacobian matrix $J(\alpha)$ can be written as

$$J(\alpha) = \begin{pmatrix} a(\alpha) & b(\alpha) \\ c(\alpha) & d(\alpha) \end{pmatrix}$$

which entries are smooth functions of α. Its eigenvalues are the roots of the characteristic equation

$$\lambda^2 - \text{tr } J\lambda + \det J = 0,$$

where $\text{tr } J = \text{tr } J(\alpha) = a(\alpha) + d(\alpha)$, and $\det J = \det J(\alpha) = a(\alpha)d(\alpha) - b(\alpha)c(\alpha)$. So,

$$\lambda_{1,2}(\alpha) = \frac{1}{2}\left(\text{tr } J(\alpha) \pm \sqrt{\text{tr } J(\alpha)^2 - 4\det J(\alpha)}\right).$$

The fold bifurcation conditions implies

$$\text{tr } J(0) \neq 0, \quad \det J(0) = 0.$$

Andronov-Hopf bifurcation

The bifurcation corresponding to the presence of $\lambda_{1,2} = \pm i\omega_0,\ \omega_0 > 0$ is called a *Hopf* (or Andronov-Hopf) bifurcation. Consider the following system of two differential equations depending on one parameter:

$$\begin{cases} \dot{x_1} = \alpha x_1 - x_2 - x_1(x_1^2 + x_2^2) \\ \dot{x_2} = x_1 + \alpha x_2 - x_2(x_1^2 + x_2^2) \end{cases}$$

This system has the equilibrium $x_1 = x_2 = 0$ for all α with the Jacobian matrix

$$J(\alpha) = \begin{pmatrix} \alpha & -1 \\ 1 & \alpha \end{pmatrix},$$

having eigenvalues $\lambda_{1,2} = \alpha \pm i$. This equilibrium is a stable focus for $\alpha < 0$ and an unstable focus for $\alpha > 0$. At the critical parameter value $\alpha = 0$ the equilibrium is nonlinearly stable and topologically equivalent to the focus (sometimes it is called a weakly attracting focus). This equilibrium is surrounded for each value of $\alpha > 0$ by an isolated closed orbit (limit cycle) that is unique and stable. Similarly, the system

$$\begin{cases} \dot{x_1} = \alpha x_1 - x_2 + x_1(x_1^2 + x_2^2) \\ \dot{x_2} = x_1 + \alpha x_2 + x_2(x_1^2 + x_2^2) \end{cases}$$

undergoes the Andronov-Hopf bifurcation at $\alpha = 0$, and the equilibrium at the origin has the same stability for $\alpha \neq 0$: it is stable for $\alpha < 0$ and unstable for $\alpha > 0$. Contrary to the previous system, its stability at the critical parameter value is opposite: it is (nonlinearly) unstable at $\alpha = 0$, and there is an unstable limit cycle for each $\alpha < 0$, which disappears when α crosses zero from negative to positive values.

If we consider the general form

$$\begin{cases} \dot{x_1} = \alpha x_1 - \omega x_2 + l_1 x_1 (x_1^2 + x_2^2) \\ \dot{x_2} = \omega x_1 + \alpha x_2 + l_1 x_2 (x_1^2 + x_2^2) \end{cases}$$

where $\omega,\ l_1 \in \mathbb{R}$ and $\omega > 0$, we can rewrite the system in polar coordinates

$$\begin{cases} \dot{\rho} = \alpha\rho + l_1 \rho^3 \\ \dot{\phi} = \omega. \end{cases}$$

This last form shows that the trajectory spirals around the origin at constant angular velocity ω, while the distance from the origin varies in accordance with the first ODE, which is the normal form of the pitchfork. Thus, the stability of the cycle depends upon the sign of l_1, called the *first Lyapunov coefficient*. Moreover, the Hopf bifurcation is *supercritical* if $l_1 < 0$ and *subcritical* if $l_1 > 0$. In terms of collisions, this bifurcation involves an equilibrium and a cycle which, however, shrinks to a point when the collision occurs. In the supercritical case, a stable cycle has in its interior an unstable focus. When the parameter is varied the cycle shrinks until it collides with the equilibrium and after the collision only a stable equilibrium remains. By contrast, in the subcritical case the cycle is unstable and is the boundary of the basin of attraction of the stable equilibrium inside the cycle. Thus, after the collision there is only a repeller.

Let us now define the condition for a Hopf bifurcation. Consider now the generic two-dimensional system

$$\dot{x} = f(x, \alpha), \quad x = (x_1, x_2)^T \in \mathbb{R}^2,\ \alpha \in \mathbb{R},$$

with a smooth function f, which has at $\alpha = 0$ the equilibrium $x = 0$ with eigenvalues $\lambda_{1,2} = \pm i\omega_0,\ \omega_0 > 0$. The Jacobian matrix $J(\alpha)$ can be written as

$$J(\alpha) = \begin{pmatrix} a(\alpha) & b(\alpha) \\ c(\alpha) & d(\alpha) \end{pmatrix}$$

with smooth functions of α as its elements. Its eigenvalues are the roots of the characteristic equation

$$\lambda^2 - \text{tr } J\lambda + \det J = 0,$$

where $\text{tr } J = \text{tr } J(\alpha) = a(\alpha) + d(\alpha)$, and $\det J = \det J(\alpha) = a(\alpha)d(\alpha) - b(\alpha)c(\alpha)$. So,

$$\lambda_{1,2}(\alpha) = \frac{1}{2}\left(\text{tr } J(\alpha) \pm \sqrt{\text{tr } J(\alpha)^2 - 4\det J(\alpha)}\right).$$

The Hopf bifurcation condition implies

$$\text{tr } J(0) = 0, \quad \det J(0) = \omega_0^2 > 0.$$

Two-parameter bifurcations

Consider a two-parameter continuous-time dynamical system

$$\dot{x} = f(x, \alpha)$$

where $x = (x_1, x_2, \ldots, x_n)^T \in \mathbb{R}^n$ is the vector of the phase variables, $\alpha = (\alpha_1, \alpha_2)^T \in \mathbb{R}^2$ is the vector of parameters, and f is a sufficiently smooth function of (x, α). Suppose that at $\alpha = \alpha_*$ the system has an equilibrium $x = x_*$ for which either the fold or Hopf bifurcation conditions are satisfied. Then, generically, there is a bifurcation curve $\mathcal{B}$ in the (α_1, α_2)-plane along which the system has an equilibrium exhibiting the same bifurcation.

More precisely, assume that at $\alpha = \alpha_* = (\alpha_{1*}, \alpha_{2*})$ the system

$$\dot{x} = f(x, \alpha), \quad x \in \mathbb{R},\ \alpha = (\alpha_1, \alpha_2)^T \in \mathbb{R}^2,$$

has an equilibrium $x = x_*$ with eigenvalue $\lambda = f_x(x_*, \alpha_*) = 0$. The system of two scalar nonlinear equations in $\mathbb{R}^3$

$$\begin{cases} f(x, \alpha) = 0 \\ f_x(x, \alpha) = 0 \end{cases}$$

generically defines a smooth one-dimensional manifold $\Gamma \subset \mathbb{R}^3$, in particular a curve, passing through the point $(x_*, \alpha_{1*}, \alpha_{2*})$. Each point $(x, \alpha) \in \Gamma$ defines an equilibrium point x with zero eigenvalue at the parameter value α. The standard projection $\pi : (x, \alpha) \to \alpha$ maps Γ onto a curve $\mathcal{B}_t$ in the parameter plane, called *fold bifurcation curve*, and a fold bifurcation takes place on this curve.

Consider now a planar system

$$\dot{x} = f(x, \alpha), \quad x = (x_1, x_2)^T \in \mathbb{R}^2,\ \alpha = (\alpha_1, \alpha_2)^T \in \mathbb{R}^2,$$

having at $\alpha = \alpha_* = (\alpha_{1*}, \alpha_{2*})^T$ an equilibrium $x_* = (x_{1*}, x_{2*})^T$ with a pair of eigenvalues on the imaginary axis $\lambda_{1,2} = \pm i\omega_*$. The system of three scalar nonlinear equations in $\mathbb{R}^4$ with coordinates $(x_1, x_2, \alpha_1, \alpha_2)$

$$\begin{cases} f(x, \alpha) = 0, \\ \mathrm{tr}\ J(x, \alpha) = 0, \end{cases}$$

defines a curve $\Gamma \subset \mathbb{R}^4$ passing through (x_*, α_*). Each point on the curve specifies an equilibrium of the system with $\lambda_{1,2} = \pm i\omega_*,\ \omega_* > 0$ as long as $\det J(x, \alpha) > 0$.

The standard projection of Γ onto the (α_1, α_2)-plane yields the Hopf bifurcation boundary $\mathcal{B}_H$.

Let the parameters (α_1, α_2) be varied simultaneously to track a bifurcation curve Γ. The the following events might happen to the monitored nonhyperbolic equilibrium at some parameter values: extra eigenvalues can approach the imaginary axis, thus changing the dimension of the center manifold W^c, or some of the genericity conditions for the codimension one bifurcation can be violated.

First, we consider the fold bifurcation curve $\mathcal{B}_t$. A typical point on this curve defines an equilibrium with a simple zero eigenvalue $\lambda_1 = 0$ and no other eigenvalues on the imaginary axis. The restriction of the system to a center manifold W^c has the form

$$\dot{\xi} = a\xi^2,$$

where, by definition, the coefficient a is nonzero at a nondegenerate fold bifurcation point. While the curve is being tracked, the following singularities can be met:

- An additional real eigenvalue λ_2 approaches the imaginary axis, and W_c becomes two-dimensional:

  $$\lambda_1 = 0, \quad \lambda_2 = 0.$$

  These are the conditions for the *Bogdanov-Takens* (or double-zero) bifurcation. To have this bifurcation, we need $n \geq 2$. Clearly, the Bogdanov-Takens bifurcation can also be located along a Hopf bifurcation curve, as ω_0 approaches zero. At this point, two purely imaginary eigenvalues collide and we have a double zero eigenvalue.

- Two extra complex eigenvalues $\lambda_{2,3}$ arrive at the imaginary axis, and W^c becomes three-dimensional:

  $$\lambda_1 = 0, \quad \lambda_{2,3} = \pm i\omega_0,$$

  for $\omega_0 > 0$. These conditions correspond to the *fold-Hopf bifurcation*. Obviously, this bifurcation can occur only if $n \geq 3$.

- The eigenvalue $\lambda_1 = 0$ remains simple and the only one on the imaginary axis ($dim W_c = 1$), but the normal form coefficient a vanishes:

  $$\lambda_1 = 0, \quad a = 0.$$

  These are the conditions for a cusp bifurcation, which is possible in systems with $n \geq 1$.

We consider now a Hopf bifurcation curve $\mathcal{B}_H$. At a typical point on this curve, the system has an equilibrium with a simple pair of purely imaginary eigenvalues $\lambda_{1,2} = \pm\omega_0,\ \omega_0 > 0$, and no other eigenvalues with $Re\lambda = 0$. The center manifold W^c is two-dimensional in this case, and there are (polar) coordinates (ρ, ϕ) for which the restriction of the system to this manifold is orbitally equivalent to

$$\begin{cases} \dot{\rho} = l_1\rho^3, \\ \dot{\phi} = 1, \end{cases}$$

where by definition, the first Lyapunov coefficient $l_1 \neq 0$ at a nondegenerate Hopf point. While moving along the curve, we can encounter the following possibilities:

- Two extra complex-conjugate eigenvalues $\lambda_{3,4}$ approach the imaginary axis, and W^c becomes four-dimensional:

  $$\lambda_{1,2} = \pm i\omega_0, \quad \lambda_{3,4} = \pm i\omega_1,$$

  with $\omega_{0,1} > 0$. These conditions define the *Hopf-Hopf bifurcation*. It is possible only if $n \geq 4$.

- The first Lyapunov coefficient l_1 might vanish while $\lambda_{1,2} = \pm i\omega_0$ remain simple and, therefore, $dimW^c = 2$:

  $$\lambda_{1,2} = \pm i\omega_0, \quad l_1 = 0.$$

  At this point, a subcritical Andronov-Hopf bifurcation turns into a supercritical one (or vice versa). We call this event a *Bautin bifurcation* or *generalized Hopf bifurcation*. It is possible if $n \geq 2$. As for the cusp bifurcation, the Bautin bifurcation cannot be detected by merely monitoring the eigenvalues.

Thus, five bifurcation points can be met in generic two-parameter systems while moving along codimension-one bifurcation curves. Each of these bifurcations is characterized by two independent conditions. There are no other codimension-two bifurcations in generic continuous-time systems. It follows that in a planar system, only three codimension-two bifurcation are possible, the Bautin, the cusp and the Bogdanov-Takens. We report more details for these three types.

Cusp bifurcation

Consider the system

$$\dot{x} = f(x, \alpha), \quad x \in \mathbb{R},\ \alpha = (\alpha_1, \alpha_2)^T \in \mathbb{R}^2,$$

with a smooth function f which has at $\alpha_* = 0$ an equilibrium $x_* = 0$. The system has a *cusp bifurcation* in (x_*, α_*) if

$$\lambda = f_x(x_*, \alpha_*) = 0, \quad a = \frac{1}{2} f_{xx}(x_*, \alpha_*) = 0. \tag{0.1}$$

Assume also that the following genericity conditions are satisfied:

$$f_{xxx}(0,0) = 0, \quad (f_{\alpha_1} f_{x\alpha_2} - f_{\alpha_2} f_{x\alpha_1})(0,0) = 0. \tag{0.2}$$

Then there are smooth invertible coordinate and parameter changes transforming the system into

$$\dot{\eta} = \beta_1 + \beta_2 \eta \pm \eta^3,$$

that is the topological normal form for the cusp bifurcation. This system (consider for instance the plus) can have from one to three equilibria. A fold bifurcation occurs at a bifurcation curve $T = (\beta_1, \beta_2) : 4\beta_2^3 - 27\beta_1^2 = 0$ on the (β_1, β_2)-plane, given by the projection onto the parameter plane of the curve Γ:

$$\begin{cases} \beta_1 + \beta_2 \eta - \eta^3 = 0, \\ \beta_2 - 3\eta_2 = 0. \end{cases}$$

The curve T has two branches, T_1 and T_2, which meet tangentially at the cusp point $(0,0)$ (see Figure 0.1). The resulting wedge divides the parameter plane into two regions. In region 1, inside the wedge, there are three equilibria, two stable and one unstable; in region 2, outside the wedge, there is a single equilibrium, which is stable, and a fold bifurcation (with respect to the parameter β_1) takes place if we cross either T_1 or T_2 at any point other than the origin. If the curve T_1 is crossed from region 1 to region 2, the right stable equilibrium collides with the unstable one and both disappear. The same happens to the left stable equilibrium and the unstable equilibrium at T_2. If we approach the cusp point from inside region 1, all three equilibria merge together into a triple root of the right-hand side of the normal form.

An useful way to present this bifurcation is to plot the equilibrium manifold of the normal form

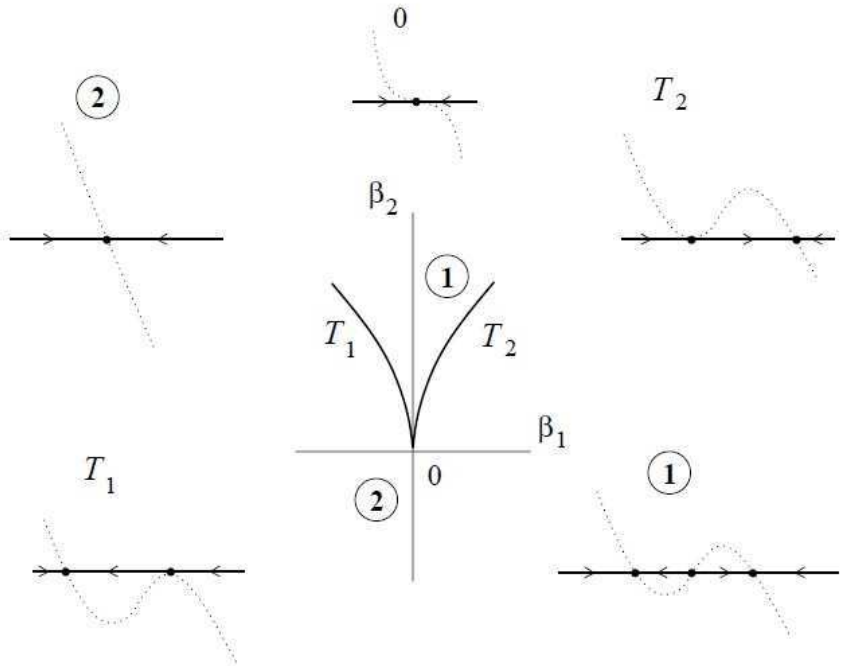

Fig. 0.1. Bifurcation diagram in the parameter space of a one-dimensional cusp point [66].

$$\mathcal{M} = \{(\eta, \beta_1, \beta_2) : \beta_1 + \beta_2\eta \pm \eta^3 = 0\},$$

in $\mathbb{R}^3$. The standard projection of $\mathcal{M}$ onto the (β_1, β_2)- plane has singularities of fold type along the fold bifurcation curve except in the origin, where a cusp singularity shows up. Notice that the fold bifurcation curve is smooth everywhere and has no geometrical singularity at the cusp point, but it is the projection that makes the fold parametric boundary nonsmooth.

The cusp bifurcation implies the presence of the phenomenon known as *hysteresis*, a catastrophic jump to a different stable equilibrium (caused by the disappearance of a traced stable equilibrium via a fold bifurcation as the parameters vary).

Bautin (generalized Hopf) bifurcation

Consider the planar system

$$\dot{x} = f(x, \alpha), \quad x = (x_1, x_2)^T \in \mathbb{R}^2,\ \alpha = (\alpha_1, \alpha_2)^T \in \mathbb{R}^2,$$

with a smooth function f which has at $\alpha_* = 0$ an equilibrium $x_* = 0$. The system has a *Bautin bifurcation* in (x_*, α_*) if the equilibrium has purely imaginary eigenvalues

and the first Lyapunov coefficient vanishes:

$$\lambda_{1,2} = \pm i\omega_0,\ \omega_0 > 0, \quad l_1 = 0.$$

In the presence of this bifurcation, we can expect the existence of two limit cycles for nearby parameter values. Moreover, they will collide and disappear along a curve emanating from the codimension-2 point.

More precisely, the normal form in polar coordinates (ρ, ϕ) has two independent equations

$$\begin{cases} \dot{\rho} = \rho(\beta_1 + \beta_2\rho^2 - \rho^4), \\ \dot{\phi} = 1. \end{cases}$$

The second equation describes a rotation with unit angular velocity. The system admits a trivial equilibrium $\rho = 0$ and positive equilibria of the first equation satisfy

$$\beta_1 + \beta_2\rho^2 - \rho^4 = 0$$

and describe circular limit cycles. This equation can have zero, one, or two positive solutions (cycles). As can be seen in Figure 0.2, these solutions branch from the trivial one along the line

$$H = \{(\beta_1, \beta_2) : \beta_1 = 0\}$$

and collide and disappear at the half-parabola

$$T = \{(\beta_1, \beta_2) : \beta_2^2 + 4\beta_1 = 0, \beta_2 > 0\}.$$

The line H corresponds to the Hopf bifurcation. The equilibrium is stable for $\beta_1 < 0$ and unstable for $\beta_1 > 0$. The first Lyapunov coefficient $l_1(\beta) = \beta_2$. Therefore, the Bautin bifurcation point $\beta_1 = \beta_2 = 0$ separates two branches, H_- and H_+, corresponding to a Hopf bifurcation with negative and with positive Lyapunov coefficient. A stable limit cycle bifurcates from the equilibrium if we cross H_- from left to right, while an unstable cycle appears if we cross H_+ in the opposite direction. The cycles collide and disappear on the curve T, corresponding to a nondegenerate fold bifurcation of the cycles. The curves divide the parameter plane into three regions. In region 1 in the parameter plane the system has a single stable equilibrium and no cycles. Crossing the Hopf bifurcation boundary H_- from region 1 to region 2 implies the appearance of a unique and stable limit cycle, which survives when we enter region 3. Crossing the Hopf boundary H_+ creates an extra unstable cycle inside the first one, while the equilibrium regains its stability. Two cycles of opposite stability exist inside region 3 and disappear at the curve T through a fold bifurcation that leaves a single stable equilibrium.

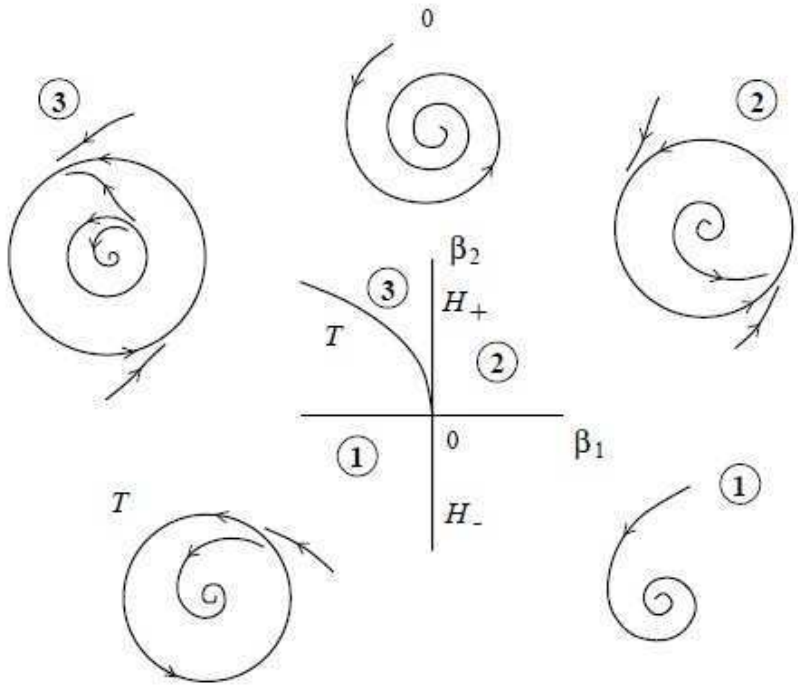

Fig. 0.2. Bifurcation diagram in the parameter space of a Bautin point [66].

Bogdanov-Takens (double-zero) bifurcation

Consider the planar system

$$\dot{x} = f(x, \alpha), \quad x = (x_1, x_2)^T \in \mathbb{R}^2, \ \alpha = (\alpha_1, \alpha_2)^T \in \mathbb{R}^2,$$

with a smooth function f which has at $\alpha_* = 0$ an equilibrium $x_* = 0$. The system has a *Bogdanov-Takens bifurcation* in (x_*, α_*) if the equilibrium has two zero eigenvalues

$$\lambda_{1,2} = 0.$$

The bifurcation condition implies that

$$\det J(x_*, \alpha_*) = 0, \quad \text{tr } J(x_*, \alpha_*) = 0.$$

As for the Bautin bifurcation, the Bogdanov-Takens bifurcation gives rise to a limit cycle bifurcation, namely, the appearance of the homoclinic orbit, for nearby parameter values.

It can be proved that any generic planar two-parameter system $\dot{x} = f(x, \alpha)$, having, at $\alpha = 0$, an equilibrium that exhibits the Bogdanov-Takens bifurcation, is locally topologically equivalent near the equilibrium to one of the following normal forms:

$$\begin{cases} \dot{\eta_1} = \eta_2, \\ \dot{\eta_2} = \beta_1 + \beta_2\eta_1 + \eta_1^2 \pm \eta_1\eta_2. \end{cases}$$

The equilibria of the system are located on the horizontal axis, $\eta_2 = 0$, and satisfy the equation

$$\beta_1 + \beta_2\eta_1 + \eta_1^2 = 0,$$

which can have between zero and two real roots. The discriminant parabola

$$T = \{(\beta_1, \beta_2) : 4\beta_1 - \beta_2^2 = 0\}$$

corresponds to a fold bifurcation. If $\beta_2 \neq 0$, then the fold bifurcation is nondegenerate and crossing T from right to left implies the appearance of two equilibria, E_1 and E_2. The point $\beta = 0$ separates two branches T_- ($\beta_2 < 0$) and T_+ ($\beta 2 > 0$) of the fold curve. That passage through T_- implies the coalescence of a stable node E_1 and a saddle point E_2, while crossing T_+ generates an unstable node E_1 and a saddle E_2. The vertical axis $\beta_1 = 0$ is a line on which the equilibrium E_1 has a pair of eigenvalues with zero sum: $\lambda_1 + \lambda_2 = 0$. The lower part,

$$H = \{(\beta_1, \beta_2) : \beta_1 = 0, \beta_2 < 0\},$$

corresponds to a nondegenerate Hopf bifurcation, while the upper half-axis is a nonbifurcation line corresponding to a neutral saddle. The Hopf bifurcation gives rise to a stable limit cycle, ($l_1 < 0$). The cycle exists near H for $\beta_1 < 0$. The equilibrium E_2 remains a saddle for all parameter values to the left of the curve T and does not bifurcate. There are no other local bifurcations in the dynamics of this system. Looking at Figure 0.3, in region 1 there are no equilibria (and thus no limit cycles). Entering from region 1 into region 2 crossing the component T_- of the fold curve yields two equilibria: a saddle and a stable node. Then the node turns into a focus and loses stability as we cross the Hopf bifurcation boundary H. A stable limit cycle is present for parameter values close to the left of H, which does not bifurcate in region 3 and approaches the saddle, turning into a homoclinic orbit at P. Then, an unstable node and a saddle, existing for the parameter values in region 4, collide and disappear at the fold curve T_+.

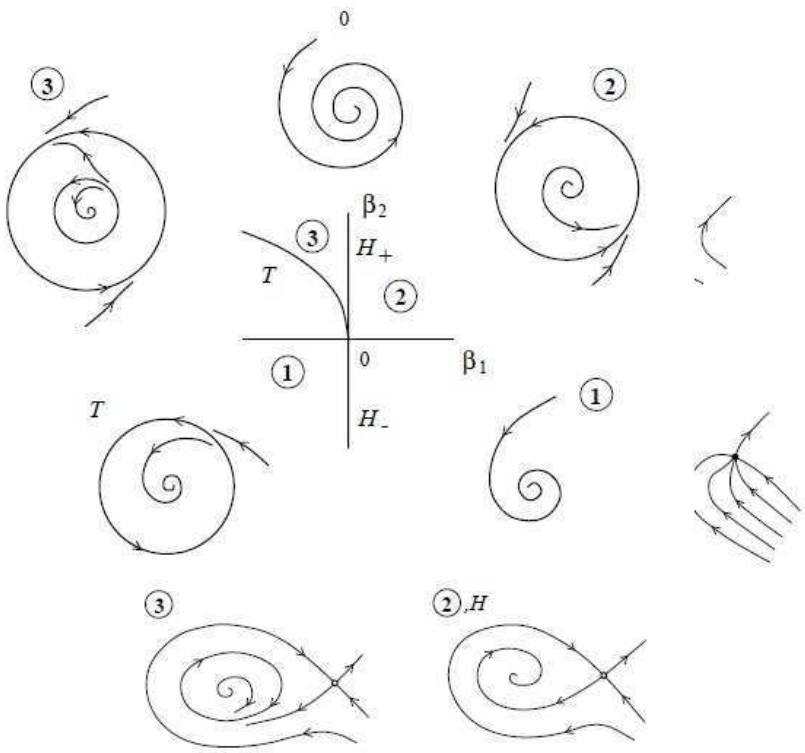

Fig. 0.3. Bifurcation diagram in the parameter space of a Bogdanov-Takens point [66].

Diffusion-driven instability in reaction-diffusion systems

Reaction-diffusion equations are widely used for modeling chemical reactions, biological systems, population dynamics and nuclear reactor physics. They are of the form

$$u_t = D\Delta u + f(u, \lambda)$$

where $u = (u_1, \ldots, u_k)$ represents various substances in a chemical reaction or species of a biological system; $\lambda \in \mathbb{R}^p$ is a vector of control parameters, Δ is the Laplace operator in the spatial variables and $D \in \mathbb{R}^{k\times k}$ is often diagonal and corresponds to the diffusion rates: they describe diffusion of different substances or species. The function $f : \mathbb{R}^k \times \mathbb{R}^p \to \mathbb{R}^k$ is a vector of smooth non-linear functions and represents the reaction among the substances.

Looking at chemical reactions, Turing (1952) suggested that, under certain conditions, chemicals can react and diffuse in such a way as to produce steady state

heterogeneous spatial patterns, due to a diffusion-driven instability of the steady state.

A reaction-diffusion system exhibits *diffusion-driven instability*, sometimes called *Turing instability*, if the homogeneous steady state is stable to small perturbations in the absence of diffusion but unstable to small spatial perturbations when diffusion is present. The interplay between *interaction* (the nonlinear kinetics) and *diffusion* is crucial in driving the spatially inhomogeneous instability: these mechanism determine the spatial pattern that evolves. In the following, we deduce necessary and sufficient conditions for diffusion-driven instability of the steady state in the case of linear diffusion (diagonal D) and also in the case of cross diffusion (more complex diffusion terms).

Turing instability analysis

We deduce here the necessary and sufficient conditions for diffusion-driven instability of the steady state and the initiation of spatial pattern for a general system of two reaction-diffusion equations.

We assume that the process happens in a bounded region $\Omega \subset \mathbb{R}^N$, assumed to be smooth ($\mathcal{C}^2$), bounded and connected, where the "molecules" (individuals) are moving. We shall concentrate on the case when the "molecules" diffuse (each species has its own diffusion velocity) within a non-reactive background (supposed to be at rest). All reaction-diffusion systems can be adimensionalized and scaled to take the general form

$$\begin{aligned} u_t - \Delta u &= \gamma f(u,v), \\ v_t - d\Delta v &= \gamma g(u,v), \end{aligned}$$

where the unknowns are $u := u(x,t)$ and $v := v(x,t)$ $(t \in \mathbb{R}, x \in \Omega)$, f, g are smooth non-linear functions and represent the reaction among the substances (or the interaction mechanisms between species), $d > 0$ is the ratio of diffusion coefficients and γ represents the relative strength of the reaction terms. We shall assume that molecules (species) are confined in the region Ω, so that the flux of density of each species at the boundary $\partial\Omega$ is 0. This gives the homogeneous Neumann boundary conditions, no density flux of each species at the boundary:

$$\hat{n}(x) \cdot \nabla_x u = 0, \quad \hat{n}(x) \cdot \nabla_x v = 0, \quad x \in \partial\Omega,$$

where $\partial\Omega$ is the closed boundary of the reaction diffusion domain Ω and $\hat{n}$ is the unit outward normal to $\partial\Omega$. In addition, we consider initial conditions

$$u(x,0) = u_0(x), \quad v(x,0) = v_0(x), \quad x \in \Omega.$$

Since we are concerned with diffusion-driven instability, we are interested in linear instability of homogeneous steady state that is solely spatially dependent. In detail, with no spatial variation u and v satisfy the ODE system

$$\begin{aligned} u_t &= \gamma f(u,v), \\ v_t &= \gamma g(u,v); \end{aligned}$$

an homogeneous steady state (u_0, v_0) is a steady state for the reaction part with no spatial variation, namely the solution of

$$f(u,v) = 0, \quad g(u,v) = 0.$$

A necessary condition to have Turing instability is that, in absence of any spatial variation, the homogeneous steady state must be linearly stable: we first determine the conditions for this to hold. Linearising about the steady state (u_0, v_0), we set

$$w = \begin{pmatrix} u - u_0 \\ v - v_0 \end{pmatrix},$$

and the homogeneous system becomes, for $|w|$ small,

$$w_t = \gamma J w, \quad J = \begin{pmatrix} f_u & f_v \\ g_u & g_v \end{pmatrix}_{|(u_0,v_0)}.$$

We now look for solutions of the form

$$w \propto e^{\lambda t}$$

where λ is the eigenvalue. The steady state $w = 0$ is linearly stable if $Re\lambda < 0$ since in this case the perturbation $w \to 0$ as $t \to \infty$. The eigenvalues λ are the solutions of $\det(\gamma J - \lambda I) = 0$, which is equivalent to

$$\lambda^2 - \gamma(f_u + g_v)\lambda + \gamma^2(f_u g_v - f_v g_u) = 0.$$

Linear stability, that is $Re\lambda < 0$, is guaranteed if and only if

$$\text{tr } J = f_u + g_v < 0, \quad \det J = f_u g_v - f_v g_u > 0,$$

which in general impose certain constraints on the parameters.

Now consider the full reaction diffusion system and again linearise around the steady state, which is $w = 0$, to get

$$w_t = \gamma J w + D \Delta_x w, \quad D = \begin{pmatrix} 1 & 0 \\ 0 & d \end{pmatrix}.$$

To solve this system of equations subject to the boundary conditions, we first define $W(x)$ to be the time-independent solution of the spatial eigenvalue problem defined by

$$\Delta_x W + k^2 W = 0, \qquad \hat{n}(x) \nabla_x W = 0$$

for x on $\partial \Omega$ where k is the eigenvalue.

If the domain is one-dimensional, for example the interval $[0, a]$, we have that $W \propto \cos(n\pi x/a)$ where n is an integer. The eigenvalue in this case is $k = n\pi/a$ and $1/k$ is a measure of the wavelike pattern and it is proportional to the wavelength $\omega = 2\pi/k = 2a/n$; the eigenvalue k is called *wavenumber*. From now on, we refer to k as the wavenumbers. With finite domains there is a discrete set of possible wavenumbers since n is an integer. If we consider a two-dimensional domain, for example the rectangle $[0, L_x] \times [0, L_y]$, we have that $W \propto \cos(k_1 \pi x/L_1) \cos(k_2 \pi y/L_2)$ with $k_1,\ k_2 \in \mathbb{N}$ and

$$k^2 = \left(\frac{k_1 \pi}{L_x}\right)^2 + \left(\frac{k_2 \pi}{L_y}\right)^2.$$

Let $W_k(x)$ be the eigenfunction corresponding to the wavenumber k. Each eigenfunction W_k satisfies zero flux boundary conditions. Because the problem is linear we now look for solutions $w(x, t)$ in the form

$$w(x, t) = \sum_k c_k e^{\lambda t} W_k(x),$$

where the constants c_k are determined by a Fourier expansion of the initial conditions in terms of $W_k(x)$, and λ is the eigenvalue which determines temporal growth. Substituting this form into the linearized reaction-diffusion equation and eliminating $e^{\lambda t}$, we get, for each k,

$$\lambda W_k = \gamma J W_k - D k^2 W_k.$$

We look for nontrivial solutions for W_k so the λ are determined by the roots of the characteristic polynomial

$$\det(\lambda I - \gamma J + D k^2) = 0,$$

which is equivalent to find the eigenvalues of the matrix $\boldsymbol{M}_k = \gamma J - Dk^2$. We get the eigenvalues $\lambda(k)$ as functions of the wavenumber k as the roots of

$$\lambda^2 + \lambda[k^2(1+d) - \gamma(f_u + g_v)] + h(k^2) = 0,$$

where

$$h(k^2) = dk^4 - \gamma(df_u + g_v)k^2 + \gamma^2 \det J.$$

Note that the coefficient of λ is $-\mathrm{tr}\, \boldsymbol{M}_k$, while $h(k^2) = \det \boldsymbol{M}_k$; since $\mathrm{tr}\, \boldsymbol{M}_k < 0$ for all k, the only way to have an unstable steady state to spatial disturbances is that $\det \boldsymbol{M}_k < 0$ for some k. Let us consider the equation for λ. The steady state (u_0, v_0) is unstable to spatial disturbances if $Re\lambda(k) > 0$ for some $k \neq 0$. Since $\mathrm{tr}\, J = (f_u + g_v) < 0$ and $k^2(1+d) > 0$ for all $k \neq 0$, the only way is that $h(k^2) < 0$ for some k. Since we required $\det J > 0$ for the homogeneous steady state, the only possibility for $h(k^2)$ to be negative is that $(df_u + g_v) > 0$. Since $(f_u + g_v) < 0$, this implies that $d \neq 1$ and f_u and g_v must have opposite signs. So, a further requirement to those implicated by the linear stability of the homogeneous steady state is $df_u + g_v > 0$, so that $d \neq 1$. This inequality is necessary but not sufficient for $Re\lambda > 0$. For $h(k^2)$ to be negative for some non-zero k, the minimum h_{min} must be negative. Elementary differentiation with respect to k^2 shows that

$$h_{min} = \gamma^2 \left[\det J - \frac{(df_u + g_v)^2}{4d}\right], \qquad k^2_{min} = \gamma \frac{df_u + g_v}{2d},$$

thus the condition that $h(k^2) < 0$ for some $k^2 \neq 0$ is

$$(df_u + g_v)^2 - 4d \det J > 0.$$

At bifurcation, when $h_{min} = 0$, from the definition of h_{min}, we require $\det J = (df_u + g_v)^2/4d$, which is equivalent to

$$d^2 f_u^2 + 2(2f_v g_u - f_u g_v)d + g_v^2 = 0,$$

and so for fixed parameters this defines a critical diffusion coefficient ratio $d_c (> 1)$ as the appropriate root of this equation. The critical wavenumber k_c is then given by

$$k_c^2 = \gamma \frac{d_c f_u + g_v}{2d_c} = \gamma \sqrt{\frac{\det J}{d_c}}.$$

Whenever $h(k^2) < 0$, the equation for λ has a solution which is positive for the same range of wavenumbers that make $h < 0$. With $d > d_c$ the range of unstable wavenumbers $k_1^2 < k^2 < k_2^2$ is obtained from the zeros k_1^2 and k_2^2 of $h(k^2) = 0$ as

$$k_{1,2}^2 = \frac{\gamma}{2d}\left((dfu + gv) \pm \sqrt{(df_u + g_v)^2 - 4d\det J}\right).$$

If we consider the solution w, the dominant contributions as t increases are those modes for which $Re\lambda(k^2) > 0$ since all other modes tend to zero exponentially. We determine the range $k_1^2 < k^2 < k_2^2$, where

$$w(x,t) \propto \sum_{k_1} k_2 c_k e^{\lambda(k^2)t} W_k(x)$$

for large t.

Summarizing, the conditions for the generation of spatial patterns by two-species reaction-diffusion mechanisms are

$$\begin{aligned}
&\text{tr } J = f_u + g_v < 0,\\
&\det J = f_u g_v - f_v g_u > 0,\\
&df_u + g_v > 0,\\
&(df_u + g_v)^2 - 4d(f_u g_v - f_v g_u) > 0,
\end{aligned}$$

remembering that all derivatives are evaluated at the homogeneous steady state (u_0, v_0).

Turing instability analysis with cross-diffusion

Recently, non-linear diffusion terms, or *cross-diffusion*, have appeared to model different physical phenomena in different contexts like population dynamics, ecology, and chemical reactions [36, 96, 39]. Cross-diffusion terms should be introduced when the gradient of the density of one species induces a flux of another species. In this context, the general two-species reaction-cross-diffusion system is

$$\begin{aligned}
u_t - \Delta_x(a(u,v)) &= f(u,v)\\
v_t - \Delta_x(b(u,v)) &= g(u,v),
\end{aligned}$$

where the unknowns are $u := u(x,t)$ and $v := v(x,t)$ $(t \in \mathbb{R}, x \in \Omega)$, f, g are smooth non-linear functions and represent the reaction among the substances (or the interaction mechanisms between species), a, b are smooth functions depending on both u, v. Also in this case, we consider homogeneous Neumann boundary conditions

$$\hat{n}(x) \cdot \nabla_x u = 0, \quad \hat{n}(x) \cdot \nabla_x v = 0, \quad x \in \partial\Omega,$$

where $\partial\Omega$ is the closed boundary of the reaction diffusion domain Ω and $\hat{n}$ is the unit outward normal to $\partial\Omega$, and given initial conditions

$$u(x,0) = u_0(x), \quad v(x,0) = v_0(x), \quad x \in \Omega.$$

Here we study the Turing bifurcation in the presence cross-diffusion, looking at determining the threshold as usual by a linear stability analysis. Following the linear case, we consider an homogeneous steady state (u_0, v_0), which is stable for the reaction part. The linearised system in the neighbourhood of (u_0, v_0) is

$$w_t = Jw + D\Delta_x w, \qquad w = \begin{pmatrix} u - u_0 \\ v - v_0 \end{pmatrix},$$

where now

$$J = \begin{pmatrix} J_{11} & J_{12} \\ J_{21} & J_{22} \end{pmatrix} := \begin{pmatrix} f_u & f_v \\ g_u & g_v \end{pmatrix}_{|(u_0,v_0)}, \qquad D = \begin{pmatrix} d_{11} & d_{12} \\ d_{21} & d_{22} \end{pmatrix} := \begin{pmatrix} a_u & a_v \\ b_u & b_v \end{pmatrix}_{|(u_0,v_0)}.$$

In this case, the diffusion matrix is no longer a diagonal matrix as in the previous section because generally non-zero off-diagonal elements appear in the matrix D. Furthermore, the cross-diffusion coefficients become effectively constant; their value is determined by the homogeneous steady state of the system. If the cross-diffusion term is positive, $d_{kj} > 0$, then the flux of species k is directed toward decreasing values of the concentration of species j , whereas $d_{kj} < 0$ implies that the flux is directed toward increasing values of the concentration of species j.

We are interested in the eigenvalues of the matrix

$$\boldsymbol{M}_k = J - Dk^2 = \begin{pmatrix} J_{11} - d_{11}k^2 & J_{12} - d_{21}k^2 \\ J_{21} - d_{21}k^2 & J_{22} - d_{22}k^2 \end{pmatrix}.$$

The Turing instability sets in when at least one of the following conditions is violated for some k:

$$\text{tr } \boldsymbol{M}_k < 0, \qquad \det \boldsymbol{M}_k > 0,$$

where

$$\text{tr } \boldsymbol{M}_k = \text{tr } J - \text{tr } D,$$

$$\det \boldsymbol{M}_k = \det D \; k^4 - (d_{11}J_{22} - d_{12}J_{21} - d_{21}J_{12} + d_{22}J_{11})k^2 + \det J.$$

In general the sign of the elements of the diffusion matrix D, and then of the trace and the determinant, is not prescribed. If we assume that both main (linearized) diffusion

coefficients $d_{11},\ d_{22}$ are positive, the condition on the trace of $\boldsymbol{M}_k$ is always satisfied when the homogeneous steady state is linearly stable for the reaction part. Hence, only the violation of the second condition gives rise to diffusion-driven instability. Thus, the condition for diffusion-driven instability occurs when

$$\det \boldsymbol{M}_k = \det D\ k^4 - (d_{11}J_{22} - d_{12}J_{21} - d_{21}J_{12} + d_{22}J_{11})k^2 + \det J < 0.$$

Again, in general we sign of the determinant of the diffusion matrix D is not prescribed. However, for instance for chemical systems, thermodynamics imposes, in addition, the constraint that all eigenvalues of the diffusion matrix must be real and positive, which implies that $\operatorname{tr} D > 0$ and $\det D > 0$ [75]. If we also assume that $\det D > 0$, then

$$d_{11}J_{22} - d_{12}J_{21} - d_{21}J_{12} + d_{22}J_{11} > 0$$

is a necessary, but not a sufficient, condition for a Turing instability. The onset of the Turing instability occurs when $\det \boldsymbol{M}_k < 0$ which holds if

$$(d_{11}J_{22} - d_{12}J_{21} - d_{21}J_{12} + d_{22}J_{11})^2 > 4 \det J \det D.$$

Summarizing as in the linear case, when $\operatorname{tr} D < 0$ and $\det D > 0$, the conditions for the generation of spatial patterns by two-species reaction-diffusion mechanisms are

$$\begin{aligned}
&\operatorname{tr}\ J < 0,\\
&\det J > 0,\\
&d_{11}J_{22} - d_{12}J_{21} - d_{21}J_{12} + d_{22}J_{11} > 0,\\
&(d_{11}J_{22} - d_{12}J_{21} - d_{21}J_{12} + d_{22}J_{11})^2 > 4 \det J \det D.
\end{aligned}$$

If these conditions holds, then the equilibrium (u_0, v_0) is cross-diffusion-driven instability (Turing instability).

Part I

Dynamics of predator-prey models with a strong Allee effect on the prey and predator-dependent trophic functions

1

Introduction

This Part[1] deals with the dynamics of a predator-prey system described in terms of a lumped parameter model [68, 24], in which the demographic structure of the populations is neglected, in particular the stage structure for insects and mites (eggs, larvae, pupae, adults). Thus, the predator and prey populations may be characterized by just one state variable, representing their abundance in terms of biomass/spatial unit. Moreover, we assume a limited and controlled environment (for instance a greenhouse, in which temperature and humidity are maintained approximately constant) so that we can consider time independent bioecological parameters, and neglect the spatial distribution of the individuals.

In this framework, the local dynamics of a predator-prey system is described by a system of two ordinary differential equations and is mainly characterized by the formulations of the prey growth rate, in the absence of predators, and of the prey consumption rate by predators. Let these rate be expressed as

$$\text{prey growth rate} = rXG(X), \tag{1.1}$$

$$\text{prey consumption rate} = YF(X,Y), \tag{1.2}$$

where X and Y are prey and predator abundances (here we assume that it is measured in terms of biomass/spatial unit). The model functions $G(X)$ and $F(X,Y)$ are specific rates and their shapes determine the type of prey growth (r is, in general, the maximum specific growth rate) and predation processes, respectively. They strongly depend on the basic assumptions made on the bioecological processes to be simulated and their shape is often unknown, thus only some of their qualitative properties can be specified. In this case, we are dealing with a *generalized* or *partially specified model* [47, 63, 103], which retains considerable structure, but involves a much less specific

[1] Most of the contents of this Part appeared on *Nonlinear Analysis: Real World Applications* 30 (2016): 143-169 [26].

assumption about the nature of the predation process and the type of growth than a *fully specified model*, where the main functions are spelled out clearly with a specific parametric expression. The hope is that models specified in this fairly general way will be capable of closer approximation to reality than more tightly specified ones, especially by the model fitting point of view.

The main purpose of this work is to investigate the dynamical behaviours of a predator-prey system, when the model functions describing the biological processes occurring in the considered trophic chain are not specified by analytical expressions, but by some characteristic properties determining their shapes. It will be shown that this is feasible for the existence and stability analysis of the equilibrium states of the system: indeed, existence and stability conditions of the equilibrium states can be established in a general framework in terms of some crucial parameters. Unfortunately, the stability analysis of limit cycles cannot be easily performed following this general approach, and the model functions have to be specified to go further in the qualitative analysis. Other authors [47, 63] presented a quite similar approach to the investigation of the dynamics in generalized models, in which the processes that are taken into account are not restricted to specific functional forms (in some cases there are no hypothesis on the general functions). As in this work, that approach allows to study the dynamical properties of generalized models in the framework of local bifurcation theory. On the contrary, the key assumption is that at least one steady state exists and the local asymptotic stability analysis of that (unknown) steady state is then performed. Our point of view is different: assumptions on the prey growth function and on the functional response are required, in order to take into account biological properties and also to limit the number of the equilibrium states admitted by the system. Furthermore, the stability and bifurcation analysis is studied for each equilibrium state.

In the development of predator-prey theory, different formulations of the prey growth rate, in absence of predators, have been proposed in the literature. In the classical predator-prey model of Lotka-Volterra $G(X) = 1$, i.e. the growth of the prey is exponential. This assumption holds for small X: when all trophic relations in the system are strained and almost all the prey is consumed by the predator, always hungry (a quite frequent situation in nature). This choice has been criticized since it neglects the overcrowding effect, i.e. the restriction in population growth due to the limits of the habitat's carrying capacity: in this case $G(X)$ should become negative for sufficiently large X. To this end, Volterra himself [101] proposed the use of the logistic model

$$G(X) = 1 - \frac{X}{K^+}, \tag{1.3}$$

where K^+ is the carrying capacity of the habitat [100]. Another classical model, taking into account the overcrowding effect, is the Gompertz model [45, 102]: $G(X) = log(K^+/X)$; we note that in this case r in (1.1) does not represent the maximum specific growth rate, but a dimensional scale for the growth rate itself. Also Kolmogorov [62], in his very general predator-prey model, considered only the overcrowding effect in the prey growth by assuming $G(X)$ not specified by any analytical expression, but characterized by the monotonicity condition

$$G'(X) < 0, \qquad G(0) = 1, \qquad \lim_{x \to +\infty} G(X) < 0. \tag{1.4}$$

In the last decades, the predator-prey dynamics resulting from the choice of a monotonic $G(X)$, namely considering only the overcrowding effect on the prey growth, have been widely investigated by many authors (for more details see [23] and references therein).

On the other hand, it is known that natural populations may exhibit either negative or positive correlation between $G(X)$ and X, depending on the range of abundance ([8], [93], [92] p.17, [104] p.275). In particular, these effects are found in populations of bisexual organisms and/or with a team behaviour and a mutual help [65]. A detailed treatment, from the ecological viewpoint, of different types of these non-monotonic relationships (the so-called *Allee effect* [91]) is given in Allee et al. [9].

Mainly two types of Allee effects in prey population have been considered in the literature (see for instance [7, 19, 20, 30, 42, 61, 65, 46, 91, 90, 94, 98, 106]): the weak and the strong (or critical) Allee effect, depending on the fact that the prey growth function $G(X)$ is non-negative or negative, respectively, for small X [94]. According to [94], if there is an Allee effect, then the prey growth function must have a positive slope at $X = 0$. In addition, in case of strong Allee effect, the function $G(X)$ becomes negative for sufficiently small values of X. Thus, the problem of minimum population size arises ([43], [104] p.275), and it is worth noticing that the extinction thresholds are often difficult to quantify ([104] p.275, [95], [19]).

To simulate the Allee effect, many authors [20, 42, 61, 46, 94, 98, 106] use a multiplicative factor to the logistic term $(1 - X/K^+)$, while other authors [7, 30, 65, 90] use an additive term (which can be rewritten, in the case of strong Allee effect, as multiplicative factors with real zeros). Also the models listed in [19] (except one, namely [60]), for a single species dynamics, simulate the Allee effect in the same way. In all these models the growth function $G(X)$ can be expressed as

$$G(X) = g\Big(\frac{X}{K^+}\Big) = \frac{a_0 + a_1\, X/K^+ - (x/K^+)^2}{b_0 + b_1\, X/K^+} = \frac{(a_0 + X/K^+)\,(1 - X/K^+)}{b_0 + b_1\, X/K^+}, \tag{1.5}$$

where a_i, b_i are adimensional coefficients with $a_1 = 1 - a_0$, $b_0 > 0$, $b_1 = 0, 1$. The function $G(X)$ defined in (1.5) has one positive zero in $X = K^+$. When $a_0 \geq 0$ the second zero is non-positive, and $G(X)$ simulates a weak Allee effect. Otherwise, when $a_0 < 0$ the second zero is positive and $G(X)$ simulates a strong Allee effect. We note that also the prey flux model considered in [61] and [98] can be described by a function $G(X)$ as in (1.5) with $b_0 = 0$ and $b_1 = 1$. The weak Allee effect, considered by Zhou et al. [106] is instead modeled by decreasing the Malthusian prey growth rate using a monotonic Holling-type II factor (Allee effect I in [106]).
The functions $G(x)$ defined by (1.5) are not bounded for increasing X:

$$\lim_{X \to +\infty} |G(X)| = +\infty.$$

However, the overcrowding effect can be taken into account also in terms of bounded functions. As a first bounded model, let $G(X)$ be defined as follows

$$G(X) \text{ as in (1.5) for } X \leq X_M; \;\; G(X) = G(X_M) \text{ for } X > X_M > K^+. \tag{1.6}$$

A second bounded model can be formulated in terms of a birth rate which is increasing for small X, and then decreasing and vanishing as $X \to +\infty$, together with a constant death rate. A possible analytical realization of this model is given by

$$G(X) = g\Big(\frac{X}{K^+}\Big) \propto \left[\left(\frac{X}{K^+}\right)^{\gamma} \exp\left(\gamma \frac{1 - X/K^+}{X_0/K^+}\right) - 1\right], \tag{1.7}$$

where $0 < \gamma \leq 1$, and X_0 is the maximum point for $G(X)$; its expression in terms of the two zeros K^- and K^+ of $G(X)$ is

$$\frac{X_0}{K^+} = -\frac{1 - \epsilon}{\log \epsilon} \qquad \text{with} \quad \epsilon = \frac{K^-}{K^+}.$$

In absence of predators, the evolution of the prey population is governed by the equation

$$\frac{dX}{dt} = rXG(X). \tag{1.8}$$

If the function $G(X)$, describing the strong Allee effect, is defined as in (1.5)-(1.7), then we have three equilibrium states for the equation (1.8): $X_{eq} = 0,\ K^-,\ K^+$. Their stability properties are independent of the choice of the specific shape of $G(X)$: $0,\ K^+$ are asymptotically stable, while K^- is unstable. Typical behaviours of the growth functions $G(X)$ as defined in (1.5)-(1.7) and the corresponding trends of $XG(X)$ are shown in Figure 1.1.

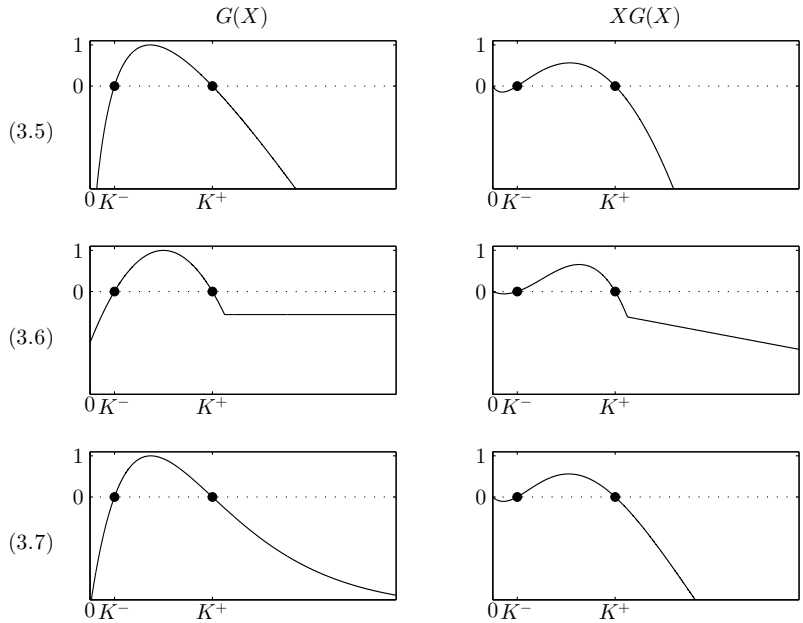

Fig. 1.1. Typical behaviours of the growth functions $G(X)$ as defined in (1.5)-(1.7) (left) and the corresponding trends of $XG(X)$ (right).

The general function in (1.2) $F(X,Y)$ is called the trophic function and describes the predator functional response to prey abundance ([92, p. 80]). It was introduced in predator-prey models to take into account the saturation limiting the predation process. To have a biologically meaningful interpretation some qualitative assumptions on $F(X,Y)$ about the dependence on X and Y have to be required:

$$F(X,Y) > 0 \quad X > 0,\ Y \geq 0, \qquad F(0,Y) = 0, \qquad \lim_{X \to +\infty} F(X,Y) < +\infty$$
$$\frac{\partial F}{\partial X} > 0, \quad \frac{\partial F}{\partial Y} < 0.$$

At first, the trophic function was assumed to be dependent only on prey abundance ([13, 55, 58, 86] and [92, p. 109-112]). Moreover, the Holling-type II [55] or the Ivlev type [58, 86] models were introduced to simulate the saturation effect of the predation process. This formulation of F only in terms of X gives rise to the "paradoxes of enrichment and biological control" [11, 16, 44], and it is unable to generate the outcome of the extinction of the two populations [11] without taking into account a strong Allee effect in the prey growth [20].

Later, the notion of per-capita availability of food was introduced. It was suggested that the trophic function should be expressed in terms of the ratio X/Y of prey to predator abundance [11, 44, 49]:

$$F(X,Y) = bf\left(\frac{PX}{Y}\right), \tag{1.9}$$

where b is the maximum prey consumption rate and P is referred to as the efficiency of the predation process. This formulation solves the above-mentioned paradoxes, and in addition allows to describe experimental observations, in particular the extinction of predator or both prey and predator populations, without resorting to the Allee effect. However, in this approach the trophic function has a singularity in the origin X=0, Y=0. This problem is solved by some authors by the blow-up method [15] or by a time rescaling [4]. Some other authors [97] modified the ratio X/Y by adding a small constant A in the denominator, so that they wrote $f(PX/(Y+A))$, and this trick [97] "...would alleviate the problem. Although this addition may appear difficult to justify biologically, Gutierrez [49] used an exponent of this form in his functional response term" of Ivlev type. It is worth noticing that the total extinction is a possible outcome when $A = 0$, while it cannot be obtained with this non-singular trophic function for any $A > 0$, as treated in detail in [23]. The efficiency P in (1.9) is assumed to be constant by some authors in their models [11, 15, 44]. On the other hand, it could be assumed predator-dependent [1, 14, 29, 50]: $P(Y)$ has to increase with Y, with a saturation effect for increasing Y due to the predator interference during foraging, and $P(Y)/Y$ has to decrease with Y to satisfy $\partial F/\partial Y < 0$. Note that, under the assumption that $P(Y) \propto Y$ as $Y \to 0$, the trophic function is no more singular in the origin. Different formulations have been proposed in the literature for $f(P(Y)X/Y)$. Gutierrez et al. [50] proposed an Ivlev-type formulation for both $f(\cdot)$ and $P(\cdot)$, while Beddington, DeAngelis and co-authors [1, 14, 29, 88] proposed a Holling-type II for both $f(\cdot)$ and $P(\cdot)$.

In this Part we will study a two-species, one-sex prey-predator model with a sufficiently general formulation, regarding both the growth of the prey and the interaction between prey and predator. The general properties of $G(X)$ and $F(X,Y)$ assumed in this work are here enlightened. We will consider non-monotonic $G(X)$ to include the effects of both undercrowding and overcrowding of the prey. The growth function $G(X)$ is not specified by an analytical expression, but by the main properties of the functions defined in (1.5)-(1.7) (Figure 1.1), suitable to model a strong or critical Allee effect (according to [7, 19, 42, 65, 91, 94]): $G(X)$ should be negative and increasing for sufficiently small X, positive between K^-, referred to as the minimum population size ([43]; [104], p. 275), and K^+, often referred to as the carrying capac-

ity of the environment ([92, p. 26]), and negative and non-increasing for sufficiently large X. The predator-dependent trophic function given by

$$F(X,Y) = bf\left(\frac{P_0 X}{K_0 + H_0 Y}\right), \tag{1.10}$$

where K_0 is a reference biomass, P_0 and H_0 are adimensional parameters: P_0 denotes the predation efficiency and H_0 is a measure of the predator interference process. Regarding the trophic function $f(\cdot)$, we prefer, until it is feasible, to introduce just one argument, instead of using a two-arguments function; this allows us to formulate its properties in a more concise form. The behaviour described by such functions shows some interesting features, e.g. the appearance of further equilibrium states, with different stability properties. Consequently, the dynamics of the system would exhibit a richer set of outcomes, depending on the range of values of the ecological parameters introduced in the model equations.

This Part is organized as follows. In Chapter 2 the basic assumptions and equations for the local dynamics of a predator-prey system are presented: the equations are written in terms of the adimensional variables X/K^+ and Y/K^+, the growth of the prey takes into account a strong Allee effect, and the interactions between prey and predator are determined by a trophic function as in (1.10). Then the stability properties of the non-coexistence equilibrium states are summarized and an existence and stability analysis of the coexistence equilibrium states is performed: parameters related to P_0 and H_0 will be assumed as bifurcation ones. In Chapter 3 results of numerical simulations, obtained for some concrete realization of the model functions, are presented to illustrate the behaviours of the system. Such results confirm analytical predictions and throw light on some aspects of the dynamics of the system. In Chapter 4 some concluding remarks can be found and results are commented on with reference to the existing literature. At the end of this Part, in Appendix A details on some crucial parameters can be found; in Appendix B more detail about the detected cusp bifurcation point are reported. For the readers' convenience, the symbols used in this Part have been collected in Appendix C.

2

The prey-predator model and the equilibrium stability analysis

In this Chapter we introduce the model equations of the considered predator-prey system, where the model functions describing the biological processes occurring in the considered trophic chain are not specified by analytical expressions, but by some characteristic properties determining their shapes. It will be shown that this is feasible for the existence and stability analysis of the equilibrium states of the system, assuming two bifurcation parameters.

2.1 Basic assumptions and model equations

We consider the dynamics of a predator-prey system described in terms of a lumped parameter model [68, 24], in which the demographic structure of the populations is neglected, in particular the stage structure for insects and mites (eggs, larvae, pupae, adults). Thus, the predator and prey populations may be characterized by just one state variable, representing their abundance in terms of biomass/spatial unit. Moreover, we assume a limited and controlled environment (for instance a greenhouse, in which temperature and humidity are maintained approximately constant) so that we can consider time independent bioecological parameters, and neglect the spatial distribution of the individuals. With these assumption, and taking into account the expression (1.10) for the trophic function, the balance equations for the local dynamics of the two trophic levels in a controlled environment are written as

$$\begin{cases} \dfrac{dX}{dt} = r_x X G(X) - bY f\left(\dfrac{P_0 X}{K_0 + H_0 Y}\right) \\ \dfrac{dY}{dt} = cbY f\left(\dfrac{P_0 X}{K_0 + H_0 Y}\right) - mY \end{cases}$$

where X and Y are prey and predator abundances (here we assume that it is measured in terms of biomass/spatial unit), and the model functions $G(X)$ and $f(X,Y)$ are specific rates and their shapes determine the type of prey growth (r_x is, in general, the maximum specific growth rate of the prey) and predation processes, respectively. The parameters b is the maximum specific rate of prey consumption, m is the specific rate of predator mortality, c is a conversion factor which measures the conversion efficiency from prey to predator biomass; K_0 is a reference biomass, P_0 and H_0 are adimensional parameters: P_0 denotes the predation efficiency and H_0 is a measure of the predator interference process. Let

$$x = \frac{X}{K^+}, \qquad y = \frac{Y}{K^+}, \qquad p = P_0\frac{K^+}{K_0}, \qquad h = H_0\frac{K^+}{K_0},$$

then the previous system can be rewritten in terms of adimensional variables (and considering also the initial conditions)

$$\begin{cases} \dfrac{dx}{dt} = r_x x g\left(x\right) - byf\left(\dfrac{px}{1+hy}\right) \\ \dfrac{dy}{dt} = cbyf\left(\dfrac{px}{1+hy}\right) - my \\ x(0) = \tilde{x}, \quad y(0) = \tilde{y}, \end{cases} \tag{2.1}$$

where p and h are adimensional parameters referred to as predation efficiency and predator interference during the predation process. The functions $g(\cdot)$ and $f(\cdot)$ should satisfy some regularity and general assumptions dictated by biological considerations. It is assumed that

$$\exists\, \epsilon: \ 0 < \epsilon < 1, \ g(\epsilon) = g(1) = 0; \quad g(s)(s-\epsilon)(1-s) > 0, \ \ s \neq \epsilon, 1; \tag{2.2}$$

$$f(0) = 0, \qquad \lim_{s\to+\infty} f(s) = 1, \qquad f'(s) > 0, \ s > 0. \tag{2.3}$$

Hereafter the prime indicates the derivative with respect to the argument. The assumption (2.2) implies that the function g has only two zeroes, ϵ and 1, that it is positive when $\epsilon < x < 1$ and negative when $0 < x < \epsilon$ or $x > 1$. The parameter ϵ is the ratio between minimum and maximum population size

$$\epsilon = K^-/K^+,$$

so that it represent the minimum population size, while 1 is the carrying capacity of the adimensional system. With these assumptions, such g is suitable to model a strong

Allee effect (according to [7, 19, 42, 65, 91, 94]). With the assumption (2.3) we are taking into account the saturation in the predation process. Moreover, some further technical assumptions on the smoothness of these functions are required to limit the number of equilibrium states of (2.1) and to make the stability analysis tractable. We will assume: just one maximum when $g(s)$ is positive, just one inflection point of $sg(s)$ when $g(s)$ is positive and increasing, a weaker than negative convexity when $g(s)$ is positive and decreasing, and a weaker than negative convexity for $f(s)$. These conditions can be written as

$$\exists\, \xi_0 :\ \epsilon < \xi_0 < 1,\ g(\xi_0) = 1,\ g'(\xi_0) = 0;\ g'(s)(\xi_0 - s) > 0,\ \epsilon < s < 1,\ s \neq \xi_0, \tag{2.4}$$

$$\exists\, \eta_0 :\ \epsilon < \eta_0 < \xi_0,\ [sg(s)]''_{s=\eta_0} = 0,\ [sg(s)]''\,(\eta_0 - s) > 0,\ \epsilon < s < \xi_0,\ s \neq \eta_0; \tag{2.5}$$

$$[sg'(s)]' < 0, \quad \xi_0 < s \leq 1; \tag{2.6}$$

$$\left[\frac{f(s)}{s}\right]' < 0, \qquad s > 0. \tag{2.7}$$

Remarks.

(I) Condition (2.4) on the prey-growth function requires that only one maximum point ξ_0 exists in $(0, 1)$ (where the function is positive). Then, the function $g(s)$ is normalized so that $g(\xi_0) = 1$, in order to have r_x as the maximum specific growth rate. This means that there is an optimal population size corresponding to a maximum rate of growth r_x: for value smaller than ξ_0, the individual could be very few and too sparse, while for greater values the competition for resources becomes evident.

(II) The expression in conditions (2.5) and (2.6) can be written as

$$[sg(s)]'' = \frac{1}{s}\left[s^2 g'(s)\right]' = 2g'(s) + sg''(s), \qquad [sg'(s)]' = g'(s) + sg''(s).$$

Thus, for $\xi_0 < s \leq 1$, namely when $g(s)$ is positive and decreasing, condition (2.6) is stronger than (2.5). Moreover, these conditions allow the function $sg(s)$ to have an inflection point in (ε, ξ_0), which is fundamental for the description of the Allee effect. Then, they could be considered as the minimal assumptions on the growth function to describe a strong Allee effect.

(III) Conditions (2.6) and (2.7) are weaker than $g''(s) < 0$ and $f''(s) < 0$, respectively. In fact, when $g'(s) < 0$, as it is in the interval $(\xi_0, 1]$, we have that

$g''(s) < 0 \Rightarrow \ [sg'(s)]' < 0$. Furthermore, it can be proved that conditions (2.3) and (2.7) implies that the function f does not have any inflection point, and f has negative concavity. This excludes for instance the Holling-type III trophic function. Since the argument of this function is $px/(1+hy)$, this means that for small prey densities or large number of predators, either the case in which the predator has an alternative source of food or the prey has a number of shelters inaccessible to the predator are excluded [13].

The required properties (2.2)-(2.7) are fulfilled for instance by the following model functions, widely used in literature (see references in [25]):

Prey growth:

$$g(s) = g_0(s-\epsilon)(1-s), \tag{2.8}$$

$$g(s) = g_0\left(s\exp\left(\frac{1-s}{\xi_0}\right)-1\right), \tag{2.9}$$

Trophic Functions:

$$f(s) = \frac{s}{1+s}, \tag{2.10}$$

$$f(s) = 1-\exp(-s), \tag{2.11}$$

where g_0 is such that $g(\xi_0) = 1$ (namely, $g_0 = 4/(1-\epsilon)^2$ in (2.8) and $g_0 = [\xi_0 \exp((1-\xi_0)/\xi_0)-1]^{-1}$ in (2.9), with $\xi_0 = -(1-\epsilon)/\log\epsilon$). The function (2.8) is the Gilpin model [42], (2.9) is from [25], (2.10) is the Holling-type II trophic function [55] and (2.11) is the Ivlev model [58, 86]. It is worth noticing that, choosing the expression (2.10) for the trophic function f leads to the Beddington-DeAngelis functional response:

$$f\left(\frac{px}{1+hy}\right) = \frac{px}{1+px+hy}.$$

2.2 Attractive invariant set

We are interested in positive solutions to (2.1). It is possible to show that all solutions initiating in $\mathbb{R}_2^+$ are bounded and eventually enter an attracting set, that it is shown in Figure 2.1.

Theorem 2.1. *Under the assumptions* (2.2) *and* (2.3) *the closed set*

$$\Omega = \left\{(x,y) \in \mathbb{R}_2^+ \mid \ 0 \le x \le 1,\, 0 \le x + \frac{y}{c} \le 1 + \frac{r_x}{m}\right\}$$

is positively invariant, and for all initial states $\tilde{E} = (\tilde{x}, \tilde{y}) \in \mathbb{R}_2^+$ *the trajectory* $(x(t), y(t))$ *eventually enters into* Ω *as* $t \to +\infty$.

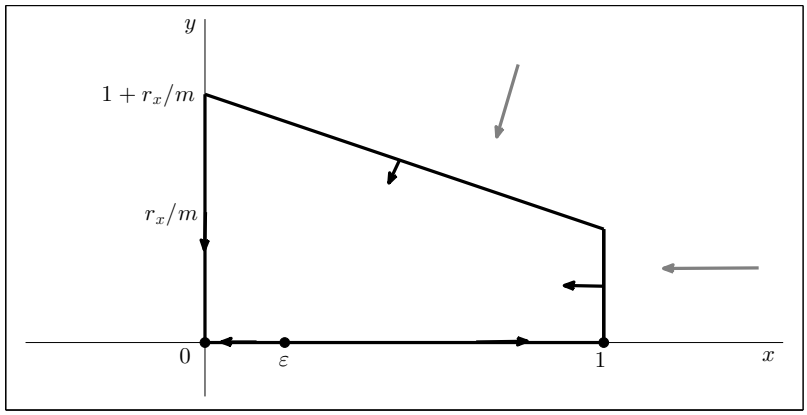

Fig. 2.1. Positively invariant and attractive set for system (2.1).

Proof. The proof is a straightforward application of the comparison theorem for ODE's and makes use of suitable bounds for the right hand side of (2.1) [38].

First, we have that the axes are trajectories, then they can not be crossed; this ensures that the solutions starting from positive initial conditions remain positive. In particular, if we choose an initial conditions on the y-axis, the first equation of (2.1) reduces to $\dot{x} = 0$ and the second to $\dot{y} = -my$; then, the y-axis is a trajectory pointing towards the origin. Analogously, if we choose an initial condition on the x-axis, the second equation of (2.1) reduces to $\dot{y} = 0$ and the first to $\dot{x} = r_x x g(x)$; then, the positive x-axis is an union of three trajectories, separated by three stationary states $x = 0,\ x = \varepsilon,\ x = 1$.

Consider now $(x(t), y(t))$ solution of (2.1) with initial condition $x(0) = x_0 > 0$ and $y(0) = y_0 > 0$. Due to the positivity of y and assumption (2.3), we have that

$$\dot{x} = r_x x g(x) - byf\left(\frac{px}{1+hy}\right) \leq r_x x g(x).$$

We can consider the reduced system

$$\begin{cases} \dot{\bar{x}} = r_x \bar{x} g(\bar{x}) \\ \bar{x}(0) = \bar{x}_0, \end{cases} \tag{2.12}$$

for which $\bar{x}(t) = 1$ is a stationary solution. Therefore, if $0 < \bar{x}_0 < 1$ then $0 < \bar{x}(t) < 1$. Thanks to the comparison theorem for ODE's applied to system (2.12) and

$$\begin{cases} \dot{x} = r_x x g(x) - byf\left(\dfrac{px}{1+hy}\right) \\ x(0) = \bar{x}_0, \end{cases} \tag{2.13}$$

with $0 < x(t) \leq \bar{x}_0 < 1$ and where y is thought as a positive parameter; it follows that $0 < x(t) < 1$ if $0 < x_0 < 1$.

Consider now initial data (x_0, y_0) such that

$$x_0 + \frac{y_0}{c} \leq 1 + \frac{r_x}{m},$$

and a linear combinations of the differential equations of (2.1) for which we have

$$\dot{x} + \frac{\dot{y}}{c} = r_x x g(x) - m\frac{y}{c} \pm mx = x(r_x g(x) + m) - m\left(x + \frac{y}{c}\right).$$

Because $0 < x < 1$ and $0 < g(x) < 1$, we have

$$\dot{x} + \frac{\dot{y}}{c} + m\left(x + \frac{y}{c}\right) = x(r_x g(x) + m) \leq m\left(\frac{r}{m} + 1\right).$$

Putting $z = x + y/c$ (then $z_0 = x_0 + y_0/c$), we obtain that

$$\dot{z} + mz \leq m\left(\frac{r_x}{m} + 1\right)$$

which can be multiplied by e^{mt} and integrated from 0 to τ; we obtain

$$\int_0^\tau \dot{z} + mze^{mt}dt \leq m\left(\frac{r_x}{m} + 1\right)\int_0^\tau e^{mt}dt$$

or equivalently

$$\int_0^\tau \frac{d}{dt}(ze^{mt})dt \leq \left(\frac{r_x}{m} + 1\right)\int_0^\tau \frac{d}{dt}(e^{mt})dt.$$

Then we have (substituting τ with t)

$$z \leq z_0 e^{-mt} + \left(\frac{r_x}{m} + 1\right)(1 - e^{-mt}) = e^{-mt}\left[z_0 - \left(\frac{r_x}{m} + 1\right)\right] + \left(\frac{r_x}{m} + 1\right) \leq \left(\frac{r_x}{m} + 1\right).$$

Therefore, we have that

$$0 \leq z(t) = x(t) + \frac{y(t)}{c} \leq \left(\frac{r_x}{m} + 1\right)$$

which conclude the proof of the positively invariance of Ω.

We want to prove that Ω is also an attractive set. Let now choose initial data $(x_0, y_0) \in \mathbb{R}^2_+ - \Omega$. Looking at(2.12), we observe that $\dot{\bar{x}} < 0$ when $\bar{x} > 1$; then we fix $\bar{x}(0) = \bar{x}_0 > 1$, so its solution decreases and then has a limit. Necessarily, because $\bar{x} = 1$ is a stationary solution of (2.12), we have

$$\lim_{t \to +\infty} \bar{x}(t) = 1.$$

Applying the comparison theorem for ODE's to systems (2.12) and (2.13) with $\bar{x}_0 \geq x_0 > 1$ we have

$$\lim_{t \to +\infty} x(t) = \lim_{t \to +\infty} \bar{x}(t) = 1.$$

Analogously, thanks to the comparison theorem for ODE's applied to systems

$$\begin{cases} \dot{x} + \dfrac{\dot{y}}{c} = -m\left(x + \dfrac{y}{c}\right) + mx\left(\dfrac{r}{m} + 1\right) \\ x(0) + \dfrac{y(0)}{c} = x_0 + \dfrac{y_0}{c} \end{cases}$$

and

$$\begin{cases} \dot{\bar{x}} + \dfrac{\dot{\bar{y}}}{c} = -m\left(\bar{x} + \dfrac{\bar{y}}{c}\right) + m\bar{x}\left(\dfrac{r}{m} + 1\right) \\ \bar{x}(0) + \dfrac{\bar{y}(0)}{c} = \bar{x}_0 + \dfrac{\bar{y}_0}{c} \end{cases}$$

with

$$\bar{x}_0 + \frac{\bar{y}_0}{c} \geq x_0 + \frac{y_0}{c} \geq \left(\frac{r}{m} + 1\right),$$

we obtain that

$$\lim_{t \to +\infty} x(t) + \frac{y(t)}{c} = \lim_{t \to +\infty} \bar{x}(t) + \frac{\bar{y}(0)}{c} = \left(\frac{r}{m} + 1\right).$$

□

2.3 Non-coexistence equilibria and their stability properties

The existence and stability analysis of the non-negative equilibrium states $E = (x_{eq}, y_{eq})$ for the system (2.1) is performed assuming the parameters h and p as bifurcation parameters, while the remaining parameters are fixed.

For any $h \geq 0$ and $p > 0$, the system admits as equilibrium states the null state $E_0 = (0,0)$ and, under the assumptions (2.2) on $g(\cdot)$, two non-coexistence states:

$$E_\epsilon = (\epsilon, 0), \qquad E_1 = (1,0).$$

Let r_y be the maximum specific growth rate of the predator. From (2.1) and (2.3) we have that

$$r_y = cb - m = cb(1-\alpha), \quad \text{with} \quad \alpha = \frac{m}{cb}. \tag{2.14}$$

If $r_y < 0$, i.e. $\alpha > 1$, then $y'(t) < 0$ for any $x,\ y > 0$. Thus, coexistence equilibrium states cannot exist. $y(t)$ is always decreasing and, as $t \to +\infty$, it can be easily seen that $(x(t), y(t))$ converges to either E_0 or E_1, depending on the initial conditions. In the following, we will assume $r_y > 0$, i.e.

$$\alpha < 1. \tag{2.15}$$

In this case, the following implication holds

$$r_y > 0 \quad \Longrightarrow \quad \exists\, p_0 = f^{-1}(\alpha) > 0, \tag{2.16}$$

and p_0 turns out to be a critical value of p for the existence and stability of the equilibrium states associated with (2.1). It depends only on the ratio α: $p_0 = p_0(\alpha)$, and we have

$$\frac{dp_0}{d\alpha} > 0, \quad p_0(0) = 0, \quad \lim_{\alpha \to 1} p_0(\alpha) = +\infty.$$

According to the Hartman-Grobman Theorem [80], the local stability properties of the equilibrium states E_ι, $\iota = 0, \epsilon, 1$, are determined by the analysis of the eigenvalues of the Jacobian matrix associated with system (2.1)

$$J(x,y) = \begin{pmatrix} r_x g(x) + r_x x g'(x) - bp\, u f'(pv) & -bf(pv) + bph\, uv f'(pv) \\ \\ cbp\, u f'(pv) & cbf(pv) - m - cbph\, uv f'(pv) \end{pmatrix}$$

where

$$u = \frac{y}{1+hy}, \quad v = \frac{x}{1+hy},$$

and evaluated in E_ι. We obtain

$$J(0,0) = \begin{pmatrix} r_x g(0) & 0 \\ \\ 0 & -m \end{pmatrix}, \qquad J(\epsilon,0) = \begin{pmatrix} r_x g'(\epsilon) & -bf(p\epsilon) \\ \\ 0 & cbf(p\epsilon) - m \end{pmatrix},$$

$$J(1,0) = \begin{pmatrix} r_x g'(1) & -bf(p) \\ \\ 0 & cbf(p) - m \end{pmatrix}.$$

Thanks to (2.2), the matrix $J(0,0)$ has two negative eigenvalues independent of the values of the parameters h and p. From (2.4), it follows that $g'(\epsilon) > 0$ and $g'(1) < 0$, so that $J(\epsilon, 0)$ and J(1,0) have a positive and a negative eigenvalue respectively; assuming that $r_y > 0$ so that (2.16) holds, we have that

$$\begin{aligned} cbf(p\epsilon) - m > 0 \quad &\Longleftrightarrow \quad p > \frac{p_0}{\epsilon}, \\ cbf(p) - m > 0 \quad &\Longleftrightarrow \quad p > p_0. \end{aligned}$$

Thus, the classification of the non-coexistence equilibrium states is the following:

E_0 is a locally stable node for any $p > 0$;

E_ϵ is always unstable: it is a saddle for $p < p_0/\epsilon$ (with unstable manifold $W_u(E_\epsilon)$ lying on the x-axis), and an unstable node for $p > p_0/\epsilon$;

E_1 is a locally stable node for $p < p_0$, and a saddle for $p > p_0$ (with stable manifold $W_s(E_1)$ lying on the x-axis).

It is worth noticing that the eigenvalues, and then the stability properties of the non-coexistence states, turn out to be independent of h. Moreover, it follows that the stability properties of E_0 and E_ϵ are independent of p, while those of E_1 depend on p.

2.4 Coexistence equilibria

Coexistence equilibrium states $E_*(h,p) = (x_*(h,p), y_*(h,p))$ are found as the solutions of

$$\begin{cases} r_x x g(x) - byf\left(\dfrac{px}{1+hy}\right) = 0 \\ cbf\left(\dfrac{px}{1+hy}\right) - m = 0, \end{cases}$$

such as the intersections of the nullclines of system (2.1), written as

$$y = \beta x g(x), \qquad f\left(\frac{px}{1+hy}\right) = \alpha, \tag{2.17}$$

where

$$\beta = \frac{r_x c}{m}.$$

It is worth noticing that the first nullcline in (2.17) is a humped curve in the phase plane, which is independent of parameters h and p. Under the assumption (2.15) and the definition (2.16) of p_0, we have that the second nullcline in (2.17) is the straight line

$$\frac{p}{p_0}x = 1 + hy,$$

whose position and slope depend on both parameters h and p. Substituting y from the first equation in (2.17), we obtain the equation for x

$$\frac{p}{p_0} = \phi(x,h) := \frac{1}{x} + h\beta g(x). \tag{2.18}$$

We are interested in solutions to (2.18) $x_*(h,p) \in (\epsilon, 1)$, in order to have $y_*(h,p) > 0$. In fact, from the assumption (2.2), $g(x) > 0$ only in $(\epsilon, 1)$ and this implies that $p > p_0$. In the following we will assume $h > 0$. The case $h = 0$ has been studied in detail in [25].

2.4.1 Shape of $\phi(x,h)$

The shape of $\phi(x,h)$, and consequently the number of solutions to (2.18) in $(\epsilon, 1)$, strongly depends on the parameter h. We have

$$\frac{\partial \phi}{\partial x} = \frac{1}{x^2}\left[-1 + h\psi(x)\right], \quad \text{with} \quad \psi(x) = \beta x^2 g'(x), \tag{2.19}$$

and

$$\frac{\partial \phi}{\partial h} = \beta g(x) > 0, \quad x \in (\epsilon, 1). \tag{2.20}$$

From the assumption (2.4), $g'(x) < 0$, and then $\partial\phi/\partial x < 0$, for $x \in (\xi_0, 1)$. Thus, $\phi(x,h)$ may be non-monotonic, with respect to x, only when $x \in (\epsilon, \xi_0)$ and $h \neq 0$. The points where $\partial\phi/\partial x = 0$ are solutions of the equation

$$\psi(x) = \frac{1}{h}, \quad h > 0. \tag{2.21}$$

We have $\psi(\epsilon) > 0$, $\psi(\xi_0) = 0$, and, from the assumption (2.5), $\psi(x)$ has only one maximum η_0 for $x \in (\epsilon, \xi_0)$. According to the shape of $\psi(x)$ (Figure 2.2) in (ϵ, ξ_0), it follows that there are two solutions for equation (2.21) when $\psi(\epsilon) \leq 1/h < \psi(\eta_0)$, and one solution when $1/h < \psi(\epsilon)$. Let η_1 be the unique point in the range (η_0, ξ_0) such that $\psi(\eta_1) = \psi(\epsilon)$. Let us define

$$h_0 = \frac{1}{\psi(\eta_0)}, \quad h_1 = \frac{1}{\psi(\epsilon)}$$

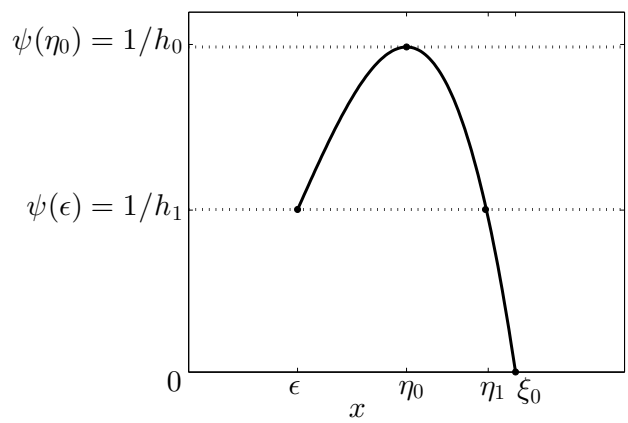

Fig. 2.2. Shape of the function $\psi(x)$.

and denote with $\xi_1(h)$ and $\xi_2(h)$ the two possible solutions to equation (2.21) ($\xi_2(h)$ exists only for $h_0 \leq h \leq h_1$, $\xi_1(h)$ for $h \geq h_0$). In Table 2.1 we summarize the results about the number of solutions to (2.21). From (2.21) it follows also that the two

h	number of solutions to $\partial\phi/\partial x = 0$	position on the x axis
$0 \leq h < h_0$	0	
$h = h_0$	1	$\xi_2(h_0) = \eta_0 = \xi_1(h_0)$
$h_0 < h < h_1$	2	$\epsilon < \xi_2(h) < \eta_0 < \xi_1(h) < \eta_1$
$h = h_1$	2	$\epsilon = \xi_2(h_1) < \eta_0 < \xi_1(h_1) = \eta_1$
$h > h_1$	1	$\eta_1 < \xi_1(h) < \xi_0$

Table 2.1. Number of solutions $\xi_j(h)$ to equation (2.21), and their positions on the x axis, for different ranges of h.

functions $\xi_1(h)$ and $\xi_2(h)$ are monotonic

$$\frac{d\xi_1}{dh} > 0 \quad h \geq h_0, \qquad \frac{d\xi_2}{dh} < 0 \quad h_0 \leq h \leq h_1$$

and, moreover, $\lim_{h \to +\infty} \xi_1(h) = \xi_0$. Let

$$\phi_0 = \phi(\eta_0, h_0), \qquad \phi_j(h) = \phi(\xi_j(h), h), \quad j = 1, 2.$$

From the expression of $\partial\phi/\partial x$ and $\psi(x)$ given in (2.19), we have that $\xi_2(h)$ is a local minimum and $\xi_1(h)$ is a local maximum of $\phi(x,h)$. Since $\xi_2(h) < \xi_1(h)$, it follows that

$$\phi_2(h) < \phi_1(h).$$

Since

$$\frac{\partial\phi}{\partial h} > 0, \quad \left(\frac{\partial\phi}{\partial x}\right)_{x=\xi_j} = 0,$$

from

$$\frac{d\phi_j}{dh} = \left(\frac{\partial\phi}{\partial h}\right)_{x=\xi_j} + \left(\frac{\partial\phi}{\partial x}\right)_{x=\xi_j} \frac{d\xi_j}{dh}$$

it follows that $\phi_j(h)$ are monotonic: $d\phi_j/dh > 0$. Moreover,

$$1 < \phi_0 = \frac{1}{\eta_0} + \beta h_0 g(\eta_0) = \phi_1(h_0) = \phi_2(h_0) < \frac{1}{\epsilon}, \quad \phi_1(h_1) > \phi_2(h_1) = \frac{1}{\epsilon},$$

and

$$\phi_1(h) > \phi(\xi_0, h), \quad \phi_1(h) \to \phi(\xi_0, h) = \beta h + \frac{1}{\xi_0} \quad \text{as} \quad h \to +\infty.$$

Lastly, $\phi_1(h)$ may be greater or less than $1/\epsilon$ for $h_0 < h < h_1$. Let h_ϵ be the unique solution to the equation $\phi_1(h) = 1/\epsilon$. Now we are able to plot the qualitative shape of $\phi(x,h)$ for $x \in (\epsilon, 1)$ and different ranges of h (Figure 2.3). This figure is representative of the qualitative behaviours of $\phi(x,h)$ (defined in (2.18)) with $g(x)$ satisfying the properties (2.2), (2.4), (2.5) and (2.6). The function $\phi(x,h)$, strictly increasing in h, when $0 \le h < h_0$ (Figure 2.3(a)) is strictly decreasing in x; when $h_0 < h < h_1$ (Figures 2.3(b), 2.3(c)), it shows a local minimum for x between ϵ and η_0 and a local maximum for x between η_0 and 1; finally, when $h > h_1$ (Figure 2.3(d)), $\phi(x,h)$ has only a local maximum.

2.4.2 Solutions to $\phi(x,h) = p/p_0$

Taking into account the results of the previous subsection, we can determine the ranges of p/p_0 for which we have solutions to (2.18), with $x \in (\epsilon, 1)$, in the various intervals of the parameter h in which $\phi(x,h)$ shows different trends versus x (Figure 2.3). For $0 \le h < h_0$ we have one solution to (2.18). For $h_0 < h < h_1$ we may have from one to three solutions; in Figure 2.4 we illustrate the positions of the local minimum and maximum of $\phi(x,h)$ with respect to $1/\epsilon$, which determine the regions in the parameter space (h,p) of existence of the solutions to (2.18). In detail, for $0 < h < h_0$ we have only one solution to (2.18) independent of the value of p, as it

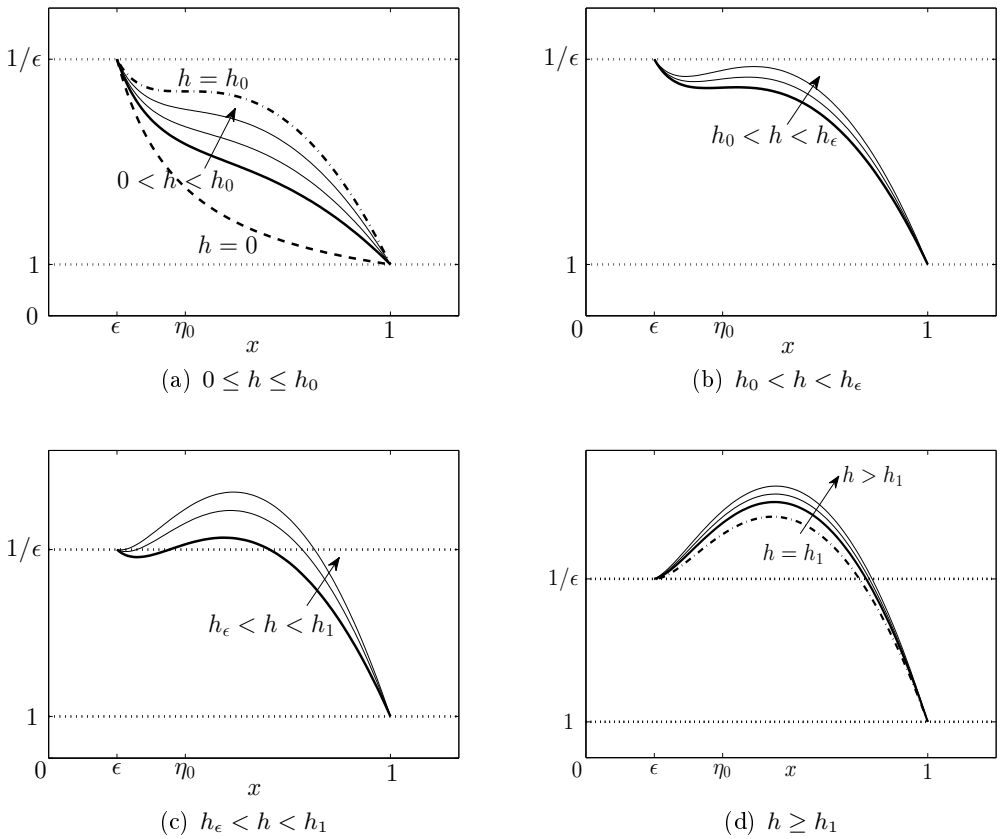

Fig. 2.3. Trend of $\phi(x,h)$ for $x \in (\epsilon, 1)$ and different values of h. The arrows indicate the direction of increasing h.

can be seen in Figure 2.4(a) related to the scenario sketched in Figure 2.3(a). Figure 2.4(b) represents the scenario for $h_0 < h < h_\epsilon$ sketched in Figure 2.3(b), where for increasing p from p_0 to p_0/ϵ, $p \neq p_0\phi_i$, $i = 1, 2$, we can have one, three, one equilibria. Figure 2.4(c) represents instead the situation for $h_\epsilon < h < h_1$ sketched in Figure 2.3(c), where for increasing p from p_0 to $p_0\phi_1$, $p \neq p_0\phi_2$, we can have one, three, two equilibria. For $h > h_1$ we may have one or two solutions to (2.18) depending on the value of p/p_0 compared to $1/\epsilon$, as it can be seen in Figure 2.4(d) related to the scenario sketched in Figure 2.3(d). The results are collected in the following Table 2.2 and shown in Figure 2.6.

In the parameter space (h, p) (Figure 2.6) the curves $p = p_0\phi_1(h)$, $h \in (h_0, h_\epsilon)$, and $p = p_0\phi_2(h)$, $h \in (h_0, h_1)$, are stationary bifurcation curves. For $h \in (h_0, h_1)$ and increasing p from p_0, when $p = p_0\phi_2(h)$ the states E_{*2} and E_{*3} appear, but

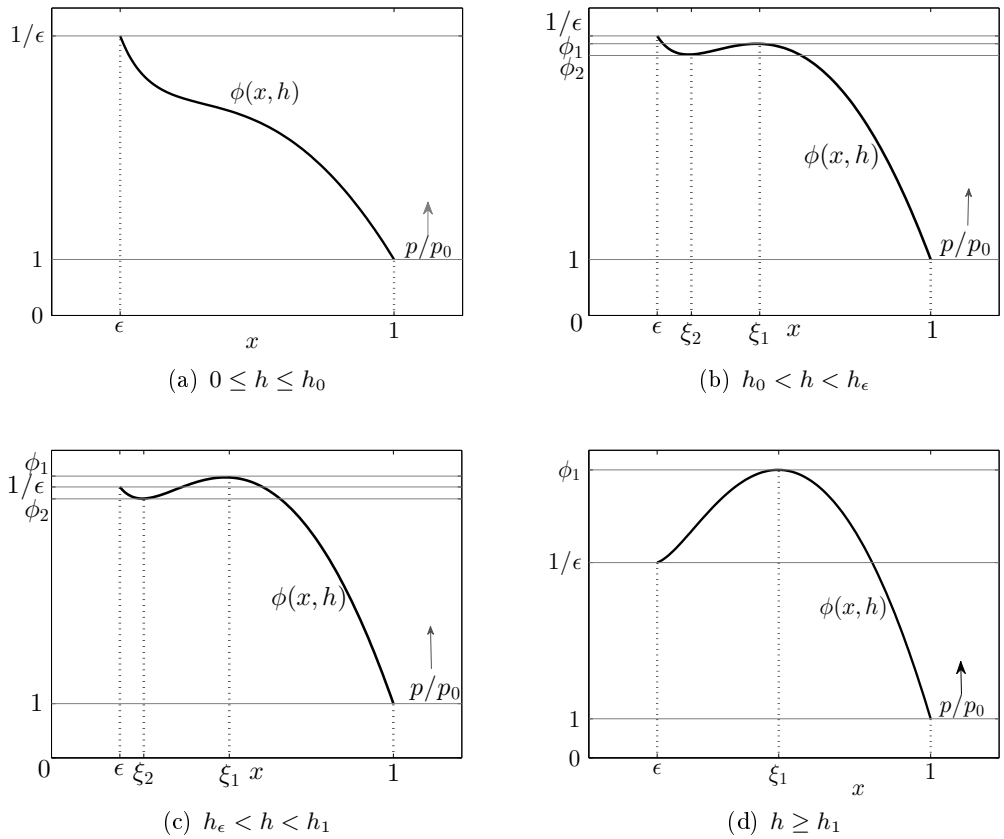

Fig. 2.4. Solutions to $\phi(x,h) = p/p_0$ for $x \in (\epsilon, 1)$.

they do not collide with E_{*1}. Otherwise, when $p = p_0\phi_1(h)$ the states E_{*1} and E_{*2} collide and disappear, but do not collide with E_{*3}. On these curves the determinant of the Jacobian matrix $J(E_{*j}(h,p))$ associated with (2.1) is zero when evaluated at the colliding equilibria (it will be shown in Section 2.5). This behaviour is typical of a saddle-node bifurcation. In addition, the two bifurcation curves $p = p_0\phi_1(h)$ and $p = p_0\phi_2(h)$ intersect at the critical point $B_0 = (h_0, p_0\phi_0)$, the unique one in the parameter space where the three equilibrium states coincide. At this point, the two bifurcation curves share a common tangent, since $x_{*j} = \eta_0,\ j = 1,2,3$ and, from (2.20), $\partial\phi_1/\partial h = \partial\phi_2/\partial h = \beta g(\eta_0)$; then B_0 is a mathematical cusp in the (h,p) plane. Moreover, we notice that at point B_0 we have, from (2.19),

$$\frac{\partial\phi}{\partial x}(x_{*j}, h_0) = 0 \quad \text{and} \quad \frac{\partial^2\phi}{\partial x^2}(x_{*j}, h_0) = 0.$$

h	p/p_0	number of solutions to $\phi = p/p_0$	position on the x axis
$0 \le h < h_0$	$1 < p/p_0 < 1/\epsilon$	1	$\epsilon < x_{*1} < 1$
$h = h_0$	$1 < p/p_0 < \phi_0$	1	$\eta_0 < x_{*1} < 1$
	$p/p_0 = \phi_0$	1	$\eta_0 = x_{*1} = x_{*2} = x_{*3}$
	$\phi_0 < p/p_0 < 1/\epsilon$	1	$\epsilon < x_{*1} = x_{*3} < \eta_0$
$h_0 < h < h_\epsilon$	$1 < p/p_0 < \phi_2$	1	$\xi_1 < x_{*1} < 1$
	$p/p_0 = \phi_2$	2	$x_{*3} = x_{*2} = \xi_2 < \xi_1 < x_{*1}$
	$\phi_2 < p/p_0 < \phi_1$	3	$\epsilon < x_{*3} < \xi_2 < x_{*2} < \xi_1 < x_{*1} < 1$
	$p/p_0 = \phi_1$	2	$x_{*3} < \xi_2 < x_{*2} = x_{*1} = \xi_1$
	$\phi_1 < p/p_0 < 1/\epsilon$	1	$\epsilon < x_{*3} < \xi_2$
$h_\epsilon < h < h_1$	$1 < p/p_0 < \phi_2$	1	$\xi_1 < x_{*1} < 1$
	$p/p_0 = \phi_2$	2	$x_{*3} = x_{*2} = \xi_2 < \xi_1 < x_{*1}$
	$\phi_2 < p/p_0 < 1/\epsilon$	3	$\epsilon < x_{*3} < \xi_2 < x_{*2} < \xi_1 < x_{*1} < 1$
	$1/\epsilon < p/p_0 < \phi_1$	2	$\xi_2 < x_{*2} < \xi_1 < x_{*1} < 1$
	$p/p_0 = \phi_1$	1	$x_{*2} = x_{*1} = \xi_1$
$h \ge h_1$	$1 < p/p_0 \le 1/\epsilon$	1	$\xi_1 < x_{*1} < 1$
	$1/\epsilon < p/p_0 \le \phi_1$	2	$\epsilon < x_{*2} \le \xi_1 \le x_{*1} < 1$
	$p/p_0 = \phi_1$	1	$x_{*2} = x_{*1} = \xi_1$

Table 2.2. Ranges of p/p_0 for the existence of solutions $x_{*j} = x_{*j}(h,p) \in (\epsilon, 1)$ to equation (2.18), their number, and their positions on the x axis, depending on h; $\phi_j = \phi_j(h)$, $\xi_j = \xi_j(h)$.

All these results indicate the presence of a cusp singularity, according to Whitney's theory [12], for the equilibrium surface implicitly defined by $p = p_0\phi(x,h)$ and shown in Figure 2.5 in the three dimensional space (h,p,x). The projection on the (h,p) plane of such surface can be seen if Figure 2.6, while the level sets in the (x,p) plane for fixed h can be deduced from Figure 2.3, or equivalently from Figure 2.7. In Appendix B more detail about the detected cusp bifurcation point are reported.

In the (h,p) plane the lines

$$\frac{p}{p_0} = 1, \qquad \frac{p}{p_0} = \frac{1}{\epsilon}, \qquad \frac{p}{p_0} = \phi_j(h),\ j = 1,2$$

are boundary lines of existence regions (Figure 2.6) for the coexistence equilibrium states $E_{*j}(h,p) = (x_{*j}(h,p), y_{*j}(h,p))$.

For $x_{*j} \neq \xi_1(h), \xi_2(h)$, from equation (2.18) it follows that

$$\frac{\partial x_{*j}}{\partial h} = -\beta g(x_{*j}) \left(\frac{\partial \phi}{\partial x}\right)^{-1}_{x_{*j}}, \qquad \frac{\partial x_{*j}}{\partial p} = \left(p_0 \frac{\partial \phi}{\partial x}\right)^{-1}_{x_{*j}}.$$

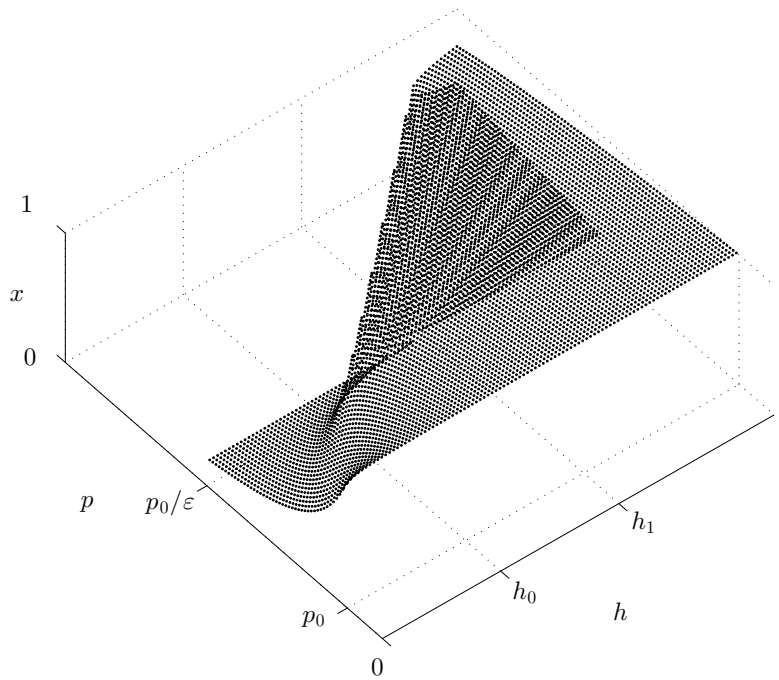

Fig. 2.5. View of the equilibrium surface $p = p_0\phi(x,h)$ in the (h,p,x) space; the level sets of such surface in the (x,p) plane for fixed h can be deduced from Figure 2.3.

Since $(\partial\phi/\partial x)$ is negative for $x = x_{*1},\ x_{*3}$ and positive for $x = x_{*2}$, we have the following monotonicity properties for x_{*j}:

$$\frac{\partial x_{*j}}{\partial h} > 0, \qquad \frac{\partial x_{*j}}{\partial p} < 0,\ j = 1,3; \qquad \frac{\partial x_{*2}}{\partial h} < 0, \qquad \frac{\partial x_{*2}}{\partial p} > 0.$$

The bifurcation process is described in detail in the bifurcation diagrams (Figure 2.7), where x_{*j} are reported versus p for different values of h, corresponding to the four different ranges of h of Figure 2.3. With reference also to Figure 2.6, we can see in detail in Figure 2.7 how the equilibrium states collide and disappear. In all subplots transcritical bifurcation points, marked with BP, are located on the lines $p = p_0$ and $p = p_0/\epsilon$ of Figure 2.6; saddle-node bifurcation points (LP) lie on the curves $p = p_0\phi_1(h)$ and $p = p_0\phi_2(h)$.

The coexistence equilibrium states, when they exist, lie on the curve $y = \beta x g(x),\ x \in (\epsilon, 1)$, in the phase space. Obviously, their number and their position depend on the parameters h and p, and their behaviour is determined by the

trends of $x_{*j}(h,p),\ j=1,2,3$, versus h and p.

Remark.

(IV) On the boundary line $h=h_0,\ p\in(p_0\phi_0, p_0/\epsilon)$ (Figure 2.6) the determinant of $J(E_{*1}(h,p))$ is positive (see Section 2.5), and therefore it is not a local bifurcation line. On this line, the trend of x_{*1} versus p is reported in Figure 2.7(a) and shows an inflection point with vertical tangent at $p=p_0\phi_0$. When $p_0\phi_0<p<p_0/\epsilon$, we have that

$$\lim_{h\to h_0^+} E_{*3}(h,p)=\lim_{h\to h_0^-} E_{*1}(h,p),$$

namely the equilibria swap names; this line has been introduced in order to allow a smooth transition of the equilibrium E_{*3}, instead of an abrupt change from E_{*3} to E_{*1}, on the bifurcation line $p=p_0\phi_1(h)$ (see Figure 2.7(b)).

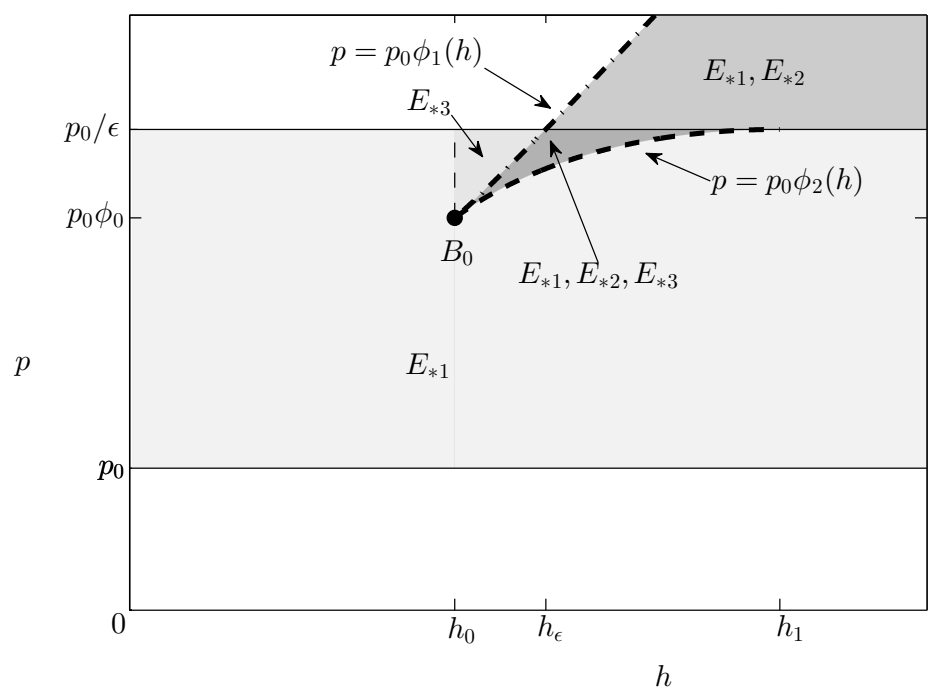

Fig. 2.6. Existence regions of coexistence equilibrium states in the (h,p) plane, displayed in grey; a different shade denotes a different number of equilibria lying in the region.

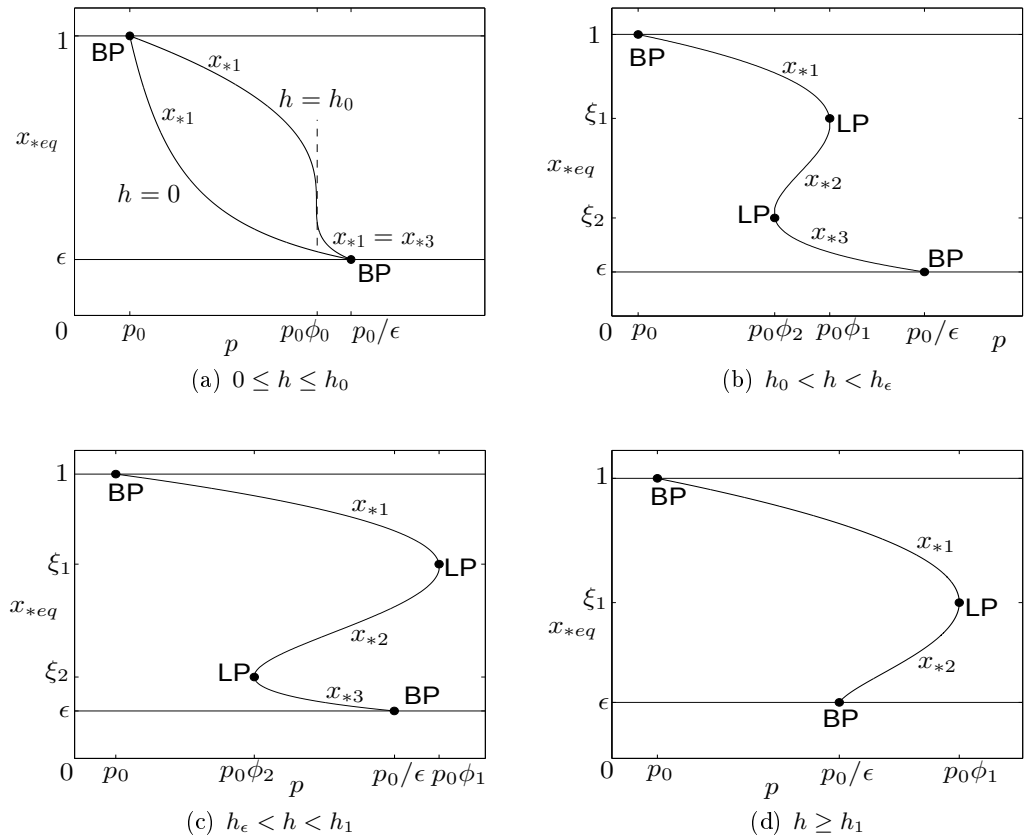

Fig. 2.7. Qualitatively trend of x_{*j} versus p for different values of h. BP: transcritical bifurcation, LP: saddle-node bifurcation.

2.5 Stability properties of coexistence equilibrium states

We want now study the stability properties of the coexistence equilibrium states found in the previous Section. Let $E_*(h,p) = (x_*(h,p), y_*(h,p))$ be a generic coexistence equilibrium state. We recall that $x_*(h,p)$ and $y_*(h,p)$ satisfy the relations (2.17), that are

$$y_* = \beta x_* g(x_*), \quad \frac{p x_*}{1 + h y_*} = p_0, \quad f\left(\frac{p x_*}{1 + h y_*}\right) = \alpha, \qquad \alpha = \frac{m}{cb}, \quad \beta = \frac{r_x c}{m},$$

with $x_* = x_*(h,p)$. We define

$$\mu_0 := \mu(p_0), \quad 0 < \mu_0 < 1,$$

where $\mu(s) = sf'(s)/f(s)$ (its properties are discussed in appendix A). From the expression of the Jacobian matrix displayed in Section 2.3, we can simplify the entries of the Jacobian matrix evaluated at $E_*(h,p)$:

$$\begin{aligned}
J_{11}(E_*(p,h)) &= r_x g(x_*) + r_x x_* g'(x_*) - b\frac{py_*}{1+hy_*} f'\left(\frac{px_*}{1+hy_*}\right) \\
&= r_x g(x_*) + r_x x_* g'(x_*) - by_* \frac{p_0 f'(p_0)}{f(p_0)} \frac{f(p_0)}{x_*} \\
&= r_x g(x_*) + r_x x_* g'(x_*) - r_x \mu_0 g(x_*)
\end{aligned}$$

$$\begin{aligned}
J_{12}(E_*(p,h)) &= -bf\left(\frac{px_*}{1+hy_*}\right) + bh\frac{px_* y_*}{(1+hy_*)^2} f'\left(\frac{px_*}{1+hy_*}\right) \\
&= -bf(p_0) + bhy_* \frac{px_*}{1+hy_*} \frac{p_0 f'(p_0)}{f(p_0)} \frac{f(p_0)}{px_*} \\
&= -\frac{r_x}{\beta} + bhy_* p_0 \mu_0 \frac{f(p_0)}{px_*} \\
&= -\frac{r_x}{\beta} + r_x h \mu_0 \frac{p_0}{p} g(x_*)
\end{aligned}$$

$$\begin{aligned}
J_{21}(E_*(p,h)) &= cb\frac{py_*}{1+hy_*} f'\left(\frac{px_*}{1+hy_*}\right) \\
&= cby_* \frac{p_0 f'(p_0)}{f(p_0)} \frac{f(p_0)}{x_*} \\
&= r_x c \mu_0 g(x_*)
\end{aligned}$$

$$\begin{aligned}
J_{22}(E_*(p,h)) &= cbf\left(\frac{px_*}{1+hy_*}\right) - m - cbh\frac{px_* y_*}{1+hy_*} f'\left(\frac{px_*}{1+hy_*}\right) \\
&= -cby_* p_0 \frac{p_0 f'(p_0)}{f(p_0)} \frac{f(p_0)}{px_*} \\
&= -r_x c \mu_0 \frac{p_0}{p} g(x_*).
\end{aligned}$$

Then, the Jacobian matrix associated with $E_*(h,p)$ is

$$J(E_*(p,h)) = r_x \begin{pmatrix} (1-\mu_0)g(x_*) + x_* g'(x_*) & -1/\beta + \mu_0 g(x_*) hp_0/p \\ c\mu_0 g(x_*) & -c\mu_0 g(x_*) hp_0/p \end{pmatrix}.$$

We want study the sign of the trace and the determinant of this matrix, which are functions of $h,\ p,\ x_*$, denoted by

$$T(h,p,x_*) = \text{tr } J(E_*(h,p)), \quad D(h,p,x_*) = \det J(E_*(h,p)).$$

By direct computation, and taking into account (2.18) and (2.19) at the equilibrium, written in the form

$$h\frac{p_0}{p}g(x_*) = \frac{1}{\beta x_*}\left(x_* - \frac{p_0}{p}\right),$$

we obtain

$$T(h,p,x_*) = r_x\left(\Lambda(h,p)g(x_*) + x_* g'(x_*)\right), \tag{2.22}$$

where

$$\Lambda(h,p) = 1 - \mu_0 - c\mu_0 h\frac{p_0}{p},$$

and

$$\begin{aligned} D(h,p,x_*) &= -r_x^2 c\mu_0 g(x_*)\left[h\frac{p_0}{p}g(x_*) + h\frac{p_0}{p}x_* g'(x_*) - \frac{1}{\beta}\right] \\ &= -r_x^2 c\mu_0 g(x_*)\frac{p_0}{p}\left[-\frac{1}{\beta x_*} + h x_* g'(x_*)\right] \\ &= -\frac{r_x m\mu_0 p_0 g(x_*)}{p x_*}[-1 + h\beta x_*^2 g'(x_*)] = -\frac{r_x m\mu_0 p_0 g(x_*)x_*}{p}\left(\frac{\partial\phi}{\partial x}\right)_{x=x_*}. \end{aligned}$$

Since $(\partial\phi/\partial x)_{x=x_{*2}} > 0$, it follows that $\det J(E_{*2}(h,p)) < 0$ for h and p not belonging to the bifurcation curves of Figure 2.6; thus, $E_{*2}(h,p)$ is a saddle point. Otherwise, for $j = 1,3$, since $(\partial\phi/\partial x)_{x=x_{*j}} < 0$, it follows that $\det J(E_{*j}(h,p)) > 0$, for h and p not belonging to bifurcation curves; thus, $E_{*j}(h,p),\ j = 1,3$, is locally asymptotically stable if and only if $T(h,p,x_{*j}) < 0$. We want now to study the sign of the trace of the Jacobian matrix evaluated at $E_{*1}(h,p)$ and $E_{*3}(h,p)$.

Looking at the formula (2.22) since we know that $\epsilon \le x_* \le 1$ and $g(x_*) > 0$, we are interested in determine the sign of $\Lambda(h,p)$ and $g'(x_*)$.

As regards the equilibrium $E_{*1}(h,p)$, an important role for its stability properties is played by the two implications

$$\Lambda(h,p) \le 0 \iff \frac{p}{p_0} \le \gamma h; \tag{2.23}$$

$$x_{*1}(h,p) \ge \xi_0 \iff \frac{p}{p_0} \le \phi(\xi_0,h) = \beta h + \frac{1}{\xi_0}, \tag{2.24}$$

where

$$\gamma = \frac{c\mu_0}{1-\mu_0}. \tag{2.25}$$

Two scenarios emerge, depending on the intersection of the two straight lines

$$\frac{p}{p_0} = \gamma h, \qquad \frac{p}{p_0} = \beta h + \frac{1}{\xi_0}$$

in the (h, p) plane; the intersection occurs when $\beta < \gamma$, i.e. when

$$r_x < r_0 := \frac{m\mu_0}{1-\mu_0}. \tag{2.26}$$

As regards the equilibrium $E_{*3}(h, p)$, since we know that it exists in the range $h_0 < h < h_1$, and that $0 < x_{*3} < \xi_2 < \eta_0 < \xi_0$ which implies $g'(x_{*3}) > 0$, we have that only the implication (2.23) is important for its stability properties.

In the next subsections we study the sign of the trace of Jacobian matrices. We write here the expressions of the derivatives of $T(h, p, x_*)$ used in the following:

$$\frac{\partial T}{\partial h} = -r_x c\mu_0 \frac{p_0}{p} g(x_*) < 0, \qquad \frac{\partial T}{\partial p} = r_x c\mu_0 \frac{p_0 h}{p^2} g(x_*) > 0, \tag{2.27}$$

$$\frac{\partial T}{\partial x_*} = r_x \Lambda g'(x_*) + (x_* g'(x_*))'. \tag{2.28}$$

2.5.1 State E_{*1}: the case of $r_x \geq r_0$

Under the assumption $r_x \geq r_0$, or equivalently $\beta \geq \gamma$, we have that in the (h, p) plane

$$\beta h + \frac{1}{\xi_0} > \gamma h \quad \forall h > 0,$$

so that the two lines $p/p_0 = \beta h + 1/\xi_0$ and $p/p_0 = \gamma h$ do not intersect. We refer to Figure 2.8 to illustrate the results of this case. We are able to prove that there exists a Hopf bifurcation curve $p = p_1(h)$ on which tr $J(E_{*1}(h, p_1(h)) = 0$; this curve is monotonically increasing and

$$p_0 \max\{1, \gamma h\} < p_1(h) < p_0 \left(\beta h + \frac{1}{\xi_0}\right).$$

Theorem 2.2. *Assume* (2.2)-(2.7) *and* $r_x \geq r_0$. *Then, for any* $h \geq 0$,

$$\exists\, p_1(h): \quad p_0 \ \max\{1,\ \gamma h\} < p_1(h) < p_0 \left(\beta h + \frac{1}{\xi_0}\right),$$

such that

$$T(h, p_1(h), x_{*1}(p_1, h)) = 0, \quad T(h, p, x_{*1}(h, p)) < 0 \textit{ for } p \in [p_0, p_1(h)),$$

and $T(h, p, x_{*1}(h, p)) > 0$ *in the existence region of* E_{*1} *of the* (h, p) *plane where* $p > p_1(h)$*:*

$$0 \leq h \leq h_0,\ p_1(h) < p < \frac{p_0}{\epsilon} \quad \textit{and} \quad h_0 < h,\ p_1(h) < p < p_0\phi_1(h).$$

Moreover,

$$\frac{dp_1}{dh} > 0.$$

Proof. From the implications (2.23) and (2.24) it follows that in the region $\boxed{1}$ of the (h, p) plane (Figure 2.8)

$$h \geq \frac{1}{\gamma}, \quad 1 \leq \frac{p}{p_0} \leq \gamma h$$

we have

$$\Lambda \leq 0 \quad \text{and} \quad x_{*1} > \xi_0,\ g'(x_{*1}) < 0,$$

which imply $T(h, p, x_{*1}) < 0$. Consider now the region $\boxed{2}$ (Figure 2.8)

$$\max\{1, \gamma h\} \leq \frac{p}{p_0} \leq \beta h + \frac{1}{\xi_0} < \phi_1(h).$$

On the boundaries we have that

$$T(h, p, x_{*1}) < 0 \quad \text{for} \quad \frac{p}{p_0} = \max\{1, \gamma h\},$$

where either $p = p_0,\ x_{*1}(h, p_0) = 1$ or $p = p_0\gamma h,\ \xi_0 < x_{*1}(h, p_0\gamma h) < 1$, and

$$T\left(h, p_0\left(\beta h + \frac{1}{\xi_0}\right), \xi_0\right) > 0 \quad \text{for} \quad \frac{p}{p_0} = \beta h + \frac{1}{\xi_0}.$$

From the implications (2.23), (2.24) we have

$$\Lambda > 0 \quad \text{and} \quad x_{*1} > \xi_0,\ g'(x_{*1}) < 0,\ (x_{*1}g'(x_{*1}))' < 0.$$

Taking into account (2.27), (2.28), (2.23), (2.24) and the monotonicity property of x_{*1} ($\partial x_{*1}/\partial p < 0$), we have that

$$\frac{\partial T}{\partial x_{*1}} < 0, \qquad \frac{dT}{dp} = \frac{\partial T}{\partial p} + \frac{\partial T}{\partial x_{*1}}\frac{\partial x_{*1}}{\partial p} > 0.$$

It follows that $T(h, p, x_{*1})$, considered as a function of p for fixed $h \geq 0$, is negative for $p/p_0 = \max\{1, \gamma h\}$, is increasing with p for $\max\{1, \gamma h\} < p/p_0 < \beta h + 1/\xi_0$ and positive for $p/p_0 = \beta h + 1/\xi_0$. Thus, there is just one zero of $T(h, p, x_{*1})$, denoted by $p_1(h)$, for $p_0 \max\{1, \gamma h\} < p < p_0(\beta h + 1/\xi_0)$.

Moreover, in the existence region $\boxed{3}$ (Figure 2.8) of E_{*1} of the (h, p) plane where $p > p_1(h)$ we have

$$\Lambda > 0 \quad \text{and} \quad x_{*1} < \xi_0,\ g'(x_{*1}) > 0,$$

which imply $T(h, p, x_{*1}) > 0$.

Finally, the monotonicity property of $p_1(h)$ follows from $\partial T/\partial h < 0$.

□

For all the considered functions $g(\cdot)$ and $f(\cdot)$ in (2.8)-(2.11) and the parameter values specified in appendix A, $p_1(h)$ turns out to be very close to $\beta h + 1/\xi_0$. The existence region of $E_{*1}(h, p)$ in the (h, p) plane is divided in three subregions (Figure 2.8): the white regions $\boxed{1}$ and $\boxed{2}$, where $E_{*1}(h, p)$ is locally stable, and the grey region $\boxed{3}$, where it is unstable.

Let $\Delta(h, p, x_{*1}) = T^2(h, p, x_{*1}) - 4D(h, p, x_{*1})$. For fixed $h \geq 0$, at $p = p_1(h)$ we have

$$T(h, p_1(h), x_{*1}(h, p_1(h))) = 0, \quad \Delta(h, p_1(h), x_{*1}(h, p_1(h))) < 0,$$

so that the Jacobian matrix has a simple pair of pure imaginary eigenvalues. Moreover, $dT/dp > 0$ for $\max\{1, \gamma h\} < p/p_0 < \beta h + 1/\xi_0$. Thus, $p = p_1(h)$ is a Hopf bifurcation curve for the equilibrium $E_{*1}(h, p)$ (the dotted one in Figure 2.8), and limit cycles emerge for p in a neighbourhood of $p_1(h)$. The stability of the limit cycles can be determined by the sign of the first Lyapunov coefficient associated with the system (2.1) ([48] p. 152, formula (3.4.11); [66] p. 178, formula (5.62)) once the model functions are fixed. The dependence of this coefficient on the parameters h and p is very intricate, and a theoretical analysis is a substantial undertaking. The sign was then determined numerically (and also checked with the specific software MATCONT [34]) for special systems characterized by different prey growth and trophic functions, and the set of bioecological parameters given in appendix A; also the side of the Hopf bifurcation curve on which the limit cycles exist has been found numerically. The results will be illustrated in the next section.

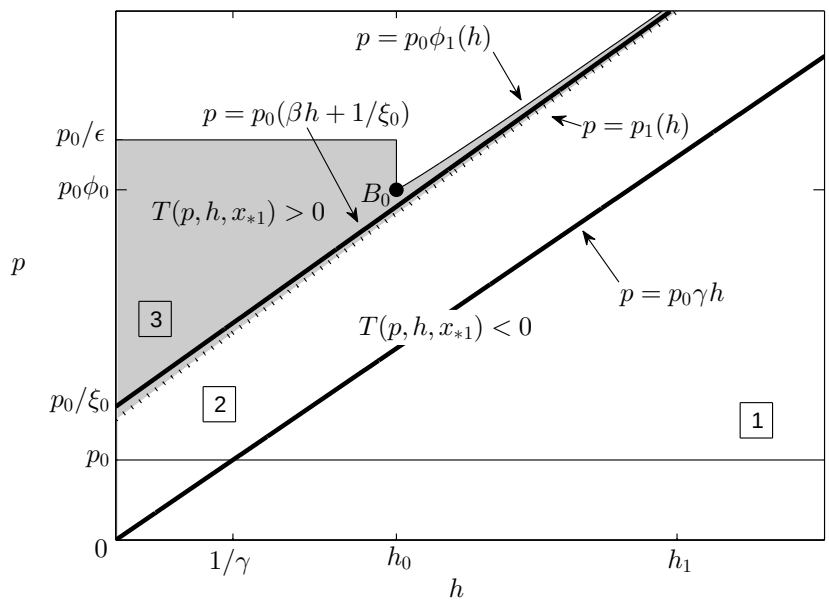

Fig. 2.8. Local stability and instability regions in the (h, p) plane of the coexistence equilibrium state $E_{*1}(h, p)$ in the case $r_x \geq r_0$. In grey the region in which $T(h, p, x_{*1}) > 0$.

2.5.2 State E_{*1}: the case of $r_x < r_0$

The situation is somewhat more involved than in the previous case. We refer to Figure 2.9 to illustrate the results of this case. Under the assumption $r_x < r_0$, or equivalently $\beta < \gamma$, we have that in the (h, p) plane the line $p/p_0 = \gamma h$ intersects the line $p/p_0 = \beta h + 1/\xi_0$ and the curve $p = p_0\phi_1(h)$ at points R and S, respectively. Let h_R (independent of p) and h_S (dependent on p) be the h-coordinates of the intersection points R and S; we have

$$h_R = \frac{1}{\xi_0(\gamma - \beta)} = \frac{1}{\xi_0\beta(r_0/r_x - 1)}, \qquad h_S = \phi_1^{-1}\left(\frac{p}{p_0}\right). \tag{2.29}$$

Also in this case, we can prove that there exists a Hopf bifurcation curve $p = p_1(h)$ for $h < h_R$ which is monotonically increasing (Figure 2.9). Theorem 2.2 can be reformulated as follows.

Theorem 2.3. *Assume* (2.2)-(2.7) *and* $r_x < r_0$. *Then,*

(i) for $0 \leq h < h_R$, $\exists\, p_1(h)$: $\quad p_0 \max\{1,\ \gamma h\} < p_1(h) < p_0\left(\beta h + \dfrac{1}{\xi_0}\right)$,
such that

$$
\begin{aligned}
&T(h, p_1(h), x_{*1}(p_1, h)) = 0,\\
&T(h, p, x_{*1}(h, p)) < 0 \textit{ for } p \in [p_0, p_1(h)),\ h \geq 0\\
&T(h, p, x_{*1}(h, p)) > 0 \textit{ for } 0 \leq h \leq h_0,\ p_1(h) < p < \frac{p_0}{\epsilon} \textit{ and}\\
&\qquad\qquad h_0 < h < h_R,\ p_1(h) < p < p_0\phi_1(h).
\end{aligned}
$$

Moreover,

$$\frac{dp_1}{dh} > 0.$$

(ii) A further region with positive trace is

$$h_R < h < h_S, \quad \gamma h < \frac{p}{p_0} < \phi_1(h),$$

where h_S is the unique solution to the equation $\gamma h = \phi_1(h)$.

The proof of Theorem 2.3 is omitted because it follows the lines of the proof of the previous Theorem 2.2.

In general, the stability properties of $E_{*1}(h, p)$ cannot be established in the subregion of existence (marked with dark grey in Figure 2.9(b)) defined by

$$h > h_R, \qquad \beta h + \frac{1}{\xi_0} < \frac{p}{p_0} < \min\{\gamma h, \phi_1(h)\}. \tag{2.30}$$

Indeed, in this region the implications (2.23) and (2.24) do not hold and we have no information about the sign of $T(h, p, x_{*1})$. It is possible nevertheless to check the sign of the trace $T(h, p, x_{*1})$ along the curve $p = p_0\phi_1(h)$ and it turns out that for h slightly above h_S $T(h, p, x_{*1}) > 0$ and $\lim_{h\to+\infty} T(h, p, x_{*1}) = r_x(1 - \mu_0)(1 - \gamma/\beta)$. Such value is negative only when $r_x < r_0$ and then, thanks to the monotonicity properties (2.27), there exists a unique value h_{BT} wherein $T(h_{BT}, p, x_{*1}) = 0$. These facts reveal the presence of a Bogdanov-Takens point, intersection of a saddle-node, a Hopf and a separatrix homoclinic loop curve, that will be discussed in the next section. Also in this case, the stability of the limit cycles has been numerically studied and the results will be discussed in the next section.

2.5.3 State E_{*3}

As regards the equilibrium $E_{*3}(h, p)$, we know that it exists when

$$h_0 < h < h_1, \quad \phi_2(h) < \frac{p}{p_0} < \frac{1}{\epsilon},$$

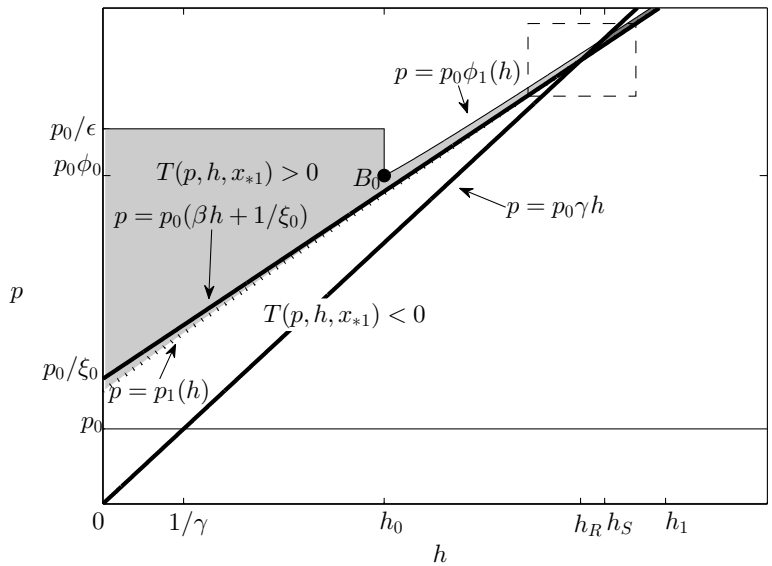

(a)

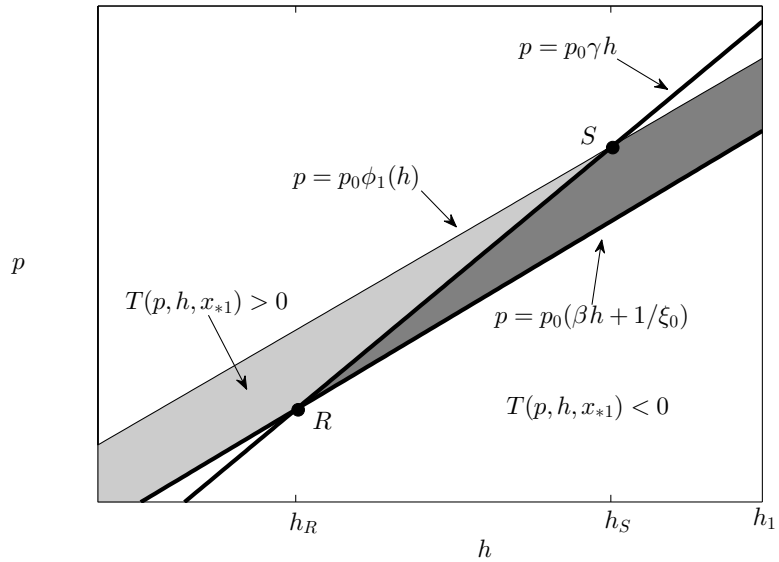

(b)

Fig. 2.9. Local stability and instability regions in the (h, p) plane of the coexistence equilibrium state $E_{*1}(h, p)$ in the case $r_x < r_0$. Light grey denotes regions in which $T(p, h, x_{*1}) > 0$; dark grey marks regions in which the stability properties of E_{*1} cannot be analytically determined. Figure (b) is an enlargement of the dashed rectangular region of Figure (a).

and that $0 < x_{*3} < \xi_2 < \eta_0 < \xi_0$ which implies $g'(x_{*3}) > 0$. It follows that only the implication (2.23) is important for its stability properties.

Then, from the existence conditions of $E_{*3}(p,h)$ and implication (2.23) it follows that for $h_0 \leq h \leq h_1$ we have

$$\max\{\phi_2(h),\ \gamma h\} < \frac{p}{p_0} < \frac{1}{\epsilon} \Longrightarrow T(p,h,x_{*3}) > 0.$$

The situation for E_{*3} is illustrated in Figure 2.10. Let $\tilde{h}_1 = 1/(\gamma\epsilon)$ be the intersection point between the straight lines $p = p_0/\epsilon$ and $p = p_0\gamma h$.

If

$$\tilde{h}_1 \geq h_1, \quad \text{i.e.} \quad \frac{r_0}{r_x} \leq \epsilon g'(\epsilon),$$

then $E_{*3}(p,h)$ is unconditionally unstable (Figure 2.10(a)). For instance, this case holds for a Holling-type II trophic function, a Gilpin model for $g(s)$ and parameters as in A with $r_x > r_0$.

If

$$\tilde{h}_1 < h_1, \quad \text{i.e.} \quad \frac{r_0}{r_x} > \epsilon g'(\epsilon),$$

then, in general, the stability properties of $E_{*3}(h,p)$ cannot be established in the region defined by

$$\tilde{h}_2 \leq h \leq h_1, \qquad \phi_2(h) \leq \frac{p}{p_0} \leq \min\left\{\gamma h, \frac{1}{\epsilon}\right\},$$

where $\tilde{h}_2$ is the unique solution to the equation $\gamma h = \phi_2(h)$ (dark grey region in Figure 2.10(b)). Indeed, in this region the implication (2.23) does not hold and we have no information about the sign of $T(h,p,x_{*3})$.

The stability properties of all equilibrium states are summarized in Table 2.3.

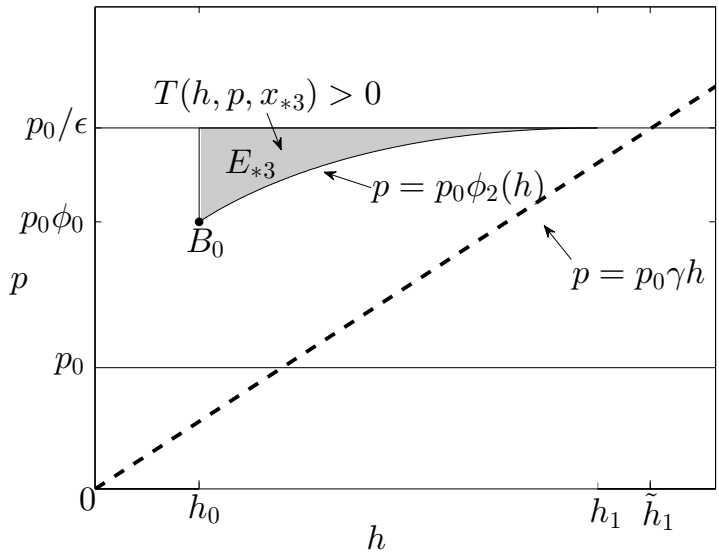

(a) $\tilde{h}_1 > h_1$

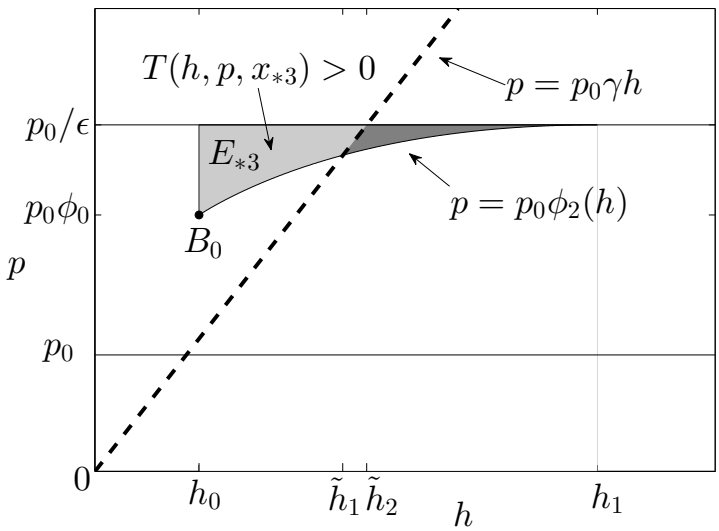

(b) $\tilde{h}_1 < h_1$

Fig. 2.10. Instability regions in the (h, p) plane of the coexistence equilibrium state $E_{*3}(h, p)$.

	$0 \le h \le h_0$		$h_0 < h < h_1$	$h > h_1$
E_0	stable node $p > 0$			
E_ϵ	saddle $0 < p < p_0/\epsilon$, unst. node $p > p_0/\epsilon$			
E_1	stable node $0 < p < p_0$, saddle $p > p_0$			
$E_{*1}(h,p)$	stable $p_0 < p < p_1(h)$ unst. $p_1(h) < p < p_0/\epsilon$	$r_x \ge r_0$	stable $p_0 < p < p_1(h)$ unst. $p_1(h) < p < p_0\phi_1(h)$	
		$r_x < r_0$	see Table 2.3(b)	stable $p_0 < p < p_0(\beta h + 1/\xi_0)$ n.d. $p_0(\beta h + 1/\xi_0) < p < p_0\phi_1(h)$
$E_{*2}(h,p)$	$\nexists$		saddle $p_0\phi_2(h) \le p \le p_0\phi_1(h)$	saddle $p_0/\epsilon \le p \le p_0\phi_1(h)$
$E_{*3}(h,p)$	$\nexists$		unst. $\max\{p_0\phi_2(h), p_0\gamma h\} \le p \le p_0/\epsilon,\ h_0 < h < \tilde{h}_1$ n.d. $p_0\phi_2(h) \le p \le \min\{p_0\gamma h, p_0/\epsilon\},\ \tilde{h}_2 < h < h_1$	$\nexists$

(a)

	$h_0 < h < h_R$	$h_R < h < h_S$	$h_S < h < h_1$
$E_{*1}(h,p)$ $(r_x < r_0,\ h_0 < h < h_1)$	stable $p_0 < p < p_1(h)$ unst. $p_1(h) < p < p_0\phi_1(h)$	stable $p_0 < p < p_0(\beta h + 1/\xi_0)$ n.d. $p_0(\beta h + 1/\xi_0) < p < p_0\gamma h$ unst. $p_0\gamma h < p < p_0\phi_1(h)$	stable $p_0 < p < p_0(\beta h + 1/\xi_0)$ n.d. $p_0(\beta h + 1/\xi_0) < p < p_0\phi_1(h)$

(b)

Table 2.3. (a) Summary of stability properties of equilibrium states (n.d.=not determinable, unst.=unstable); (b) details on stability of $E_{*1}(h,p)$ for $h_0 < h < h_1$ and $r_x < r_0$.

3

Numerical study

In the previous Chapter we have investigated the dynamical behaviours of a predator-prey system, when the model functions describing the biological processes occurring in the considered trophic chain are not specified by analytical expressions, but by some characteristic properties determining their shapes. We have shown that this is feasible for the existence and stability analysis of the equilibrium states of the system. Unfortunately, the stability analysis of limit cycles cannot be easily performed following this general approach, and the model functions have to be specified to go further in the qualitative analysis.

In this Chapter results of numerical simulations, obtained for some concrete realization of the model functions, are presented to illustrate the behaviours of the system. Such results confirm analytical predictions and throw light on some aspects of the dynamics of the system.

3.1 Behaviours of the system

Here we focus on some peculiar behaviours obtained by using the model functions (2.8)-(2.11), and the parameter values specified in appendix A. Such behaviours are of course in agreement with the analytical results obtained in the previous Chapter. Once the model functions are fixed, we can also numerically investigate the limit cycles arising from E_{*1} by Hopf bifurcation. The main features of the bifurcation structure will be shown in the following diagrams, which are only qualitative because the real bifurcation curves, simulated here by using model functions (2.8) and (2.10) and parameter values as in A, are almost indistinguishable from one another. Therefore, some of the phenomena described below can be viewed only with a very fine resolution. Anyhow, we obtain qualitatively the same scenarios with different

combinations of model functions (2.8)-(2.11). Further information on the bifurcation structure close to critical values of the bifurcation parameters detected in the following analysis (such as number of bifurcating limit cycles, higher codimension points, ...) could be obtained case by case with specific model functions and it will be matter of a future work.

- When $0 < h < h_0$, in all tested cases, independently of the value of r_x, the numerical results showed the existence of a critical value $\hat{h}$ such that:

  - for any fixed $0 \leq h < \hat{h}$, stable limit cycles emerge for p slightly above the Hopf value $p_1(h)$ and disappear by global bifurcation with the heteroclinic cycle involving equilibria E_ϵ and E_1 at a further critical value $p_2(h) > p_1(h)$ (see Figure 3.1 and 3.2(a)); in this range of h the system behaves qualitatively as the system with $h = 0$ [25, Figure 7];

  - when $h > \hat{h}$, repelling limit cycles emerge for p slightly below the Hopf value $p_1(h)$. We have numerical evidence of the existence of a further critical value h_C such that for $\hat{h} < h < h_C$ (Figure 3.1) the repelling limit cycles disappear by saddle-node bifurcation with a stable limit cycle on the curve $p = p_3(h)$, and stable limit cycles then disappear by global bifurcation involving the heteroclinic cycle between equilibria E_ϵ and E_1 (Figure 3.2(b) and 3.2(c)) on the curve $p = p_2(h)$ (Figure 3.1). The curve of heteroclinic cycles $p = p_2(h)$ intersects $p = p_3(h)$ for $h = h_C$, while it crosses the Hopf curve $p = p_1(h)$ for a value $h \in (\hat{h}, h_C)$. For $h_C < h < h_0$, the repelling limit cycles disappear instead by global bifurcation with the heteroclinic cycle involving E_ϵ and E_1 (Figure 3.2(d)) on the curve $p = p_2(h) < p_1(h)$.

  The Hopf bifurcation is thus supercritical for $h < \hat{h}$, and subcritical for $h > \hat{h}$; the curve $p = p_3(h)$ of saddle-node bifurcation of limit cycles emanates from the point $(\hat{h}, p_1(\hat{h}))$. It is possible to detect, by using the continuation software MATCONT [34], that the Hopf bifurcation curve has a Generalized Hopf (GH) codimension-two point at $h = \hat{h}$. A deeper investigation of the bifurcation occurring at $h = h_C$, where $p = p_2(h)$ and $p = p_3(h)$ intersect each other, could be performed case by case following [6], with specific model functions, and would allow to determine how many cycles bifurcate in this region of the parameter space and what is their stability; this analysis will be matter of future studies.

- When $h_0 < h < h_1$, again whatever r_x, we have that the coexistence region of the equilibria $E_{*1},\ E_{*2},\ E_{*3}$ (dark grey region in Figure 2.6) is crossed by the Hopf bifurcation curve $p = p_1(h)$ (see Figure 3.1). Again, the Hopf bifurcation curve generates unstable limit cycles for p slightly below the Hopf value $p_1(h)$; such cycles disappear by global bifurcation on the curve $p = p_2(h)$, which can occur either with the heteroclinic cycle connecting E_ϵ and E_1 or with a homoclinic cycle with the saddle point E_{*2}. In detail, let h_U be the abscissa of the intersection of the curves $p = p_2(h)$ and $p = p_0\phi_2(h)$ (Figure 3.1); then, the heteroclinic cycle occurs for $h < h_U$ and the homoclinic cycle for $h > h_U$. The transition from having heteroclinic to homoclinic orbits turns out to be caused by the formation at $h = h_U$ of a heteroclinic cycle connecting the just appeared equilibrium $E_{*2} = E_{*3}$ and E_1. This leads to the interaction of the limit cycles with the equilibrium E_{*2} and then to their disappearance by global bifurcation with a homoclinic cycle through E_{*2}, instead of by a heteroclinic cycle connecting E_ϵ and E_1. The point $h = h_U$ seems to be a codimension-three or even higher bifurcation point. Anyway, a deeper analysis aiming at detecting all possible non equivalent phase portraits around this point cannot be carried out in general and it will be matter of future investigations with specific model functions.
  Some examples of the peculiar dynamics obtained for different p and $h_0 < h < h_1$ are reported in the phase portraits in Figure 3.3. We selected cases in which all coexistence equilibria are present and we focused on bistability occurring in the system. In Figure 3.3(a) (where $p < p_2(h)$) the trajectories tend to E_0 or E_{*1} depending on the initial conditions. In Figure 3.3(b) (where $p_2(h) < p < p_1(h)$) an unstable limit cycle separates the basins of attraction of the stable equilibria E_{*1} and E_0. Lastly, in Figure 3.3(c) (where $p > p_1(h)$) all the coexistence equilibria are unstable and the system evolves towards global extinction.

- For $h > h_1$ and $r_x \geq r_0$ we have proved in Theorem 2.2 that the Hopf bifurcation curve $p = p_1(h)$ is always below the stationary bifurcation curve $p = p_0\phi_1(h)$ (Figure 2.8). The numerical investigation shows that unstable limit cycles arise below the curve $p = p_1(h)$ and disappear by global bifurcation with a homoclinic cycle through the saddle point E_{*2} on the curve $p = p_2(h) < p_1(h)$ (Figure 3.2(e)). For $h > h_1$ and $r_x < r_0$, we cannot state in general the mutual positions of the curves $p = p_1(h),\ p = p_0\phi_1(h)$. Moreover, the stability properties of E_{*1} cannot be determined in general in the region defined in (2.30) (dark grey region in Figure 2.9(b)). We have numerically detected Hopf bifurcation values $p_1(h)$ for

E_{*1} also when h is above the estimated threshold h_R (see Figure 3.4). Again, unstable limit cycles arise below the curve $p = p_1(h)$ and disappear by global bifurcation with the homoclinic cycle through E_{*2} on the curve $p = p_2(h) < p_1(h)$. The Hopf bifurcation curve $p = p_1(h)$ lies below the line $p = p_0(\beta h + 1/\xi_0)$ for $h < h_R$, intersects it for $h = h_R$ at point R (where $\gamma h = \beta h + 1/\xi_0$) and stays definitely above for $h > h_R$. Since the sign of the trace $T(h, p, x_{*1})$ along the curve $p = p_0\phi_1(h)$ changes from positive to negative, as pointed out in Subsection 2.5.2, there exists the critical value $h_{BT} > h_1$ at which the Hopf curve $p = p_1(h)$ intersects the curve $p = p_0\phi_1(h)$. Also the global bifurcation curve $p = p_2(h)$, which involves the homoclinic cycle through the saddle point E_{*2}, passes through this intersection and then we obtain a codimension-two point in the (h, p) plane in which $D(h_{BT}, p_{BT}, x_{*1}) = 0$ and $T(h_{BT}, p_{BT}, x_{*1}) = 0$, that turns out to be a Bogdanov-Takens (BT) bifurcation point. It is characterized by the typical phase diagram of Figure 3.5; this type of bifurcation has been detected by other authors in similar models [5, 87, 37, 40].

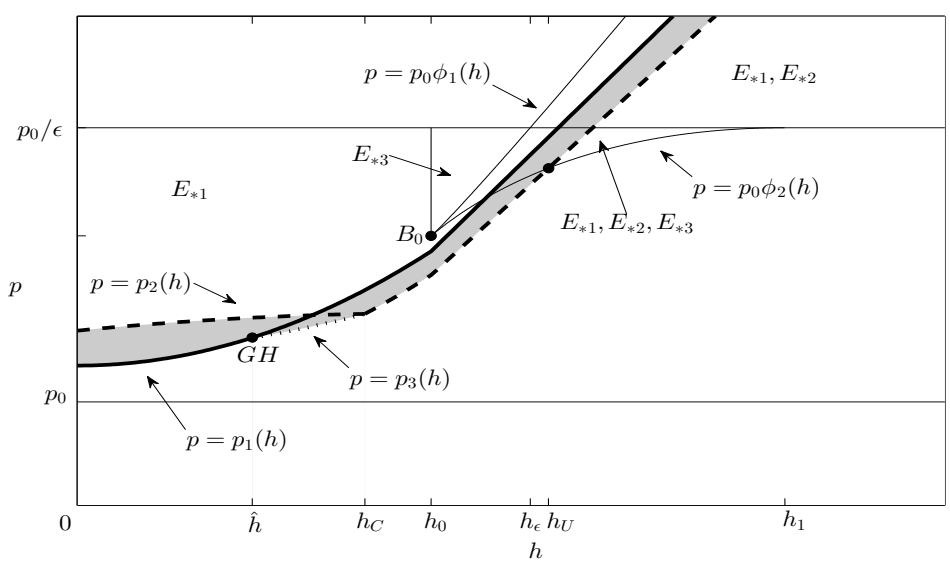

Fig. 3.1. Qualitative representation of local and global bifurcation curves for the equilibrium E_{*1} and limit cycles; in grey the regions of the (h, p) plane in which stable or unstable limit cycles exist. GH: Generalized Hopf point.

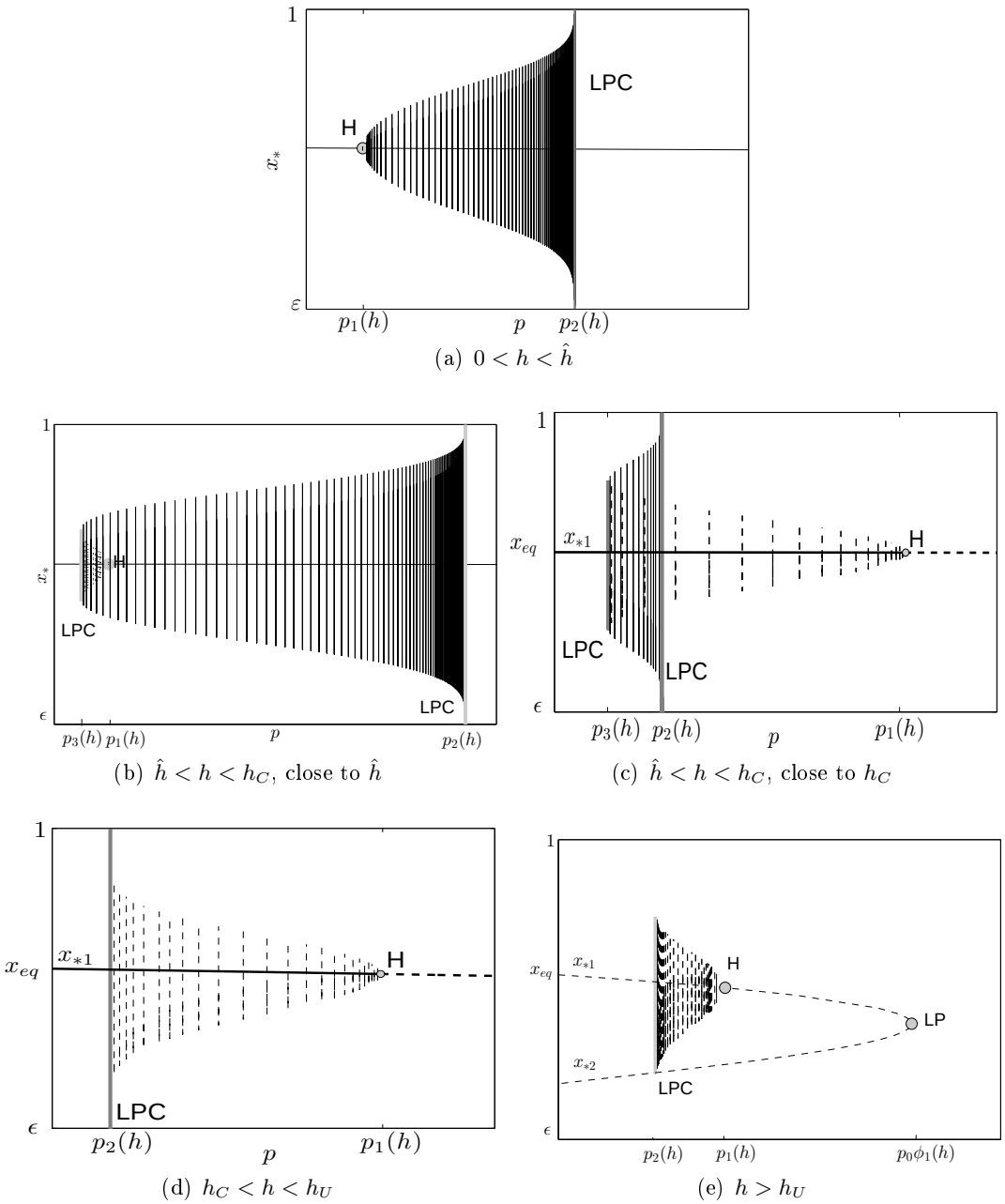

Fig. 3.2. Limit cycles behaviours versus p. (a) Stable limit cycles emerge and disappear by global bifurcation. (b-c) Repelling limit cycles emerge and disappear by saddle-node bifurcation with a stable limit cycle on the curve $p = p_3(h)$, and stable limit cycles then disappear by global bifurcation on the curve $p = p_2(h)$. The position of this curve with respect to $p = p_1(h)$ changes increasing the value of h. (d-e) Repelling limit cycles emerge and disappear instead by global bifurcation. The vertical lines represent the projections of the limit cycles on the (p, x) plane. Solid lines: stable cycles, dashed lines: unstable cycles. LPC denotes bifurcation of limit cycles detected by MATCONT, while H indicates a Hopf point.

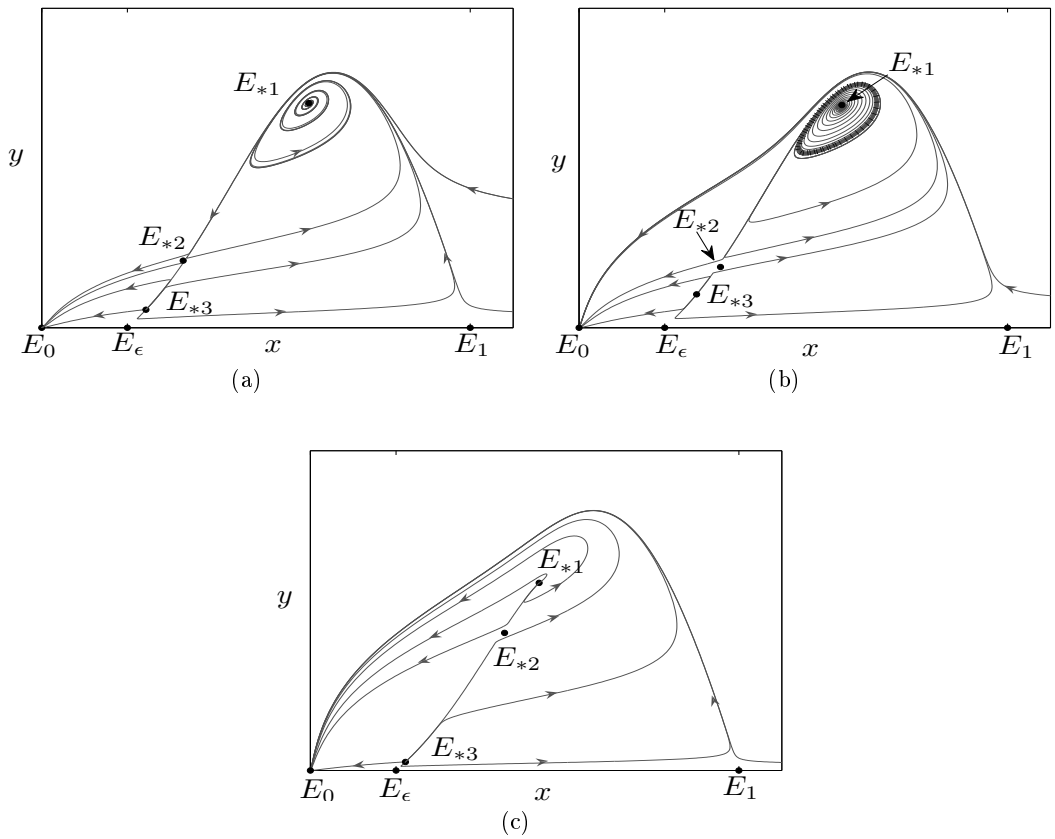

Fig. 3.3. Phase portraits for $h_0 < h < h_1$ and different p: (a) $p < p_2(h)$, (b) $p_2(h) < p < p_1(h)$, (c) $p > p_1(h)$.

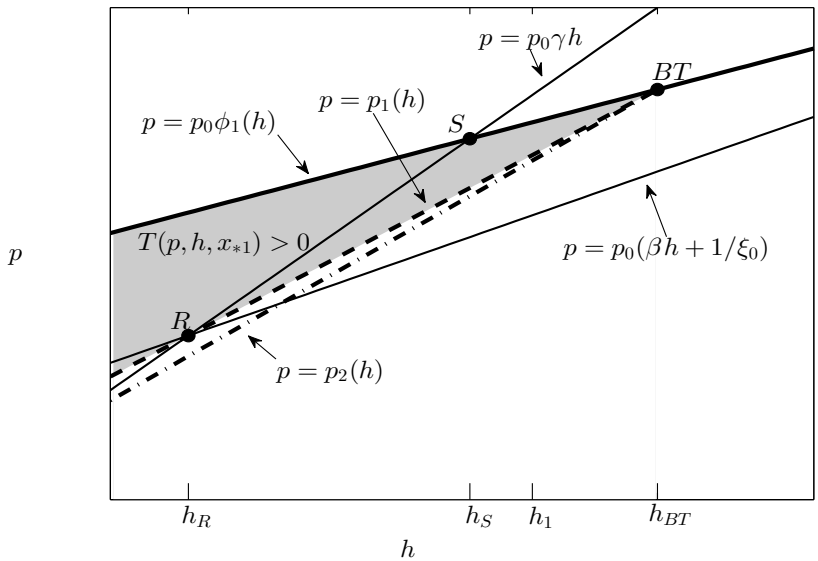

Fig. 3.4. Qualitative representation of local and global bifurcation curves for the equilibrium E_{*1} and limit cycles for $h > h_R$ in the case $r_x < r_0$. Light grey denotes the region in which $T(h, p, x_{*1}) > 0$. BT: Bogdanov-Takens point.

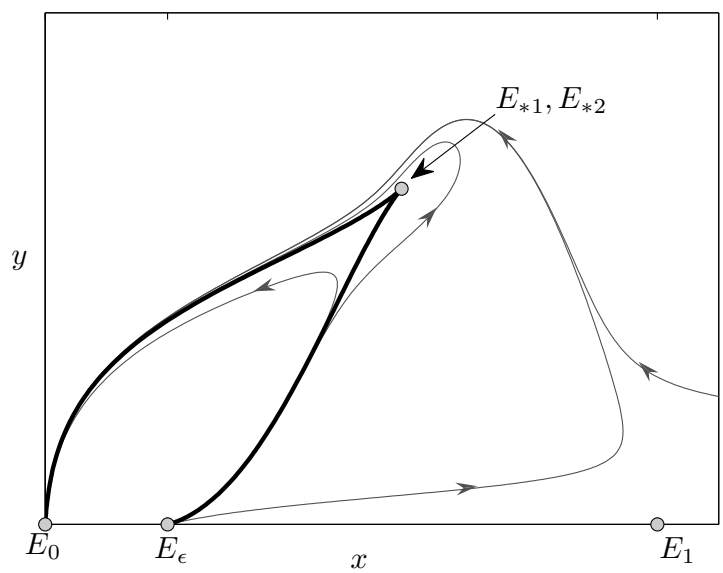

Fig. 3.5. Phase diagram close to the Bogdanov-Takens bifurcation $h = h_{BT},\ p = p_{BT}$.

4

Concluding remarks

When modeling predator-prey systems, the properties of the prey growth function $g(\cdot)$ depend on the introduction of intraspecific competition among the prey, and on the assumption of either the absence or the presence of a weak/strong Allee effect. On the other hand, the trophic function $f(\cdot)$ may be assumed either concave or S-shaped and it can be prey-dependent, ratio-dependent or predator-prey dependent. Moreover, only some of their qualitative properties are known. Thus, these functions should not be specified by any analytical expression, but only by general properties dictated by bioecological considerations; moreover, they should satisfy some technical assumptions to make the analysis tractable.

The assumptions made on the model functions limit the number of equilibrium points, and allow to perform a sufficiently general existence, stability and bifurcation analysis of the equilibrium states. This is the main difference with respect to the investigation of the dynamics in generalized models carried on by others authors [47, 63], who assume that at least one steady state exists (without hypothesis on the general functions) and then perform the local asymptotic stability analysis of the steady state under consideration. On the contrary, in this work assumptions on the prey growth function and on the functional response are required, in order to take into account proper biological properties. Moreover, these assumptions limit the number of equilibrium states admitted by the system, and the stability and bifurcation analysis is studied for each equilibrium state.

However, this approach leads to some restrictions in the analysis of the dynamics. Let us look at the assumptions (2.2)-(2.7) on g and f. These conditions imply relationships between $f(s)$, $f'(s)$ and $g(s)$, $g'(s)$, $g''(s)$. At any rate, when a Hopf bifurcation is detected, the stability properties of the limit cycles cannot be in general established from the sign of the first Lyapunov number, because it depends on the first, second and third derivatives of the right hand side of (2.1), evaluated at

the equilibrium point. In the very recent paper by Adamson and Morozov [3] it is pointed out that "the use of two different functions belonging to the same class can result in qualitatively different dynamical behaviour in the model and a different type of bifurcation. In the literature, the conventional way to avoid such ambiguity is to narrow the class of unknown functions", and they conclude that this approach may lead to cumbersome expressions, biologically meaningful. We observe that some uncertainties could be removed by carrying out many numerical simulations with different model functions.

In our approach, the use of different functions belonging to the same class leads to some common behaviours, for instance in connection with the number of equilibria and their stability properties. However, some peculiar dynamics, such as the phase diagram close to the Bogdanov-Takens bifurcation point in the case of $r_x < r_0$, can be found only with specific functions in the class. Adamson and Morozov [3] analyse in detail this crucial problem and show that where the model functions are not specified by analytical expressions, the bifurcations can be described only with a certain probability.

We wish to point out that slightly different formulations of the model equations, together with rescaling of state variables and parameters and the use of different bifurcation parameters in the stability analysis, make the comparison between the various scenarios a hard work. In any event, behaviours of predator-prey systems of type (2.1) characterized by different model functions $g(\cdot)$ and $f(\cdot)$ analysed in the literature [13, 98, 37, 5, 40, 107, 79, 87, 25], deserve some attention. Under the assumption of a strong Allee effect, the functions implemented in the aforementioned literature, and combined in different ways in system (2.1), are (2.8)-(2.11).

In the case of a prey-dependent trophic function, realized by setting $h = 0$ in (2.1), comparisons of models characterized by combinations of (2.8)-(2.9) and (2.10)-(2.11) have been reported in [25]. The existence and stability analysis of the equilibrium states had been performed by taking p and the ratio $\theta = m/(cb)$ as bifurcation parameters. All the considered models admit the same equilibrium states, and show the same qualitative behaviours regarding the local stability properties, the occurrence of a heteroclinic cycle and the consequent global bifurcation. Obviously, the stability ranges may be very different, with the same values of the bioecological parameters r_x, b, m, c.

Also the model in the recent paper [107], with an Allee effect of rational type $g(s) = g_0(s - \epsilon)(1 - s)/(\epsilon_0 + s)$ with $\epsilon_0 > 0$ (called double Allee effect) and linear trophic function $f(s) = s$ (Lotka-Volterra interaction) undergoes a heteroclinic loop bifurcation, and moreover subcritical and supercritical Hopf bifurcation.

In all the visited models with Allee effect and prey-dependent trophic function only one possible coexistence state it has been observed, which may undergo several stability changes. For instance, assuming ϵ_0 in the double Allee effect as bifurcation parameter, the coexistence equilibrium state can switch from stable to unstable and then back again to stable [108, 107].

The ratio-dependent trophic function expressed in terms of the ratio $x/(x+y)$, which is singular in the origin, has been recently introduced in models with Allee effect of quadratic type (Gilpin model (2.8)) in [87, 40, 5], and of rational type (double Allee effect) in [37]. In all these models only two coexistence states may be found, and one is always a saddle point. In the different parameter spaces considered by these authors, a Bogdanov-Takens bifurcation point of codimension-two has been detected and it is considered "as an organising centre of the global dynamics" [5]. Although these models have the same structure, the analysis and the numerical simulations performed in [87, 40] show and suggest the absence of stable limit cycles, while in [5] "for a fixed set of parameters, the following may happen: the extinction of both populations, coexistence for determined population sizes, or the oscillation of both population". The same results are obtained in [37]. A possible explanation is the following: in [5, 37] a parameter introduced in the prey growth function, associated with ϵ in our formulation, is used as bifurcation parameter, and varied in the numerical simulations, while it is maintained fixed in [87]. Furthermore, in [5, 37] more global phenomena are described: heteroclinic loop and bifurcation of limit cycles. The results obtained in [108, 107, 5, 37] suggest that the use of parameters introduced in the prey growth function as a bifurcation parameter put in evidence phenomena which are not detected by performing the analysis with other bifurcation parameters.

In our analysis, we fixed all the dimensional bioecological rates r_x, b, m, determining the time scale of the dynamics and the conversion factor c from prey to predator biomass, which are multiplicative factors in equation (2.1). Moreover, also the Allee threshold ε is maintained fixed. The parameters h and p appearing in the argument of the trophic function, which describes the predator-prey interaction, have been chosen as bifurcation parameters. In our analytical study, we found that the system admits at most three coexistence equilibria E_{*1}, E_{*2}, E_{*3} depending on the values of parameters h and p, as in Table 2.2. The coexistence equilibrium E_{*2}, when exists, is always a saddle point. The equilibrium E_{*3} is always unstable when the straight line $p = p_0\gamma h$ does not intersect its existence region in the (h, p) plane.

The study of the stability properties of E_{*1} in the (h, p) plane is more intricate. We found a Hopf bifurcation curve $p = p_1(h)$, and limit cycles emerge, stable or unstable depending on the value of h, and disappear by global bifurcation, involving the

heteroclinic cycle between the non coexistence equilibria E_ϵ, E_1 or the homoclinic cycle through the coexistence equilibrium E_{*2}, respectively. Furthermore, we have also numerically detected a region in the (h, p) plane where stable and unstable limit cycles coexist and disappear by saddle-node bifurcation of cycles. Finally, we proved the existence of a Bogdanov-Takens bifurcation point for $r_x < r_0$. We pointed out that, in some regions of the parameter space, the model presents multiple attractors. Moreover, the extinction of both populations is always possible, since the global extinction E_0 is always locally asymptotically stable and globally stable for some parameter values.

It is worth noticing that, from a mathematical viewpoint the system admits different phase portraits depending on the parameter values, but this not necessarily implies a significant difference in the biological interpretation of the results. For instance, the difference between a stable steady state and a small stable limit cycle around the same (but unstable) steady state is of minor importance, even though the mathematical study asserts that the dynamics in these two cases are not equivalent.

A last brief remark concerns the maximal specific production rates r_x and r_y. A critical value r_0, defined in (2.26), of r_x was found. It depends on the bioecological parameters b, m, c and on the type of the trophic function. The behaviour of the system shows different features depending on the sign of the difference $r_x - r_0$. This fact is independent of either the presence or the absence of an Allee effect in the model equations (see Subsections 2.5.1, 2.5.2 and [25]). It is worthwhile noting that the difference in the system behaviour due to the sign of $r_x - r_0$ becomes very marked when a trophic function singular in the origin is used [22]. Furthermore, it can be observed (see A) that with a Holling-type II trophic function we have $r_0 = r_y$, while with an Ivlev type $r_0 > r_y$ with the same bioecological parameters m, c, b. Thus, if $r_x < r_y$, then $r_x < r_0$, with a Holling-type II trophic function. Contrarily, with the Ivlev trophic function, when $r_x > r_y$ we might have either $r_x < r_0$ or $r_x > r_0$. We recall that, in general, in a food web the time needed for reproduction and growth of the individuals of a population is increasing with the trophic level [67, 22]. At any event, in some predator-prey systems, such as some acarine systems, any situation may occur.

Summarizing, the general approach to predator-prey systems used in this work, in which the mathematical formulation of model functions is unspecified except for some generic qualitative properties, has put in evidence the overall complexity of the bifurcation structure of the model, according also to recent works [4, 2, 3]. Local (stationary and Hopf) bifurcations have been determined analytically in this general framework; also the presence of the Bogdanov-Takens and the cusp codimension-two

bifurcation points is independent of the particular expression of the model functions. The next step consists in performing an analogous investigation for nonlocal and codimension-two bifurcations, such as the Generalized Hopf and the bifurcations of cycles, admitted by this general model; it will be a lot more challenging, and hopefully could give additional elements to try to explain phenomena still unclear in real ecosystems.

Appendix

A Details on some parameters

(i) Let

$$\mu(s) = \frac{sf'(s)}{f(s)}, \quad s > 0. \tag{4.1}$$

From properties (2.3) and (2.7) it follows that

$$\mu(0) = 1, \quad 0 < \mu(s) < 1, \quad \lim_{s \to +\infty} \mu(s) = 0. \tag{4.2}$$

The first two properties of $\mu(s)$ are easily verified. To prove the limit in (4.2), let us consider the identity

$$\int_{s_0}^{s} \frac{\mu(a)}{a} da = \int_{s_0}^{s} \frac{f'(a)}{f(a)} da, \tag{4.3}$$

where $s_0 > 0$ is fixed, and $s > s_0$. From (4.3) we have that there exists $\hat{a}(s)$, $s_0 < \hat{a}(s) < s$, such that

$$\mu\left(\hat{a}(s)\right) = \frac{log\ f(s)/f(s_0)}{log\ s/s_0}. \tag{4.4}$$

From (4.4), taking into account (2.3), it follows that

$$\lim_{s \to +\infty} \mu\left(\hat{a}(s)\right) = 0, \quad \lim_{s \to +\infty} \frac{\partial \mu\left(\hat{a}(s)\right)}{\partial s} = \lim_{s \to +\infty} \frac{\mu(s) - \mu\left(\hat{a}(s)\right)}{s\ \log s/s_0} = 0, \tag{4.5}$$

which imply the limit in (4.2). However, from properties (2.3) we are not able to show the monotonicity condition $\mu'(s) < 0$, which holds for the functions $f(s)$ generally used in the applications.

(ii) The dynamical behaviours of predator-prey systems may be different depending on the sign of the difference $r_x - r_0$ and $r_x - r_y$, where r_0 is given in (2.26) and r_y in (2.14) [22, 67, 70]. With respect to this issue, we point out that with a Holling-type II trophic function the parameters p_0 and μ_0 are given by

$$p_0 = \frac{\alpha}{1-\alpha}, \quad \mu_0 = 1 - \alpha,$$

so that

$$r_0 = \frac{m(1-\alpha)}{\alpha} = r_y.$$

Otherwise, with an Ivlev trophic function we obtain

$$p_0 = -\ln(1-\alpha), \quad \mu_0 = \frac{-(1-\alpha)\ln(1-\alpha)}{\alpha},$$

so that

$$r_0 = r_y \frac{-\alpha \ln(1-\alpha)}{\alpha + (1-\alpha)\ln(1-\alpha)} > r_y.$$

(iii) As a basic set of bioecological parameters to be used in numerical simulations, we have taken the values from Buffoni et al. [23], reported in the following table:

Parameter	r_x (d^{-1})	b (d^{-1})	m (d^{-1})	c	ϵ
Value	0.11	0.88	0.19	0.39	0.2

These data have been estimated in [24]. They refer to an acarine system, surveyed in biological control field experiments: the phytophagous mite *Tetranychus urticae* and its biological control agent, the predator mite *Phytoseiulus persimilis* [24]. We wish to point out that, by using this choice of parameters, some relations, characterizing the ecological system, are satisfied. The inequality (2.15) $\alpha = m/(cb) = 0.55 < 1$ is fulfilled, and then non trivial dynamics can be found. The maximum growth rate r_x of the prey is less than the one of the predator:

$$r_x = 0.11\ d^{-1} < r_y = cb - m = 0.15\ d^{-1}.$$

With a Holling-type II trophic function we have that $r_0 = r_y$. It follows that in the (h, p) plane the two straight lines $p/p_0 = \gamma h$ and $p/p_0 = \beta h + 1/\xi_0$ intersect. We have taken $r_x = 0.16\ d^{-1}$ in some numerical experiments to simulate the case $r_x > r_y$.

B The cusp bifurcation point

In Section 2.4.2 of Chapter 2, we found a cusp bifurcation point in B_0 in the (h, p)-plane regarding the coexistence equilibrium states. Here, we want to verify the conditions for a cusp bifurcation point.

First of all, we have to reduce the 2-dimensional system (2.1) on the center manifold, and then verify the conditions for a cusp bifurcation point (0.1) and (0.2). However, we can consider the following ODE

$$\dot{x} = F(x, h, p) = \frac{1}{x} + h\beta g(x) - \frac{p}{p_0}.$$

Its equilibrium points are the $x-$coordinates of the coexistence equilibria of (2.1), while the $y-$coordinates can be found thanks to

$$y_* = \beta x_* g(x_*).$$

Moreover, its equilibrium surface is the same of the general system (2.1).

- We have that $F(\eta_0, h_0, p_0\Phi_0) = 0$.
- We want to prove that $F_x(\eta_0, h_0, p_0\Phi_0) = 0$.

$$\begin{aligned} F_x &= -\frac{1}{x^2} + h\beta g'(x) = \frac{1}{x^2}\left(-1 + h\beta x^2 g'(x)\right) \\ &= \frac{1}{x^2}\left(-1 + h\psi(x)\right). \\ F_x(\eta_0, h_0, p_0\Phi_0) &= \frac{1}{\eta_0^2}\left(-1 + h_0\psi(\eta_0)\right) = 0. \end{aligned}$$

- We want to prove that $F_{xx}(\eta_0, h_0, p_0\Phi_0) = 0$.

$$\begin{aligned} F_{xx} &= -\frac{2}{x^3}(-1 + h\psi(x)) + \frac{1}{x^2}h\psi'(x). \\ F_{xx}(\eta_0, h_0, p_0\Phi_0) &= -\frac{2}{\eta_0^3}(-1 + h_0\psi(\eta_0)) + \frac{1}{\eta_0^2}h_0\psi'(\eta_0) = 0. \end{aligned}$$

- We want to prove that $F_{xxx}(\eta_0, h_0, p_0\Phi_0) \neq 0$.

$$
\begin{aligned}
F_{xxx} &= \frac{6}{x^4}(-1+h\psi(x)) - \frac{4}{x^3}h\psi'(x) + \frac{1}{x^2}h\psi''(x). \\
F_{xxx}(\eta_0, h_0, p_0\Phi_0) &= \frac{6}{\eta_0^4}(-1+h_0\psi(\eta_0)) - \frac{4}{\eta_0^3}h_0\psi'(\eta_0) + \frac{1}{\eta_0^2}h_0\psi''(\eta_0) \\
&= \frac{1}{\eta_0}h_0\psi''(\eta_0) < 0,
\end{aligned}
$$

since ψ has only one maximum in η_0.

- We want to prove that $(F_hF_{xp} - F_pF_{xh})(\eta_0, h_0, p_0\Phi_0) \neq 0$.

$$
\begin{aligned}
F_h &= \beta g(x), \\
F_{xp} &= 0, \\
F_p &= -\frac{1}{p_0}, \\
F_{xh} &= \beta g'(x). \\
(F_hF_{xp} - F_pF_{xh})(\eta_0, h_0, p_0\Phi_0) &= \beta g'(\eta_0)\frac{1}{p_0} > 0.
\end{aligned}
$$

Thus, the conditions are satisfied.

C List of main symbols

t	time (d)
x	ratio between prey biomass and maximum of prey population size
y	ratio between predator biomass and maximum of prey population size
r_x	maximum specific rate of prey growth (d^{-1})
b	maximum specific rate of prey consumption (d^{-1})
m	specific rate of predator mortality (d^{-1})
c	conversion efficiency (from prey to predator biomass)
ϵ	ratio between minimum and maximum of prey population size
$g(x)$	adimensional function specifying the type of prey growth
$f\left(\frac{px}{1+hy}\right)$	adimensional functional response of predator to prey abundance
p	predation efficiency
h	measure of the predator interference during the predation process
α	m/cb

β	$r_x c/m$
r_y	$cb - m \quad (d^{-1})$
p_0	$f^{-1}(\alpha)$
$\mu(s)$	$sf'(s)/f(s)$
μ_0	$\mu(p_0)$
γ	$c\mu_0/(1-\mu_0)$
r_0	$m\mu_0/(1-\mu_0) \quad (d^{-1})$
$\Lambda(h,p)$	$1 - \mu_0 - c\mu_0 h p_0/p$
$\phi(x,h)$	$1/x + h\beta g(x)$
$\psi(x)$	$\beta x^2 g'(x)$
ξ_0	unique solution of $g'(x) = 0$
$\phi(\xi_0, h)$	$\beta h + 1/\xi_0$
η_0	unique solution of $\psi'(x) = 0$
h_0	$1/\psi(\eta_0)$
h_1	$1/\psi(\epsilon)$
h_ϵ	unique solution of $\phi_1(h) = 1/\epsilon$
η_1	unique solution of $\psi(x) = 1/h_1$ in the range (η_0, ξ_0)
$\xi_1(h),\ \xi_2(h)$	solutions of $\psi(x) = 1/h$, $\xi_1(h) \geq \xi_2(h)$
ϕ_0	$\phi(\eta_0, h_0)$
B_0	cusp point $(h_0, p_0\phi_0)$
$\phi_j(h)$	$\phi(\xi_j(h), h), \quad j = 1, 2$
$p_1(h)$	Hopf bifurcation value for p
$p_2(h)$	global bifurcation value for p
h_R	$1/(\xi_0(\gamma - \beta))$, unique solution to $\gamma h = \beta h + 1/\xi_0$
h_S	unique solution of $\phi_1(h) = \gamma h$
h_U	unique solution of $p_2(h) = p_0\phi_2(h)$
h_{BT}	unique solution of $p_1(h) = p_0\phi_1(h)$

Part II

About reaction-diffusion predator-prey systems involving the Holling-type II and the Beddington-DeAngelis functional responses

5

Introduction

This Part[1] focuses on the study of two predator-prey models with diffusion that justify, in a suitable limit, two classical types of functional responses in the reaction part and present a cross-diffusion term in the predator equation. We also look for conditions on the parameters values which lead to Turing instability.

Complex functional responses are quite usual in predator-prey models [1, 14, 29, 55, 58]. For example, the Holling-type II functional response [55] is based on the idea that predators will catch a limited amount of prey in the case when prey are abundant. Denoting with $N := N(t)$ the prey biomass and with $P := P(t)$ the predator biomass, this type of functional response leads to the following system of two ODEs:

$$\begin{aligned} \dot{N} &= r_0 g(N) - \frac{bNP}{1+kN}, \\ \dot{P} &= \frac{cbNP}{1+kN} - \mu P, \end{aligned} \tag{5.1}$$

with $r_0,\ b,\ c,\ k,\ \mu > 0$; the function g describes the prey growth and can be either linear, that is $g(N) = N$, or involve a logistic part, so that $g(N) = (1-\eta N)N$ with $\eta \geq 0$ [13]. Note that when $g(N) = N$ and $k = 0$, one recovers the Lotka-Volterra predator-prey model.

If one also wishes to take into account the competition between predators when they try to catch prey, one can use the slightly more complex Beddington-DeAngelis functional response [14, 29]:

[1] Most of the contents of this Part will be included in the paper in preparation: F. Conforto, L. Desvillettes, C. Soresina, *About reaction-diffusion systems involving the Holling-type II and the Beddington-DeAngelis functional responses for predator-prey models.*

$$\begin{aligned} \dot{N} &= r_0 g(N) - \frac{bNP}{1+kN+hP}, \\ \dot{P} &= \frac{cbNP}{1+kN+hP} - \mu P, \end{aligned} \tag{5.2}$$

with $r_0,\ b,\ c,\ k,\ \mu > 0$ and also $h > 0$.

An important point in the sequel will be the observation that predator-prey reaction-diffusion models with the Beddington-DeAngelis functional response in the reaction part are known to produce patterns (coming out of a Turing instability) when diffusion terms with suitable rates (denoted by $d_N,\ d_P$) are added to the reaction terms [105, 51]. In this case the densities $N,\ P$ also depends on space coordinates, and the system writes

$$\begin{aligned} \partial_t N - d_N \Delta_x N &= r_0 g(N) - \frac{bNP}{1+kN+hP}, \\ \partial_t P - d_P \Delta_x P &= \frac{cbNP}{1+kN+hP} - \mu P. \end{aligned} \tag{5.3}$$

On the opposite, no Turing-patterns are known to appear in the case of a reaction-diffusion predator-prey model with a Holling-type II functional response and standard diffusion terms [10] (except when richer dynamics are considered, for example when one adds quadratic intra-predator interaction or fighting term [71, 69], or even a density-dependent predator mortality [69]; the case of non-Turing patterns, that means $d_N = d_P$, is studied in [81, 82, 72]).

An interesting modeling issue consists in finding a simple and somewhat realistic "microscopic model" (in terms of time scales) which in some limit leads, at least formally, to systems (5.1) or (5.2). Such a microscopic model was designed by Metz and Diekmann [74] for the Holling-type II functional response, and by Geritz and Gyllenberg [41], Huisman and De Boer [56], for the Beddington-DeAngelis one. Metz and Diekmann proposed a system of three ODEs, in which the predators are divided in two classes, searching and handling predators, while the interaction between predators and prey is treated in a quite simple way (a Lotka-Volterra terms are considered). Predators which are searching for prey become handling with a rate proportional to the number of prey and come back to the searching state with a constant rate. Only handling predators contribute to the reproduction and give rise to a searching predator, while the mortality rate (in absence of prey) is constant and equal for the two classes. The searching-handling switch is supposed to happen on a much faster scale than the reproduction and mortality processes. The corresponding

parameter in the system of ODEs is therefore called $1/\varepsilon$, and the system writes (for some r_0, α, $\tilde{\gamma}$, Γ, μ, $\varepsilon > 0$)

$$\begin{aligned} \dot{N}^\varepsilon &= r_0 N^\varepsilon - \alpha N^\varepsilon p_s^\varepsilon, \\ \dot{p}_s^\varepsilon &= \frac{1}{\varepsilon}\left(-\alpha N^\varepsilon p_s^\varepsilon + \tilde{\gamma} p_h^\varepsilon\right) + \Gamma p_h^\varepsilon - \mu p_s^\varepsilon, \\ \dot{p}_h^\varepsilon &= \frac{1}{\varepsilon}\left(\alpha N^\varepsilon p_s^\varepsilon - \tilde{\gamma} p_h^\varepsilon\right) - \mu p_h^\varepsilon. \end{aligned} \tag{5.4}$$

It is shown that in the formal limit $\varepsilon \to 0$, $N^\varepsilon \to N$ and $p_s^\varepsilon + p_h^\varepsilon \to P$ where N, P satisfy (5.1) (with $b = \alpha$, $k = \alpha/\tilde{\gamma}$, $c = \Gamma/\tilde{\gamma}$, and $g(N) = N$) [74].

The same procedure was applied later by Geritz and Gyllenberg [41]: they divided not only the predator population into searchers and handlers, but also structured the prey population into two classes, the class of active prey (typically foraging) and prone to predation, and the class of those prey individuals who have found a refuge and cannot be caught by predators. In this way, they derived the Beddington-DeAngelis functional response in terms of mechanisms at the individual level avoiding the usual interference between predators. Also Huisman and De Boer [56], starting from a different four-dimensional model, use a reaction schemes and quasi-steady-state assumptions, obtaining a system of two ordinary differential equations; however, they had to simplify a complicated quadratic expression with a Padé approximation to recover the standard formula of the Beddington-DeAngelis functional response. In both cases, two different time scales are exploited.

In this Part we are interested in the introduction of diffusion processes in the asymptotic problem (5.4). Denoting by d_1, d_2, d_3 the diffusion rates of prey, searching predators and handling predators respectively (and taking into account a possible logistic term in the evolution of preys), we obtain the following reaction-diffusion system:

$$\begin{aligned} \partial_t N^\varepsilon - d_1 \Delta_x N^\varepsilon &= r_0 \left(1 - \eta N^\varepsilon\right) N^\varepsilon - \alpha N^\varepsilon p_s^\varepsilon, \\ \partial_t p_s^\varepsilon - d_2 \Delta_x p_s^\varepsilon &= \frac{1}{\varepsilon}\left(-\alpha N^\varepsilon p_s^\varepsilon + \tilde{\gamma}\, p_h^\varepsilon\right) + \Gamma p_h^\varepsilon - \mu p_s^\varepsilon, \\ \partial_t p_h^\varepsilon - d_3 \Delta_x p_h^\varepsilon &= \frac{1}{\varepsilon}\left(\alpha N^\varepsilon p_s^\varepsilon - \tilde{\gamma}\, p_h^\varepsilon\right) - \mu p_h^\varepsilon. \end{aligned} \tag{5.5}$$

Note that we systematically expect the diffusion rate d_3 of handling predators to be smaller than the the one of searching predators d_2. The formal limit of this system when $\varepsilon \to 0$ is the set of two cross reaction-diffusion equations

$$
\begin{aligned}
&\partial_t N - d_1 \Delta_x N = r_0(1-\eta N)N - \frac{\tilde{\gamma}\alpha N}{\alpha N + \tilde{\gamma}} P, \\
&\partial_t P - \Delta_x \left(\frac{d_2 \tilde{\gamma} + d_3 \alpha N}{\alpha N + \tilde{\gamma}} P \right) = \Gamma \frac{\alpha N}{\alpha N + \tilde{\gamma}} P - \mu P,
\end{aligned}
\tag{5.6}
$$

in which the reaction terms are identical (up to the change of name of the constant parameters) to those of (5.1), but in which the diffusion term relative to predators is much more complicated than a constant times Laplacian of P (terms like $d\Delta_x P$ will systematically be called linear diffusive terms in the sequel, while cross diffusion will refer to terms like $\Delta_x(f(N,P)P)$, where f is a smooth non-constant functions of $N,\ P$, as in the second equation of (5.6)). In Subsection 6.3, we state a rigorous theorem showing that convergence of solutions to system (5.5) towards solutions to system (5.6) indeed holds when suitable functional spaces are introduced.

The same procedure can be applied in the case of Beddington-DeAngelis-like functional response, (that is, systems of ODEs close to (5.2)). First, we introduce a system of three ODEs modeling the interaction between preys, handling and searching predators as in (5.5), but in which we also take into account the competition among predators when they look for prey. This is done thanks to the introduction of the denominator $1 + \xi\, P$, for some $\xi > 0$, in the interaction term between predators and prey. The system writes then as follows:

$$
\begin{aligned}
&\dot{N}^\varepsilon = r_0(1-\eta N^\varepsilon)N^\varepsilon - \frac{\alpha N^\varepsilon p_s^\varepsilon}{1+\xi p_s^\varepsilon}, \\
&\dot{p}_s^\varepsilon = \frac{1}{\varepsilon}\left(-\frac{\alpha N^\varepsilon p_s^\varepsilon}{1+\xi p_s^\varepsilon} + \tilde{\gamma} p_h^\varepsilon \right) + \Gamma p_h^\varepsilon - \mu p_s^\varepsilon, \\
&\dot{p}_h^\varepsilon = \frac{1}{\varepsilon}\left(\frac{\alpha N^\varepsilon p_s^\varepsilon}{1+\xi p_s^\varepsilon} - \tilde{\gamma} p_h^\varepsilon \right) - \mu p_h^\varepsilon.
\end{aligned}
\tag{5.7}
$$

Its formal limit when $\varepsilon \to 0$ is then a system close to (5.2), and also obtained in [56] starting from a more complex system of four ODEs.

A reaction-diffusion system when $d_1,\ d_2,\ d_3$ are still diffusive rates for prey, searching and handling predators, writes

$$
\begin{aligned}
\partial_t N^\varepsilon - d_1 \Delta_x N^\varepsilon &= r_0 \left(1 - \eta N^\varepsilon\right) N^\varepsilon - \frac{\alpha N^\varepsilon p_s^\varepsilon}{1 + \xi p_s^\varepsilon}, \\
\partial_t p_s^\varepsilon - d_2 \Delta_x p_s^\varepsilon &= \frac{1}{\varepsilon}\left(- \frac{\alpha N^\varepsilon p_s^\varepsilon}{1 + \xi p_s^\varepsilon} + \tilde{\gamma} p_h^\varepsilon \right) + \Gamma p_h^\varepsilon - \mu p_s^\varepsilon, \\
\partial_t p_h^\varepsilon - d_3 \Delta_x p_h^\varepsilon &= -\frac{1}{\varepsilon}\left(- \frac{\alpha N^\varepsilon p_s^\varepsilon}{1 + \xi p_s^\varepsilon} + \tilde{\gamma} p_h^\varepsilon \right) - \mu p_h^\varepsilon.
\end{aligned}
\tag{5.8}
$$

We present in Section 6.3 a rigorous result of convergence of the solutions of this system towards the solution of a reaction-cross diffusion system where the reaction part is close to (5.2). This system writes

$$
\begin{aligned}
\frac{\partial N}{\partial t} - d_1 \Delta_x N &= r_0 \left(1 - \eta N\right) N - \tilde{\gamma} \frac{2\alpha N P}{\tilde{\gamma} + \alpha N + \tilde{\gamma}\xi P + \sqrt{(\tilde{\gamma} + \alpha N - \tilde{\gamma}\xi P)^2 + 4\tilde{\gamma}^2 \xi P}}, \\
\frac{\partial P}{\partial t} - \Delta_x \left(f(N,P) P\right) &= \Gamma \frac{2\alpha N P}{\tilde{\gamma} + \alpha N + \tilde{\gamma}\xi P + \sqrt{(\tilde{\gamma} + \alpha N - \tilde{\gamma}\xi P)^2 + 4\tilde{\gamma}^2 \xi P}} - \mu P,
\end{aligned}
\tag{5.9}
$$

where

$$
\begin{aligned}
f(N,P) = d_2 &\frac{2\tilde{\gamma}}{\tilde{\gamma} + \alpha N - \tilde{\gamma}\xi P + \sqrt{(\tilde{\gamma} + \alpha N - \tilde{\gamma}\xi P)^2 + 4\tilde{\gamma}^2 \xi P}} \\
&+ d_3 \frac{2\alpha N}{\tilde{\gamma} + \alpha N + \tilde{\gamma}\xi P + \sqrt{(\tilde{\gamma} + \alpha N - \tilde{\gamma}\xi P)^2 + 4\tilde{\gamma}^2 \xi P}}.
\end{aligned}
$$

The proof of those theorems are based on estimates coming out of two classes of methods. On one hand, we use the duality lemmas devised for reaction-diffusion systems by M. Pierre and D. Schmitt [83]. More precisely, we use a version of those lemmas allowing to recover L^p regularity for $p > 2$ for the solutions of such systems [27, 21]. On the other hand, we also use entropy-like functionals which are strongly reminiscent of those used in works in which microscopic models for the Shigesada-Kawasaki-Teramoto system [89] are studied [33].

These proofs can also be compared to recent results in which cross reaction-diffusion systems are obtained as limits of standard reaction-diffusion systems with more equations, in the context of chemistry or biology [77, 59, 28, 17, 18, 52, 53, 54, 85].

As already mentioned, Beddington-DeAngelis-like functional response is particularly interesting since it is known that predator-dependent functional responses

lead to patterns when linear-diffusion terms are added to the reaction part, like for example in the following system

$$\begin{aligned}
\frac{\partial N}{\partial t} - d_1 \Delta_x N &= r_0 \left(1 - \eta N\right) N - \tilde{\gamma} \frac{2\alpha N P}{\tilde{\gamma} + \alpha N + \tilde{\gamma}\xi P + \sqrt{(\tilde{\gamma} + \alpha N - \tilde{\gamma}\xi P)^2 + 4\tilde{\gamma}^2 \xi P}}, \\
\frac{\partial P}{\partial t} - D \Delta_x P &= \Gamma \frac{2\alpha N P}{\tilde{\gamma} + \alpha N + \tilde{\gamma}\xi P + \sqrt{(\tilde{\gamma} + \alpha N - \tilde{\gamma}\xi P)^2 + 4\tilde{\gamma}^2 \xi P}} - \mu P.
\end{aligned} \tag{5.10}$$

However, if one consider that the Beddington-DeAngelis-like functional response is coming out of an asymptotics when $\varepsilon \to 0$ of (5.8), one should rather study the possible appearance of patterns starting from a system with cross diffusion terms (5.9). Note that for Holling-type II functional response, no patterns seem to appear, even with the cross diffusion model (5.6), under the (biologically reasonable) assumption $d_3 < d_2$.

In Chapter 7, we study the Turing instability regions associated to system (5.9) and (5.10). In order to do so, we first perform an adimensionalization, which enables to keep only a small number of parameters in the equations.

Then we make explicit the condition on the parameters which lead to the existence of an homogeneous coexistence equilibrium for (5.9) and (5.10). We also perform a stability analysis of this equilibrium (when it exists) at the ODEs level. Thus, we show that the Turing instability region (in terms of parameters) is nonempty, as expected, for both systems (5.9) and (5.10), and finally, we compare the size of these regions. The main point is the fact that the Turing instability region associated to system (5.9) is always strictly included in the Turing instability region of system (5.10).

As a consequence, the use of reaction-diffusion systems for predator-prey interactions of Beddington-DeAngelis-like in which standard diffusion is simply added to the reaction terms [35] may lead to an overestimation of the possibility of appearance of patterns (in the case when the Beddington-DeAngelis functional response is a consequence of the interactions between searching and handling predators).

It is worth to mention that in many instances, the introduction of cross-diffusion terms instead of standard (linear) diffusion terms leads exactly to the opposite result, that is, the increase of the set of parameter values in which patterns develop [96, 57].

6

A justification of classical functional responses

In this chapter, we consider a predator-prey system of three reaction-diffusion equations, incorporating the dynamics of handling and searching predators, and show that its solutions converge, when a small parameter tends to 0, towards the solutions of a reaction-cross diffusion predator-prey system involving a cross-diffusion term and a Holling-type II or a Beddington-DeAngelis-like functional response. With respect to the systems presented in the Introduction, we systematically use in the sequel (except than for Section 6.3) the parameter $k := 1/\eta$ in order to stick to the traditional concept of carrying capacity. This means of course that we work only in the case when $\eta > 0$, which corresponds to a logistic prey growth.

6.1 The derivation of the Holling-type II functional response

We consider a reaction-diffusion predator-prey model in which we distinguish two types of predators, those searching for prey and those busy handling a prey caught earlier, while the interaction between predators and prey is treated in a quite simple way (a Lotka-Volterra type interaction is considered). We suppose that the predation process happens in a region $\Omega \subset \mathbb{R}^N$, $(N = 1, 2, 3)$, assumed to be smooth ($\mathcal{C}^2$), bounded and connected, where the individuals are moving. We denote with $n^\varepsilon := n^\varepsilon(x,t) \geq 0$ the density of prey, with $p_s^\varepsilon := p_s(x,t) \geq 0$ and $p_h^\varepsilon := p_h(x,t) \geq 0$ the density of searching and handling predators, respectively (where $t \in \mathbb{R}, x \in \Omega$). We assume that each species has its own diffusion velocity and diffuse within a non-reactive background (suppose to be at rest). We shall also assume that individuals are confined in the region Ω, so that the flux of density of each species at the boundary $\partial\Omega$ is zero. This gives the homogeneous Neumann boundary conditions, no flux of

density of each species at the boundary:

$$\hat{n}(x) \cdot \nabla_x n^\varepsilon = 0, \quad \hat{n}(x) \cdot \nabla_x p_s^\varepsilon = 0, \quad \hat{n}(x) \cdot \nabla_x p_h^\varepsilon = 0,$$

where $\hat{n}(x)$ is the exterior unit normal vector to $\partial\Omega$ at point x.

Predators which are searching for preys become handling with a rate proportional to the number of preys and come back to the searching state with a constant rate. Only handling predators contribute to the reproduction and give rise to a searching predator, while the mortality rate is constant and equal for the two classes. The searching-handling switch is supposed to happen on a much faster scale than the reproduction and mortality processes, and than there are far less predators than prey. The corresponding parameter in the system of ODEs is therefore called $1/\varepsilon$, and the system writes (for some r_0, α, $\tilde{\gamma}$, Γ, μ, $\varepsilon > 0$, d_1, d_2, d_3)

$$\partial_t N^\varepsilon - d_1 \Delta_x N^\varepsilon = r_0 N^\varepsilon \left(1 - \frac{N^\varepsilon}{k}\right) - \alpha N^\varepsilon p_s^\varepsilon \tag{6.1a}$$

$$\partial_t p_s^\varepsilon - d_2 \Delta_x p_s^\varepsilon = \frac{1}{\varepsilon}\big(- \alpha N^\varepsilon p_s^\varepsilon + \tilde{\gamma} p_h^\varepsilon\big) + \Gamma p_h^\varepsilon - \mu p_s^\varepsilon, \tag{6.1b}$$

$$\partial_t p_h^\varepsilon - d_3 \Delta_x p_h^\varepsilon = \frac{1}{\varepsilon}\big(\alpha N^\varepsilon p_s^\varepsilon - \tilde{\gamma} p_h^\varepsilon\big) - \mu p_h^\varepsilon, \tag{6.1c}$$

together with initial conditions and homogeneous Neumann boundary conditions. In Section 6.3 we will rigorously prove that in the limit when $\varepsilon \to 0$, the solution N^ε, p_s^ε, p_h^ε of this system converges in a suitable topology towards $N \geq 0$, $p_s \geq 0$, $p_h \geq 0$ such that

$$p_h = \frac{\alpha N p_s}{\tilde{\gamma}}.$$

We now wish to write the limiting system

$$\partial_t N - d_1 \Delta_x N = r_0 N \left(1 - \frac{N}{k}\right) - \alpha N p_s$$

$$\partial_t (p_s + p_h) - \Delta_x \left(d_2 p_s + d_3 p_h\right) = \Gamma p_h - \mu (p_s + p_h),$$

in terms of the density of the prey N and totality of predators $P := p_s + p_h$, only; the equation for the totality of predators is obtained adding (6.1b) and (6.1c). At a formal level, we expect when $\varepsilon \to 0$ to obtain $\alpha N p_s = \tilde{\gamma} p_h$, that is, rewritten in terms of P,

$$p_s = \frac{\tilde{\gamma} P}{\alpha N + \tilde{\gamma}}, \qquad p_h = \frac{\tilde{\gamma} N P}{\alpha N + \tilde{\gamma}},$$

and

$$P := p_s + p_h = p_s + \frac{\alpha N p_s}{\tilde{\gamma}} = \frac{\tilde{\gamma} p_s + \alpha N p_s}{\tilde{\gamma}}.$$

Then, the limiting system can be written with $N,\ P$ as unknowns

$$\begin{aligned} \partial_t N - d_1 \Delta_x N &= rN\left(1 - \frac{N}{k}\right) - \frac{\tilde{\gamma}\alpha N P}{\alpha N + \tilde{\gamma}} \\ \partial_t P - \Delta_x \left(\frac{d_2\tilde{\gamma} + d_3\alpha N}{\alpha N + \tilde{\gamma}} P\right) &= \frac{\Gamma \alpha N P}{\alpha N + \tilde{\gamma}} - \mu P. \end{aligned} \tag{6.2}$$

This system still satisfy Neumann boundary conditions and is associated with the initial conditions $N(0,x) = N_{in}(x),\ P(0,x) = p_{s,in}(x) + p_{h,in}(x)$. We want to note that the limiting system presents a Holling-type II trophic function in the reaction part: in this sense, we have derived this type of functional response by a time-scale argument from a more complicated model. This fact is already known in the context of predator-prey models described by ordinary differential equation [74]. Moreover, the limiting system presents a cross-diffusion in the predator equation (the diffusion rate depends on the prey biomass), while the prey diffusion is still linear. This means that the diffusion term relative to predators is much more complicated than a constant times Laplacian of P (linear diffusive term), which can be simply added to the reaction part [35]. In particular, the diffusion term obtained by the time-scale argument depends on both the diffusion coefficient of searching and handling predators d_2 and d_3. In this case, we can write the the cross-diffusion term as

$$\Delta_x \left(f(N)P\right), \qquad f(N) = \frac{d_2\tilde{\gamma} + d_3\alpha N}{\alpha N + \tilde{\gamma}},$$

which is a monotonically decreasing function with $f(0) = d_2$ and $f(N) \to d_3$ when $N \to +\infty$. We also note that if there is no prey, no handling predators are present and the diffusion coefficient reduces to a constant one equal to the diffusion coefficient of searching predators. On the contrary, when there is a huge prey abundance, we expect that handling predators are more numerous than searching predators and the diffusion coefficient again reduces to a constant equal to the diffusion coefficient of handling predators. With respect to the linear case (which can be obtain with a constant f), the cross-diffusion term reduces the predator diffusion when the prey density increases.

6.1.1 Adimensionalization

In order to simplify the notations and to keep only meaningful parameters, we now propose an adimensionalization procedure, using the new variables $T,\ n,\ p$ instead

of $t,\ N,\ P$ in the following way:

$$t = \Theta T,\ N = \Sigma n,\ P = \Pi p.$$

After simplifications, the system (6.2) becomes

$$\frac{\partial n}{\partial T} - d_1 \Theta \Delta_x n = r_0 \Theta \left(1 - \frac{n}{k/\Sigma}\right) n - \frac{\alpha \Pi \Theta n p}{\frac{\alpha \Sigma}{\tilde{\gamma}} n + 1},$$

$$\frac{\partial p}{\partial T} - \Delta_x \left(\frac{d_2 \Theta + d_3 \Theta \frac{\alpha \Sigma}{\tilde{\gamma}} n}{\frac{\alpha \Sigma}{\tilde{\gamma}} n + 1} p \right) = \Theta \Gamma \frac{\frac{\alpha \Sigma}{\tilde{\gamma}} n p}{\frac{\alpha \Sigma}{\tilde{\gamma}} n + 1} - \Theta \mu p.$$

Choosing $\Theta,\ \Sigma,\ \Pi$ in such a way that $\alpha \Pi \Theta = 1,\ \alpha \Sigma / \tilde{\gamma} = 1,\ r_0 \Theta = 1$, we end up with the system

$$\frac{\partial n}{\partial T} - d_1 \Theta \Delta_x n = \left(1 - \frac{n}{k/\Sigma}\right) n - \frac{n p}{n+1},$$

$$\frac{\partial p}{\partial T} - \Delta_x \left(\frac{d_2 \Theta + d_3 \Theta n}{n+1} p \right) = \Theta \Gamma \frac{n p}{n+1} - \Theta \mu p.$$

We set $D_1 := d_1 \Theta,\ D_2 := d_2 \Theta,\ D_3 := d_3 \Theta,\ \nu := k/\Sigma,\ c = \Theta \Gamma,\ m = \Theta \mu$. Then, we end up with

$$\begin{aligned} \partial_t n - D_1 \Delta_x n &= n \left(1 - \frac{n}{\nu}\right) - \frac{n p}{1+n} \\ \partial_t p - \Delta_x \left(\frac{D_2 + D_3 n}{1+n} p \right) &= \frac{c n p}{1+n} - m p. \end{aligned} \tag{6.3}$$

6.2 The derivation of the Beddington-DeAngelis-like functional response

As in the previous section, we introduce a system of three ODEs modeling the interaction between prey, handling and searching predators, but in which we also take into account the competition among predators when they look for prey. This is done thanks to the introduction of the denominator $1 + \xi p_s^{\varepsilon}$, for some $\xi > 0$, in the interaction term between predators and prey [13]. The system becomes

$$\frac{\partial N^\varepsilon}{\partial t} - d_1 \Delta_x N^\varepsilon = r_0 \left(1 - \frac{N^\varepsilon}{k}\right) N^\varepsilon - \frac{\alpha N^\varepsilon p_s^\varepsilon}{1 + \xi p_s^\varepsilon}, \tag{6.4a}$$

$$\frac{\partial p_s^\varepsilon}{\partial t} - d_2 \Delta_x p_s^\varepsilon = \frac{1}{\epsilon}\left(-\frac{\alpha N^\varepsilon p_s^\varepsilon}{1 + \xi p_s^\varepsilon} + \tilde{\gamma} p_h^\varepsilon\right) + \Gamma p_h^\varepsilon - \mu p_s^\varepsilon, \tag{6.4b}$$

$$\frac{\partial p_h^\varepsilon}{\partial t} - d_3 \Delta_x p_h^\varepsilon = -\frac{1}{\epsilon}\left(-\frac{\alpha N^\varepsilon p_s^\varepsilon}{1 + \xi p_s^\varepsilon} + \tilde{\gamma} p_h^\varepsilon\right) - \mu p_h^\varepsilon. \tag{6.4c}$$

In Section 6.3 we will rigorously prove that in the limit when $\varepsilon \to 0$, the solution $N^\varepsilon,\ p_s^\varepsilon,\ p_h^\varepsilon$ of this system converges in a suitable topology towards $N \geq 0,\ p_s \geq 0,\ p_h \geq 0$ such that

$$p_h = \frac{1}{\tilde{\gamma}} \frac{\alpha N p_s}{1 + \xi p_s}, \tag{6.5}$$

and

$$P := p_s + p_h = p_s + \frac{1}{\tilde{\gamma}} \frac{\alpha N p_s}{1 + \xi p_s} = \frac{\tilde{\gamma}(1 + \xi p_s) p_s + \alpha N p_s}{\tilde{\gamma}(1 + \xi p_s)}.$$

We now wish to write the limiting system

$$\begin{aligned} &\partial_t N - d_1 \Delta_x N = r_0 \left(1 - \frac{N}{k}\right) N - \frac{\alpha N p_s}{1 + \xi p_s}, \\ &\partial_t (p_s + p_h) - \Delta_x (d_2 p_s + d_3 p_h) = \Gamma p_h - \mu (p_h + p_s), \end{aligned} \tag{6.6}$$

in terms of N and P only, where the second equation is obtained adding (6.4b) and (6.4c). We notice that p_s satisfies a second degree equation (when P is given):

$$\tilde{\gamma} \xi p_s^2 + (\tilde{\gamma} + \alpha N - \tilde{\gamma} \xi P) p_s - \tilde{\gamma} P = 0.$$

Then, we consider only the positive root of this equation:

$$p_s = \frac{-A + \sqrt{\Delta}}{2\tilde{\gamma}\xi} = \frac{2\tilde{\gamma} P}{A + \sqrt{\Delta}},$$

where we have denoted

$$A := \tilde{\gamma} + \alpha N - \tilde{\gamma} \xi P, \qquad \Delta = A^2 + 4\tilde{\gamma}^2 \xi P. \tag{6.7}$$

Note that $\Delta > 0$ since $P > 0$. Denoting by

$$B := \tilde{\gamma} + \alpha N + \tilde{\gamma} \xi P, \tag{6.8}$$

we also obtain from (6.5) the formula

$$p_h = \frac{2\alpha NP}{B + \sqrt{\Delta}},$$

where Δ can be computed in terms of B:

$$\begin{aligned}
\Delta &= A^2 + 4\tilde{\gamma}^2\xi P = (\tilde{\gamma} + \alpha N - \tilde{\gamma}\xi P)^2 + 4\tilde{\gamma}^2\xi P \\
&= \tilde{\gamma}^2 + (\alpha N)^2 + (\tilde{\gamma}\xi P)^2 + 2\tilde{\gamma}\alpha N - 2\tilde{\gamma}^2\xi P - 2\alpha N\tilde{\gamma}\xi P + 4\tilde{\gamma}^2\xi P \\
&= \tilde{\gamma}^2 + (\alpha N)^2 + (\tilde{\gamma}\xi P)^2 + 2\tilde{\gamma}\alpha N + 2\tilde{\gamma}^2\xi P + 2\alpha N\tilde{\gamma}\xi P - 4\alpha N\tilde{\gamma}\xi P \\
&= (\tilde{\gamma} + \alpha N + \tilde{\gamma}\xi P)^2 - 4\alpha N\tilde{\gamma}\xi P = B^2 - 4\alpha N\tilde{\gamma}\xi P.
\end{aligned}$$

Then the limiting system can be written with $N,\ P$ as unknowns

$$\begin{aligned}
&\frac{\partial N}{\partial t} - d_1\Delta_x N = r_0\left(1 - \frac{N}{k}\right)N - \tilde{\gamma}\frac{2\alpha NP}{B + \sqrt{\Delta}}, \\
&\frac{\partial P}{\partial t} - \Delta_x\left(d_2\frac{2\tilde{\gamma}P}{A + \sqrt{\Delta}} + d_3\frac{2\alpha NP}{B + \sqrt{\Delta}}\right) = \Gamma\frac{2\alpha NP}{B + \sqrt{\Delta}} - \mu P,
\end{aligned} \tag{6.9}$$

remembering the definition of $A,\ B$ and Δ in (6.7) and (6.8). The limiting system presents a cross-diffusion term in the predator equation (the diffusion rate depends on the prey biomass), and a trophic function close to the Beddington-DeAngelis one.

This system still satisfy Neumann boundary conditions and is associated with the initial conditions $N(0,x) = N_{in}(x),\ P(0,x) = p_{s,in}(x) + p_{h,in}(x)$. We note that the limiting system presents a functional response close to the Beddington-DeAngelis in the reaction part: in this sense, we have derived this type of functional response by a time-scale argument from a more complicated model. This type of functional response was derived also by Huisman et al. [56] in the context of ordinary differential equations, starting from a system of four ODEs by a quasi-steady-state approximation. With their approach, also the logistic growth and the predator turnover terms still depend on this complex expression. Thereafter, they have simplified this complicated quadratic expression with a Padé approximation and they recovered the standard formula of the Beddington-DeAngelis functional response.

Moreover we can also note that, as in the previous Section where we have derived the Holling-type II functional response, the limiting system presents a cross-diffusion term in the predator equation (the diffusion rate depends on the prey biomass), while the prey diffusion is still linear. This means that the diffusion term relative to

predators is much more complicated than a constant times Laplacian of P (linear diffusive term), which can be simply added to the reaction part [35]. In particular, the diffusion term obtained by the time-scale argument depends on both the diffusion coefficient of searching and handling predators d_2 and d_3. Otherwise, here the cross diffusion term depends also on P: we can write the the cross-diffusion term as

$$\Delta_x \left(f(N,P)P\right), \qquad f(N,P) = d_2 \frac{2\tilde{\gamma}P}{A+\sqrt{\Delta}} + d_3 \frac{2\alpha NP}{B+\sqrt{\Delta}},$$

remembering that $\Delta := \Delta(N,P)$. As in the previous case, we have that $f(0,P) = d_2$ and $f(N,P) \to d_3$ when $N \to +\infty$.

6.2.1 Adimensionalization

In order to simplify the notations and to keep only meaningful parameters, we now propose an adimensionalization procedure, using the new variables $T,\ n,\ p$ instead of $t,\ N,\ P$ in the following way:

$$t = \Theta T,\ N = \Sigma n,\ P = \Pi p.$$

After simplifications, the system (6.9) becomes

$$\frac{\partial n}{\partial T} - d_1 \Theta \Delta_x n = r_0 \Theta \left(1 - \frac{n}{k/\Sigma}\right) n - \frac{2\tilde{\gamma}\alpha\Pi\Theta np}{B+\sqrt{\Delta}},$$

$$\frac{\partial p}{\partial T} - \Delta_x \left(d_2 \Theta \frac{2\tilde{\gamma}p}{A+\sqrt{\Delta}} + d_3 \Theta \frac{2\alpha\Sigma np}{B+\sqrt{\Delta}}\right) = \frac{2\Gamma\alpha\Sigma\Theta np}{B+\sqrt{\Delta}} - \mu\Theta p,$$

where

$$A + \sqrt{\Delta} = \tilde{\gamma} + \alpha\Sigma n - \tilde{\gamma}\xi\Pi p + \sqrt{(\tilde{\gamma} + \alpha\Sigma n + \tilde{\gamma}\xi\Pi p)^2 - 4\tilde{\gamma}\alpha\xi\Sigma\Pi np},$$
$$B + \sqrt{\Delta} = \tilde{\gamma} + \alpha\Sigma n + \tilde{\gamma}\xi\Pi p + \sqrt{(\tilde{\gamma} + \alpha\Sigma n + \tilde{\gamma}\xi\Pi p)^2 - 4\tilde{\gamma}\alpha\xi\Sigma\Pi np}.$$

Choosing $\Theta,\ \Sigma,\ \Pi$ in such a way that $2\alpha\Pi\Theta = 1,\ \alpha\Sigma = 1,\ \tilde{\gamma}\xi\Pi = 1$, we end up with the system

$$\frac{\partial n}{\partial T} - d_1 \Theta \Delta_x n = r_0 \Theta \left(1 - \frac{n}{k/\Sigma}\right) n - \frac{\tilde{\gamma}np}{B+\sqrt{\Delta}},$$

$$\frac{\partial p}{\partial T} - \Delta_x \left(d_2 \Theta \frac{2\tilde{\gamma}p}{A+\sqrt{\Delta}} + d_3 \Theta \frac{2np}{B+\sqrt{\Delta}}\right) = \frac{\Gamma\tilde{\gamma}\Sigma\xi np}{B+\sqrt{\Delta}} - \mu\Theta p,$$

where now

$$A+\sqrt{\Delta}=\tilde{\gamma}+n-p+\sqrt{(\tilde{\gamma}+n+p)^2-4np},$$
$$B+\sqrt{\Delta}=\tilde{\gamma}+n+p+\sqrt{(\tilde{\gamma}+n+p)^2-4np}.$$

We set $D_1 := d_1\Theta,\ D_2 := d_2\Theta,\ D_3 := d_3\Theta,\ r = r_0\Theta,\ \nu := k/\Sigma$. Furthermore, we denote again n by N, p by P, $\tilde{\gamma}$ by γ, and $\Gamma := \Gamma\tilde{\gamma}\Sigma\xi,\ \mu := \mu\Theta$. We end up with

$$\begin{aligned}\frac{\partial N}{\partial T}-D_1\Delta_x N &= r\left(1-\frac{N}{\nu}\right)N-\frac{\gamma NP}{B+\sqrt{\Delta}},\\ \frac{\partial P}{\partial T}-\Delta_x\left(D_2\frac{2\gamma P}{A+\sqrt{\Delta}}+D_3\frac{2NP}{B+\sqrt{\Delta}}\right) &= \frac{\Gamma NP}{B+\sqrt{\Delta}}-\mu P,\end{aligned} \tag{6.10}$$

where now

$$A=\gamma+N-P,\quad B=\gamma+N+P,\quad \Delta=(\gamma+N+P)^2-4NP. \tag{6.11}$$

Rationalizing the denominators, we can obtain an equivalent expression, which will be useful for the stability analysis of equilibrium states of the non diffusive part:

$$\begin{aligned}\frac{\partial N}{\partial T}-D_1\Delta_x N &= r\left(1-\frac{N}{\nu}\right)N-\frac{\gamma}{4}\left(B-\sqrt{B^2-4NP}\right),\\ \frac{\partial P}{\partial T}-\Delta_x\left(\frac{D_2}{2}(\sqrt{\Delta}-A)+\frac{D_3}{2}(B-\sqrt{\Delta})\right) &= \frac{\Gamma}{4}\left(B-\sqrt{B^2-4NP}\right)-\mu P,\end{aligned} \tag{6.12}$$

where $A,\ B$ and Δ are defined by (6.11).

6.3 Rigorous results of convergence

We consider in this section the family (when $\varepsilon > 0$) of systems described in (5.8), that is:

$$\partial_t N^\varepsilon - d_1\Delta_x N^\varepsilon = r_0\left(1-\eta N^\varepsilon\right)N^\varepsilon-\frac{\alpha N^\varepsilon p_s^\varepsilon}{1+\xi p_s^\varepsilon}, \tag{6.13a}$$

$$\partial_t p_s^\varepsilon - d_2\Delta_x p_s^\varepsilon = \frac{1}{\varepsilon}\left(-\frac{\alpha N^\varepsilon p_s^\varepsilon}{1+\xi p_s^\varepsilon}+\tilde{\gamma}p_h^\varepsilon\right)+\Gamma p_h^\varepsilon-\mu p_s^\varepsilon, \tag{6.13b}$$

$$\partial_t p_h^\varepsilon - d_3\Delta_x p_h^\varepsilon = -\frac{1}{\varepsilon}\left(-\frac{\alpha N^\varepsilon p_s^\varepsilon}{1+\xi p_s^\varepsilon}+\tilde{\gamma}p_h^\varepsilon\right)-\mu p_h^\varepsilon, \tag{6.13c}$$

together with homogeneous Neumann boundary conditions

$$\hat{n}(x) \cdot \nabla_x N^\varepsilon = 0, \quad \hat{n}(x) \cdot \nabla_x p_s^\varepsilon = 0, \quad \hat{n}(x) \cdot \nabla_x p_h^\varepsilon = 0,$$

where $\eta \geq 0$ and $\xi \geq 0$.

When both η and ξ are equal to zero, the reaction part of the system (6.13a)-(6.13c) reduces to (5.4). In this subsection, we assume that $\eta \geq 0$ (that is, we treat simultaneously cases with or without logistic effects for the preys). We however treat separately the case when $\xi = 0$ (leading to Holling-type II functional response) and the case when $\xi > 0$ (leading to Beddington-DeAngelis-like functional response).

We want to rigorously prove that in the limit when $\varepsilon \to 0$, the solution N^ε, p_s^ε, p_h^ε of this system converges in a suitable topology towards $N \geq 0$, $p_s \geq 0$, $p_h \geq 0$. The main results are based on the notion of very-weak solutions (see Appendix A).

The following theorem refers to the case $\xi = 0$.

Theorem 6.3.1 *Let Ω be a smooth domain of $\mathbb{R}^d$ (for some dimension $d \in \mathbb{N} - \{0\}$), $d_1, d_2, d_3 > 0$ be diffusion rates, r_0, α, $\tilde{\gamma}$, Γ, $\mu > 0$ and $\eta \geq 0$ be parameters, and $N_{in} := N_{in}(x) \geq 0$, $p_{h,in} := p_{h,in}(x) \geq 0$, $p_{s,in} := p_{s,in}(x) \geq 0$ be nonnegative initial data respectively in $L^\infty(\Omega)$, $L^2(\Omega)$, and $L^2(\Omega)$.*

Then for each $\varepsilon > 0$, there exists a unique global classical (for $t > 0$) solution (N^ε, p_h^ε, p_s^ε) of system (6.13a)-(6.13c) with $\xi = 0$, satisfying homogeneous Neumann boundary conditions (and with the initial data defined above).

Moreover, when $\varepsilon \to 0$, one can extract from N^ε a subsequence which is bounded in $L^\infty([0,T] \times \Omega)$ for all $T > 0$, and converges a.e. towards a function $N \geq 0$ lying in $L^\infty([0,T] \times \Omega)$. One can extract from p_s^ε a subsequence which converges weakly in $L^{2+\delta}([0,T] \times \Omega)$ towards a function $p_s \geq 0$ lying in $L^{2+\delta}([0,T] \times \Omega)$ for all $T > 0$ and some $\delta > 0$. Finally, one can extract from p_h^ε a subsequence which converges towards a function $p_h \geq 0$ belonging to $L^{2+\delta}([0,T] \times \Omega)$ weakly in $L^{2+\delta}([0,T] \times \Omega)$ for all $T > 0$ and some $\delta > 0$.

Moreover, N, p_s and p_h are very-weak solutions of the cross-diffusion system

$$\partial_t N - d_1 \Delta_x N = r_0(1 - \eta N)N - \alpha N p_s, \tag{6.14}$$

$$\partial_t (p_s + p_h) - \Delta_x (d_2 p_s + d_3 p_h) = \Gamma p_h - \mu(p_h + p_s), \tag{6.15}$$

$$\alpha N p_s = \tilde{\gamma} p_h, \tag{6.16}$$

with homogeneous Neumann boundary conditions

$$\hat{n}(x) \cdot \nabla_x N = 0, \quad \hat{n}(x) \cdot \nabla_x p_s = 0, \quad \hat{n}(x) \cdot \nabla_x p_h = 0,$$

and with initial data $N(0,x) = N_{in}(x)$ *and* $(p_s + p_h)(0,x) = p_{s,in}(x) + p_{h,in}(x)$. *This system can be rewritten in the simpler form (with* $P = p_h + p_s$*)*

$$\partial_t N - d_1 \Delta_x N = r_0(1-\eta N)N - \frac{\tilde{\gamma}\alpha N}{\alpha N + \tilde{\gamma}} P,$$
$$\partial_t P - \Delta_x \left(\frac{d_2\tilde{\gamma} + d_3 \alpha N}{\alpha N + \tilde{\gamma}} P \right) = \Gamma \frac{\alpha N}{\alpha N + \tilde{\gamma}} - \mu P,$$

with Neumann boundary conditions $\hat{n}(x) \cdot \nabla_x N = 0, \quad \hat{n}(x) \cdot \nabla_x P = 0$, *and with initial data* $N(0,x) = N_{in}(x)$ *and* $P(0,x) = p_{s,in}(x) + p_{h,in}(x)$.

Finally, N *lies in* $W^{1,2+\delta}([0,T]; L^{2+\delta}(\Omega)) \cap L^{2+\delta}([0,T]; W^{2,2+\delta}(\Omega))$ *for all* $T > 0$ *and some* $\delta > 0$ *(and* P *lies in* $L^{2+\delta}([0,T] \times \Omega])$*).*

The conclusion of this theorem can be somewhat extended in the case of low dimension (and strictly positive initial data). We can in fact show the following proposition.

Proposition 6.3.1 *Under the same assumptions as in Theorem 6.3.1, and under the extra assumptions that the dimension is* $d = 1$ *or* $d = 2$, *and that* $\inf ess\, N_{in}(x) > 0$, *the sequences* p_h^ε *and* p_s^ε *converge a.e. towards* p_h *and* p_s. *Moreover, the quantities* p_h, p_s *(and* P*) lie in* $L^1([0,T]; W^{1,1}(\Omega))$ *for all* $T > 0$.

We now turn to the case when $\xi \neq 0$:

Theorem 6.3.2 *Let* Ω *be a smooth domain of* $\mathbb{R}^d$ *(for some dimension* $d \in \mathbb{N} - \{0\}$*),* $d_1,\ d_2,\ d_3 > 0$ *be diffusion rates,* $r_0, \alpha, \xi, \tilde{\gamma}, \Gamma, \mu > 0$ *and* $\eta \geq 0$ *be parameters, and* $N_{in} := N_{in}(x) \geq 0$, $p_{h,in} := p_{h,in}(x) \geq 0$, $p_{s,in} := p_{s,in}(x) \geq 0$ *be nonnegative initial data respectively in* $L^\infty(\Omega)$, $L^2(\Omega)$, *and* $L^2(\Omega)$. *We assume moreover that* $\inf ess N_{in}(x) > 0$.

Then for each $\varepsilon > 0$, *there exists a unique global classical (for* $t > 0$*) solution* $(N^\varepsilon,\ p_h^\varepsilon,\ p_s^\varepsilon)$ *of system* (6.13a) -(6.13c) *satisfying homogeneous Neumann boundary conditions (and with the initial data defined above).*

Moreover, when $\varepsilon \to 0$, *one can extract from* N^ε *a subsequence which is bounded in* $L^\infty([0,T] \times \Omega)$ *for all* $T > 0$ *and converges a.e. towards a function* $N \geq 0$ *lying in* $L^\infty([0,T] \times \Omega)$, *from* p_s^ε *a subsequence which converges (strongly) in* $L^{2+\delta}([0,T] \times \Omega)$ *towards a function* $p_s \geq 0$ *lying in* $L^{2+\delta}([0,T] \times \Omega)$ *for all* $T > 0$ *and some* $\delta > 0$, *and from* p_h^ε *a subsequence which converges (strongly) towards a function* $p_h \geq 0$ *lying in* $L^{2+\delta}([0,T] \times \Omega)$ *in* $L^{2+\delta}([0,T] \times \Omega)$ *for all* $T > 0$ *and some* $\delta > 0$.

Moreover, N, p_s *and* p_h *are very-weak solutions of the cross diffusion system*

$$\partial_t N - d_1 \Delta_x N = r_0 \left(1 - \eta N\right) N - \frac{\alpha N p_s}{1 + \xi p_s}, \tag{6.17}$$

$$\partial_t (p_s + p_h) - \Delta_x (d_2 p_s + d_3 p_h) = \Gamma p_h - \mu (p_h + p_s), \tag{6.18}$$

$$\frac{\alpha N p_s}{1 + \xi p_s} = \tilde{\gamma} p_h, \tag{6.19}$$

with homogeneous Neumann boundary conditions

$$\hat{n}(x) \cdot \nabla_x N = 0, \quad \hat{n}(x) \cdot \nabla_x p_s = 0, \quad \hat{n}(x) \cdot \nabla_x p_h = 0,$$

and with initial data $N(0,x) = N_{in}(x)$ *and* $(p_s + p_h)(0,x) = p_{s,in}(x) + p_{h,in}(x)$.

Finally, N *lies in* $W^{1,p}([0,T]; L^p(\Omega))$ *and* $L^p([0,T]; W^{2,p}(\Omega))$ *for all* $T > 0$ *and all* $p \in [1, +\infty[$, p_h *lies in* $L^2([0,T]; H^1(\Omega))$, *and* p_s *lies in* $L^1([0,T]; W^{1,1}(\Omega))$.

We denote from now on by $C_T > 0$ a constant which may depend on T, the parameters, and the initial data of the considered systems.

6.3.1 Proof of Theorem. 6.3.1

We consider system (6.13a)-(6.13c) with $\xi = 0$.

The existence of global in time solutions (for which N^ε, p_s^ε, p_h^ε are nonnegative) for a given $\varepsilon > 0$ to this system, is classical [31].

The r.h.s. of equation (6.13a) is bounded above by $r_0 N^\varepsilon$. Then, for each $T > 0$, there exists $C_T > 0$ such that

$$\sup_{\varepsilon > 0} ||N^\varepsilon||_{L^\infty([0,T] \times \Omega)} \leq C_T,$$

thanks to the maximum principle (or comparison principle); in fact C_T can be bounded above by $||N_{in}||_{L^\infty} e^{r_0 T}$. As a consequence, there exists $N \in L^\infty([0,T] \times \Omega)$ and a subsequence (still denoted by N^ε) such that $N^\varepsilon \rightharpoonup N$ in $L^\infty([0,T] \times \Omega)$ weak $*$ topology.

Adding the equations for p_h^ε and p_s^ε, we end up with

$$\partial_t P^\varepsilon - \Delta_x (A^\varepsilon P^\varepsilon) = \Gamma p_h^\varepsilon - \mu P^\varepsilon \leq \Gamma P^\varepsilon, \tag{6.20}$$

with

$$P^\varepsilon = p_h^\varepsilon + p_s^\varepsilon, \qquad A^\varepsilon = \frac{d_2 p_h^\varepsilon + d_3 p_s^\varepsilon}{p_h^\varepsilon + p_s^\varepsilon}.$$

Then, thanks to a duality lemma (cf. [32] and the older reference [84]) we see that

$$\sup_{\varepsilon>0} ||P^\varepsilon||_{L^2([0,T]\times\Omega)} \leq C_T.$$

A refined version of the same lemma (cf. for example [27] or [21]) yields in fact the better estimate

$$\sup_{\varepsilon>0} ||P^\varepsilon||_{L^{2+\delta}([0,T]\times\Omega)} \leq C_T,$$

for some $\delta > 0$.

As a consequence, there exist $p_h, p_s \in L^{2+\delta}([0,T]\times\Omega)$ and subsequences (still denoted by $p_h^\varepsilon, p_s^\varepsilon$) such that $p_s^\varepsilon \rightharpoonup p_s$, $p_h^\varepsilon \rightharpoonup p_h$ in $L^{2+\delta}([0,T]\times\Omega)$ weak topology (for some $\delta > 0$).

Observing that $\partial_t N^\varepsilon - d_1 \Delta_x N^\varepsilon$ is bounded in $L^{2+\delta}([0,T]\times\Omega)$ for all $T > 0$ and some $\delta > 0$, we get thanks to the maximal regularity estimates for the heat kernel

$$\sup_{\varepsilon>0} ||\partial_t N^\varepsilon||_{L^{2+\delta}([0,T]\times\Omega)} \leq C_T,$$

$$\sup_{\varepsilon>0} ||\partial_{x_i x_j} N^\varepsilon||_{L^{2+\delta}([0,T]\times\Omega)} \leq C_T.$$

As a consequence, we see that the sequence N^ε is strongly compact in $L^2([0,T]\times\Omega)$, so that (up to an extra extraction) N^ε converges a.e. towards N. We also see that N lies in $W^{1,2+\delta}([0,T]; L^{2+\delta}(\Omega)) \cap L^{2+\delta}([0,T]; W^{2,2+\delta}(\Omega))$.

Using the bound in $L^{2+\delta}$ of p_s^ε, we end up with the convergence $N^\varepsilon p_s^\varepsilon \rightharpoonup N p_s$ in $L^{2+\delta}([0,T]\times\Omega)$ weak (for all $T > 0$ and some $\delta > 0$).

Passing to the limit in the equations (6.13a) and (6.20) in the sense of distributions, we end up with the equations (6.14) and (6.15). More precisely, passing to the limit in the very-weak formulation of equations (6.13a) and (6.20), we get the very-weak formulation of the above system together with the homogeneous Neumann boundary condition on N and P, and the initial data for N and P (that is $P(0,x) = p_{s,in}(x) + p_{h,in}(x)$).

Observing that

$$p_h^\varepsilon - N^\varepsilon p_s^\varepsilon = \varepsilon(\partial_t p_s^\varepsilon - d_2 \Delta_x p_s^\varepsilon) - \varepsilon(p_h^\varepsilon - \mu p_s^\varepsilon),$$

and passing to the limit in the sense of distributions in this statement, we get identity (6.16), which concludes the proof of Theorem. 6.3.1.

□

6.3.2 Proof of Proposition 6.3.1

We compute, for $q \in]0,1[$, the time derivative of a suitable nonnegative quantity:

$$\begin{aligned}
&\frac{d}{dt}\int\left[\frac{(p_h^\varepsilon)^{q+1}}{q+1}+\left|\frac{\alpha}{\tilde\gamma}N^\varepsilon\right|^q\frac{(p_s^\varepsilon)^{q+1}}{q+1}\right]\\
&\quad=-\underbrace{d_3 q\int(p_h^\varepsilon)^{q-1}|\nabla_x p_h^\varepsilon|^2}_{\boxed{1}}-\underbrace{d_2 q\left(\frac{\alpha}{\tilde\gamma}\right)^q\int(N^\varepsilon)^q(p_s^\varepsilon)^{q-1}|\nabla_x p_s^\varepsilon|^2}_{\boxed{2}}\\
&\qquad-\underbrace{\frac{\tilde\gamma}{\varepsilon}\int\left(p_h^\varepsilon-\left(\frac{\alpha}{\tilde\gamma}\right)N^\varepsilon p_s^\varepsilon\right)\left((p_h^\varepsilon)^q-\left(\frac{\alpha}{\tilde\gamma}N^\varepsilon p_s^\varepsilon\right)^q\right)}_{\boxed{3}}\\
&\qquad-\underbrace{\mu\int\left[(p_h^\varepsilon)^{q+1}+\left(\frac{\alpha}{\tilde\gamma}N^\varepsilon\right)^q(p_s^\varepsilon)^{q+1}\right]}_{\boxed{4}}+\underbrace{\Gamma\left(\frac{\alpha}{\tilde\gamma}\right)^q\int(N^\varepsilon)^q(p_s^\varepsilon)^q p_h^\varepsilon}_{\boxed{5}}\\
&\qquad+\underbrace{\frac{q}{q+1}\left(\frac{\alpha}{\tilde\gamma}\right)^q\int(p_s^\varepsilon)^{q+1}(N^\varepsilon)^{q-1}(\partial_t N^\varepsilon+d_2\Delta_x N^\varepsilon)}_{\boxed{6}}\\
&\qquad\qquad-\underbrace{d_2\frac{q(1-q)}{1+q}\left(\frac{\alpha}{\tilde\gamma}\right)^q\int(p_s^\varepsilon)^{q+1}(N^\varepsilon)^{q-2}|\nabla_x N^\varepsilon|^2}_{\boxed{7}}.
\end{aligned}\tag{6.21}$$

We observe that the terms $\boxed{1}$, $\boxed{2}$, $\boxed{3}$, $\boxed{4}$, $\boxed{7}$ are all nonpositive. Remembering that N^ε is bounded in L^∞, and that p_s^ε, p_h^ε are bounded in $L^{2+\delta}$ for some $\delta>0$, we see that

$$\int_0^T\int(N^\varepsilon)^q(p_s^\varepsilon)^q p_h^\varepsilon\le C_T\qquad(\text{for all } q\in]0,1[).$$

Remembering then that $\partial_t N^\varepsilon+d_2\Delta_x N^\varepsilon$ is bounded in $L^{2+\delta}$ for some $\delta>0$, we see that

$$\int_0^T\int|p_s^\varepsilon|^{q+1}|\partial_t N^\varepsilon+d_2\Delta_x N^\varepsilon|\le C_T\qquad\text{when } q\in]0,1[\text{ is small enough.}$$

As a consequence, integrating (6.21) on $[0,T]$, we see that (for $q\in]0,1[$ small enough)

$$\int \left(p_h^\varepsilon - (\alpha/\tilde{\gamma})N^\varepsilon p_s^\varepsilon\right)\left((p_h^\varepsilon)^q - ((\alpha/\tilde{\gamma})N^\varepsilon p_s^\varepsilon)^q\right) \leq C_T\varepsilon, \tag{6.22}$$

$$\int_0^T \int_\Omega (p_h^\varepsilon)^{q-1}|\nabla_x p_h^\varepsilon|^2 \leq C_T,$$

$$\int_0^T \int_\Omega (N^\varepsilon)^q (p_s^\varepsilon)^{q-1}|\nabla_x p_s^\varepsilon|^2 \leq C_T.$$

Observing that

$$(\partial_t - d_1\Delta_x)\ln N^\varepsilon = \frac{1}{N^\varepsilon}(\partial_t - d_1\Delta_x)N^\varepsilon + d_1\frac{|\nabla_x N^\varepsilon|^2}{(N^\varepsilon)^2}$$
$$\geq r_0(1-\eta N^\varepsilon) - \alpha p_s^\varepsilon \geq (-\eta r_0 - \alpha p_s^\varepsilon)C_T,$$

we see that since p_s^ε is bounded in $L^{2+\delta}([0,T]\times\Omega)$ for some $\delta > 0$, in dimension $d = 1$ or $d = 2$, we obtain that N^ε is bounded below (by a strictly positive constant). Indeed, we recall that $(\partial_t - d_1\Delta_x)^{-1}$ acts as a convolution with a function lying in $L^{3-\varepsilon}$ (when $d = 1$) or $L^{2-\varepsilon}$ (when $d = 2$) for any $\varepsilon > 0$, so that thanks to Young's inequality and the assumption that the initial datum N^ε is essentially strictly positive, $\ln N^\varepsilon$ is bounded below (by a strictly positive constant). As a consequence, still for $q \in]0,1[$ small enough,

$$\int_0^T \int_\Omega (p_s^\varepsilon)^{q-1}|\nabla_x p_s^\varepsilon|^2 \leq C_T.$$

Then, Cauchy-Schwarz inequality ensures that

$$\left(\int_0^T \int_\Omega |\nabla_x p_{s,h}^\varepsilon|\right)^2 \leq \int_0^T \int_\Omega (p_{s,h}^\varepsilon)^{q-1}|\nabla_x p_{s,h}^\varepsilon|^2 \times \int_0^T \int_\Omega (p_{s,h}^\varepsilon)^{1-q} \leq C_T. \tag{6.23}$$

Using (6.20), we see that $\partial_t P^\varepsilon$ is bounded in $L^2([0,T];H^{-2}(\Omega))$, so that thanks to Aubin's lemma [76], P^ε converges a.e. to P. Since $p_h^\varepsilon - N^\varepsilon p_s^\varepsilon \to 0$ a.e. (up to extraction of a subsequence) because of (6.22), and N^ε converges a.e. to N, we see that p_h^ε converges a.e. to p_h, and p_s^ε converges a.e. to p_s. Finally, (6.23) implies that $p_h,\ p_s \in L^1([0,T],W^{1,1}(\Omega))$ for all $T > 0$.

□

6.3.3 Proof of Theorem. 6.3.2

As in Theorem 6.3.1, existence of solutions (for which $N^\varepsilon,\ p_s^\varepsilon,\ p_h^\varepsilon$ are nonnegative) for a given ε is classical [31].

As in Theorem. 6.3.1 again, for each $T > 0$, there exists $C_T > 0$ such that

$$\sup_{\varepsilon>0} ||N^\varepsilon||_{L^\infty([0,T]\times\Omega)} \leq C_T,$$

(and as a consequence, there exists $N \in L^\infty([0,T]\times\Omega)$ and a subsequence, still denoted by N^ε, such that $N^\varepsilon \rightharpoonup N$ in $L^\infty([0,T]\times\Omega)$ weak $*$) and such that

$$\sup_{\varepsilon>0} ||P^\varepsilon||_{L^{2+\delta}([0,T]\times\Omega)} \leq C_T,$$

for some $\delta > 0$ (and as a consequence, there exist $p_h, p_s \in L^{2+\delta}([0,T]\times\Omega)$ and subsequences, still denoted by $p_h^\varepsilon, p_s^\varepsilon$, such that $p_s^\varepsilon \rightharpoonup p_s$, $p_h^\varepsilon \rightharpoonup p_h$ in $L^{2+\delta}([0,T]\times\Omega)$ weak for some $\delta > 0$).

Now observing that the r.h.s. of (6.17) is bounded in $L^\infty([0,T]\times\Omega)$ (this held only in $L^{2+\delta}([0,T]\times\Omega)$ for some $\delta > 0$ in Theorem 6.3.1), the maximal regularity estimates for the heat kernel yield the bounds

$$\sup_{\varepsilon>0} ||\partial_t N^\varepsilon||_{L^p([0,T]\times\Omega)} \leq C_T, \tag{6.24}$$

$$\sup_{\varepsilon>0} ||\partial_{x_i x_j} N^\varepsilon||_{L^p([0,T]\times\Omega)} \leq C_T, \tag{6.25}$$

for all $p \in [1,+\infty[$, $i,j = 1,..,d$, so that the sequence N^ε is strongly compact in $L^p([0,T]\times\Omega)$ for all $p \in [1,+\infty[$, and N^ε converges a.e. towards N.

We now compute the derivative of a suitable nonnegative quantity:

$$\frac{1}{2}\frac{d}{dt}\int \left[\frac{\tilde{\gamma}}{\alpha}(p_h^\varepsilon)^2 + N^\varepsilon \psi(p_s^\varepsilon)\right],$$

with $\psi(x) = 2/\xi(x - \ln(1+\xi x)/\xi)$ (so that $\psi'(x) = 2x/(1+\xi x)$, and $\psi''(x) = 2/(1+\xi x)^2$). We obtain

$$\begin{aligned}
&\frac{1}{2}\frac{d}{dt}\int \left[\frac{\tilde{\gamma}}{\alpha}(p_h^\varepsilon)^2 + N^\varepsilon \psi(p_s^\varepsilon)\right] = \\
&\qquad \int \frac{\tilde{\gamma}}{\alpha} p_h^\varepsilon \partial_t p_h^\varepsilon + \int \frac{\psi(p_s^\varepsilon)}{2}\partial_t N^\varepsilon + \frac{1}{2}\int N^\varepsilon \psi'(p_s^\varepsilon)\partial_t p_s^\varepsilon \\
&= \int \frac{\tilde{\gamma}}{\alpha} p_h^\varepsilon \left(d_3 \Delta_x p_h^\varepsilon - \frac{1}{\varepsilon}\left(\tilde{\gamma} p_h^\varepsilon - \frac{\alpha N^\varepsilon p_s^\varepsilon}{1+\xi p_s^\varepsilon}\right) - \mu p_h^\varepsilon\right) + \int \frac{\psi(p_s^\varepsilon)}{2}\partial_t N^\varepsilon \\
&\qquad + \int N^\varepsilon \frac{p_s^\varepsilon}{1+\xi p_s^\varepsilon}\left(d_2 \Delta_x p_s^\varepsilon + \frac{1}{\varepsilon}\left(\tilde{\gamma} p_h^\varepsilon - \frac{\alpha N^\varepsilon p_s^\varepsilon}{1+\xi p_s^\varepsilon}\right) - \mu p_s^\varepsilon + \Gamma p_h^\varepsilon\right)
\end{aligned}$$

$$
\begin{aligned}
&= \boxed{d_3 \frac{\tilde{\gamma}}{\alpha} \int p_h^\varepsilon \Delta_x p_h^\varepsilon} - \frac{1}{\varepsilon\alpha} \int \left(\tilde{\gamma} p_h^\varepsilon - \frac{\alpha N^\varepsilon p_s^\varepsilon}{1+\xi p_s^\varepsilon} \right)^2 - \mu \frac{\tilde{\gamma}}{\alpha} \int (p_h^\varepsilon)^2 \\
&\quad + \frac{d_1}{2} \int \psi(p_s^\varepsilon) \Delta_x N^\varepsilon + \frac{r_0}{2} \int \psi(p_s^\varepsilon)(1-\eta N^\varepsilon) N^\varepsilon - \frac{\alpha}{2} \int \psi(p_s^\varepsilon) \frac{p_s^\varepsilon}{1+\xi p_s^\varepsilon} N^\varepsilon \\
&\quad + \boxed{d_2 \int N^\varepsilon \frac{p_s^\varepsilon}{1+\xi p_s^\varepsilon} \Delta_x p_s^\varepsilon} - \mu \int \frac{N^\varepsilon (p_s^\varepsilon)^2}{1+\xi p_s^\varepsilon} + \Gamma \int \frac{N^\varepsilon p_s^\varepsilon p_h^\varepsilon}{1+\xi p_s^\varepsilon}. \qquad (6.26)
\end{aligned}
$$

The boxed terms, integrating by parts and using the boundary conditions, can be rewritten as

$$
d_3 \frac{\tilde{\gamma}}{\alpha} \int p_h^\varepsilon \Delta_x p_h^\varepsilon = -d_3 \frac{\tilde{\gamma}}{\alpha} \int |\nabla p_h^\varepsilon|^2
$$

$$
\begin{aligned}
d_2 \int N^\varepsilon \frac{p_s^\varepsilon}{1+\xi p_s^\varepsilon} \Delta_x p_s^\varepsilon &= -d_2 \int \nabla p_s^\varepsilon \nabla \left(N^\varepsilon \frac{p_s^\varepsilon}{1+\xi p_s^\varepsilon} \right) \\
&= -d_2 \int \nabla p_s^\varepsilon \nabla \left(\frac{p_s^\varepsilon}{1+\xi p_s^\varepsilon} \right) N^\varepsilon - d_2 \int \nabla p_s^\varepsilon \nabla N^\varepsilon \frac{p_s^\varepsilon}{1+\xi p_s^\varepsilon} \\
&= -\frac{d_2}{2} \int \nabla p_s^\varepsilon \nabla \psi'(p_s^\varepsilon) N^\varepsilon - \frac{d_2}{2} \int \nabla \psi(p_s^\varepsilon) \nabla N^\varepsilon \\
&= -\frac{d_2}{2} \int |\nabla p_s^\varepsilon|^2 \nabla \psi''(p_s^\varepsilon) N^\varepsilon + \frac{d_2}{2} \int \psi(p_s^\varepsilon) \Delta_x N^\varepsilon
\end{aligned}
$$

Thus, (6.26) can be rewritten as

$$
\begin{aligned}
&= -\frac{1}{\varepsilon\alpha} \underbrace{\int \left(\tilde{\gamma} p_h^\varepsilon - \frac{\alpha N^\varepsilon p_s^\varepsilon}{1+\xi p_s^\varepsilon} \right)^2}_{\boxed{1}} - \underbrace{d_3 \frac{\tilde{\gamma}}{\alpha} \int |\nabla p_h^\varepsilon|^2}_{\boxed{2}} - \underbrace{\mu \frac{\tilde{\gamma}}{\alpha} \int (p_h^\varepsilon)^2}_{\boxed{3}} \\
&\quad - \underbrace{\frac{d_2}{2} \int N^\varepsilon \psi''(p_s^\varepsilon) |\nabla p_s^\varepsilon|^2}_{\boxed{4}} + \underbrace{\frac{1}{2} \int \psi(p_s^\varepsilon) \left(\partial_t N^\varepsilon + d_2 \Delta N^\varepsilon \right)}_{\boxed{5}} \\
&\quad - \underbrace{\mu \int \frac{N^\varepsilon (p_s^\varepsilon)^2}{1+\xi p_s^\varepsilon}}_{\boxed{6}} + \underbrace{\Gamma \int \frac{N^\varepsilon p_s^\varepsilon p_h^\varepsilon}{1+\xi p_s^\varepsilon}}_{\boxed{7}}.
\end{aligned}
$$

The terms $\boxed{1}$, $\boxed{2}$, $\boxed{3}$, $\boxed{4}$ and $\boxed{6}$ are nonpositive. Then remembering that $0 \leq \psi(x) \leq 2x/\xi$, p_s^ε and p_h^ε are bounded in $L^{2+\delta}$ for some $\delta > 0$, N^ε is bounded in L^∞, and finally $\partial_t N\varepsilon$, $\Delta_x N^\varepsilon$ are bounded in L^p for all $p < +\infty$, we see that terms $\boxed{5}$ and $\boxed{7}$, once integrated on $[0,T]$, are bounded (by some constant $C_T > 0$). As a consequence, we end up with the estimates

$$\int_0^T \int_\Omega \left(\tilde{\gamma} p_h^\varepsilon - \frac{\alpha N^\varepsilon p_s^\varepsilon}{1+\xi p_s^\varepsilon}\right)^2 \leq C_T \varepsilon, \tag{6.27}$$

$$\int_0^T \int_\Omega |\nabla_x p_h^\varepsilon|^2 \leq C_T, \tag{6.28}$$

$$\int_0^T \int_\Omega N^\varepsilon \psi''(p_s^\varepsilon) |\nabla_x p_s^\varepsilon|^2 \leq C_T. \tag{6.29}$$

We see that (with $C_T := \alpha + r_0 \eta \sup_{\varepsilon>0} ||N^\varepsilon||_{L^\infty([0,T]\times\Omega)}$)

$$(\partial_t - d_1 \Delta_x) N^\varepsilon \geq -C_T N^\varepsilon,$$

so that (denoting by inf the essential infima in the formula below)

$$\inf_{\varepsilon>0, x\in\Omega} N^\varepsilon(t,x) \geq e^{-C_T} \inf_{\varepsilon>0, x\in\Omega} N^\varepsilon(0,x).$$

As a consequence, thanks to (6.29),

$$\int_0^T \int_\Omega \psi''(p_s^\varepsilon) |\nabla_x p_s^\varepsilon|^2 \leq C_T.$$

Then, the Cauchy-Schwarz inequality ensures that

$$\left(\int_0^T \int_\Omega |\nabla_x p_s^\varepsilon|\right)^2 \leq \left(\int_0^T \int_\Omega \psi''(p_s^\varepsilon) |\nabla_x p_s^\varepsilon|^2\right) \times \left(\int_0^T \int_\Omega (1+\xi p_s^\varepsilon)^2\right) \leq C_T. \tag{6.30}$$

Using (6.20), we see that $\partial_t P^\varepsilon$ is bounded in $L^2([0,T]; H^{-2}(\Omega))$, so that thanks to estimates (6.28), (6.30) and Aubin's lemma [76], P^ε converges a.e. to P. Note that $\tilde{\gamma} p_h^\varepsilon - \alpha N^\varepsilon p_s^\varepsilon/(1+\xi p_s^\varepsilon) \to 0$ a.e. (up to extraction of a subsequence) thanks to (6.27), and that N^ε converges a.e. to N. Then

$$\tilde{\gamma} P^\varepsilon - \left(\tilde{\gamma} p_h^\varepsilon - \frac{\alpha N^\varepsilon p_s^\varepsilon}{1+\xi p_s^\varepsilon}\right) = \tilde{\gamma} p_s^\varepsilon + \frac{\alpha N^\varepsilon p_s^\varepsilon}{1+\xi p_s^\varepsilon}$$

converges a.e. towards $\tilde{\gamma} P$. Observing that

$$\left|\left(\tilde{\gamma}p_s^\varepsilon + \frac{\alpha N^\varepsilon p_s^\varepsilon}{1+\xi p_s^\varepsilon}\right) - \left(\tilde{\gamma}p_s^\varepsilon + \frac{\alpha N p_s^\varepsilon}{1+\xi p_s^\varepsilon}\right)\right| \leq \frac{\alpha}{\xi}|N^\varepsilon - N|,$$

we see that

$$\tilde{\gamma}p_s^\varepsilon + \frac{\alpha N p_s^\varepsilon}{1+\xi p_s^\varepsilon} \to \tilde{\gamma}P.$$

Using the continuity and the strict monotonicity of $y \to \tilde{\gamma}y + \alpha N y/(1+\xi y)$ for all $N \geq 0$, we see that p_s^ε converges a.e. towards a nonnegative function denoted by p_s. Then, p_h^ε also converges a.e. towards a nonnegative function denoted by p_h. As a consequence, they also converge in $L^{2+\delta}$ strong when $\delta > 0$ is small enough. Finally, it is clear that

$$p_s + p_h = P, \quad \tilde{\gamma}p_h = \frac{\alpha N p_s}{1+\xi p_s},$$

so that (6.19) holds.

We now pass to the limit in equation (6.13a) and (6.20) in the sense of distributions (more precisely, in the sense of very-weak solutions, which include the Neumann boundary conditions and the initial data $N(0,x) = N_{in}(x)$ and $(p_s + p_h)(0,x) = p_{s,in}(x) + p_{h,in}(x)$), so that (6.17) and (6.18) hold.

Finally, thanks to (6.24) and (6.25), we see that N lies in $L^p([0,T], W^{2,p}(\Omega)) \cap W^{1,p}(]0,T[, L^p(\Omega))$ for all $p \in]1,+\infty[$, and thanks to (6.28) and (6.30), we see that p_s and p_h respectively belong to $L^1([0,T], W^{1,1}(\Omega))$ and $L^2([0,T], H^1(\Omega))$.

□

7

The Turing Instability analysis

In this Chapter, we study the Turing instability regions associated to system (6.3) and (6.10). We make explicit the condition on the parameters which lead to the existence of an homogeneous coexistence equilibrium and perform a stability analysis of this equilibrium (when it exists) at the ODEs level. Thus, we study Turing instability for both cross-diffusion systems and compare the results with respect to the case in which a linear diffusion term is simply added to the predator equation, instead of the cross-diffusion term.

7.1 The Holling-type II

In this Section we want to study the Turing instability of the cross-diffusion system with the Holling-type II functional response. We are also interested in the study of the associated linear-diffusion system, that is when linear-diffusion terms are simply added to the reaction part.

7.1.1 Homogeneous equilibrium states

First, we look for the homogeneous equilibrium states (that is the ODEs system of the reaction part of (6.3)):

$$\begin{aligned} \dot{n} &= n\left(1-\frac{n}{\nu}\right)-\frac{np}{1+n} \\ \dot{p} &= \frac{cnp}{1+n}-mp. \end{aligned} \tag{7.1}$$

From the first equation, if $p=0$, we obtain $n=0$ or $N=\nu$, corresponding to the total extinction $E_0(0,0)$ and the non-coexistence $E_1(\nu,0)$ equilibria. Otherwise, we

look for a coexistence equilibrium $E_*(n_*, p_*)$ (by coexistence equilibrium, we mean that $n_*,\ p_* > 0$). From the second equation, we get

$$n_* = \frac{m}{c-m}, \qquad p_* = n_* \left(1 - \frac{n_*}{\nu}\right) \frac{n_*+1}{n_*},$$

with existence conditions on the parameters

$$c - m > 0, \qquad \nu > \frac{m}{c-m}.$$

Now we study the stability properties of these equilibrium states. We denote by $J_{i,j},\ i,j = 1,2$ the elements of the Jacobian matrix of the system:

$$\begin{aligned}
J_{11} &= \frac{\partial}{\partial n}\dot{n} = 1 - \frac{2}{\nu}n - \frac{p}{(1+n)^2},\\
J_{12} &= \frac{\partial}{\partial p}\dot{n} = -\frac{n}{1+n},\\
J_{21} &= \frac{\partial}{\partial n}\dot{p} = \frac{cp}{1+n},\\
J_{22} &= \frac{\partial}{\partial p}\dot{p} = \frac{cp}{1+n} - m.
\end{aligned}$$

Evaluating the Jacobian matrix in the equilibrium states, we obtain:

$$J(E_0) = \begin{pmatrix} 1 & 0 \\ 0 & -m \end{pmatrix}, \qquad J(E_1) = \begin{pmatrix} -1 & -\dfrac{n_*}{1+n_*} \\ 0 & \dfrac{cp_*}{1+n_*} - m \end{pmatrix},$$

and we have that

$$\frac{cp_*}{1+n_*} - m < 0 \qquad \Leftrightarrow \qquad \nu < \frac{m}{c-m}.$$

Then the equilibrium E_0 is unstable (more precisely a saddle point); the equilibrium E_1 is locally asymptotically stable (more precisely a node) when E_* does not exist, and the equilibrium E_1 is unstable (more precisely a saddle point) otherwise.

The elements of the Jacobian matrix evaluated at the equilibrium E_* are

$$
\begin{aligned}
J_{11}^* &= 1 - \frac{2}{\nu} n_* - \frac{p_*}{(1+n_*)^2} \\
&= 1 - \frac{2}{\nu} n_* - n_* \left(1 - \frac{n_*}{\nu}\right) \frac{n_*+1}{n_*} \frac{1}{(1+n_*)^2} \\
&= 1 - \frac{2}{\nu} n_* - \left(1 - \frac{n_*}{\nu}\right)\left(1 - \frac{m}{c}\right) \\
&= -\frac{n_*}{\nu}\left(1 + \frac{m}{c}\right) - \frac{m}{c},
\end{aligned}
$$

$$
J_{12}^* = -\frac{n_*}{1+n_*} < 0,
$$

$$
J_{21}^* = \frac{cp_*}{1+n_*} > 0,
$$

$$
J_{22}^* = \frac{cp_*}{1+n_*} - m = 0.
$$

Then, we have that the determinant of the Jacobian matrix is positive and the trace has the same sign of J_{11}^*. In particular,

$$
J_{11}^* > 0 \qquad \Leftrightarrow \qquad \frac{m}{c-m} < \nu < 2\frac{m}{c-m},
$$

thus E_* exists stable (and unstable for greater values of ν).

7.1.2 Turing Instability analysis

We look now to the reaction-diffusion system with parameter values for which the coexistence equilibrium is stable. If we consider linear-diffusion terms, the system writes

$$
\begin{aligned}
\partial_t n - D_1 \Delta_x n &= n\left(1 - \frac{n}{\nu}\right) - \frac{np}{1+n} \\
\partial_t p - D \Delta_x p &= \frac{cnp}{1+n} - mp,
\end{aligned}
$$

where D is a constant diffusion coefficient of predators, $D \neq D_1$; in this case it is known that Turing instability can not appear [10]. In fact,

$$
\boldsymbol{M}_k^* = \begin{pmatrix} J_{11}^* - D_1 k^2 & J_{12}^* \\ J_{21}^* & -Dk^2 \end{pmatrix},
$$

and it is easy to verify that $\operatorname{tr} \boldsymbol{M}_k^* < 0$ and $\det \boldsymbol{M}_k^* > 0 \; \forall \; k$.

Now we study the cross-diffusion system (6.3); the linearization of the diffusion terms around E_* gives the matrix

$$\begin{pmatrix} D_1 & 0 \\ \dfrac{(D_3 - D_2)}{(1+n^*)^2} p_* & \dfrac{D_2 + D_3 n_*}{1+n^*} \end{pmatrix},$$

which has positive diagonal elements. The non-zero off-diagonal element is the cross-diffusion coefficient of predators in the linearized system. We note that it tends to zero when $p_* \to 0$, because in this case there can be no flux of predators. The sign of non-zero off-diagonal element is prescribed by the values of the diffusion coefficients of searching and handling predators. In particular, we can assume that $D_3 < D_2$, which means that searching predators are more diffusive than handling predators (biologically reasonable). With this assumption, $D_3 - D_2 < 0$; hence, the cross-diffusion coefficient is negative. This implies that the flux of predators is directed toward increasing values of the concentration of preys. The characteristic matrix ($k \in \mathbb{R}$ is the wavenumber) has the form

$$\boldsymbol{M}_k^* = \begin{pmatrix} J_{11}^* - D_1 k^2 & J_{12}^* \\ J_{21}^* - \dfrac{(D_3 - D_2) p_*}{(1+n^*)^2} k^2 & -\dfrac{D_2 + D_3 n_*}{1+n^*} k^2 \end{pmatrix}.$$

Thus, $\operatorname{tr} \boldsymbol{M}_k^* < 0$ and $\det \boldsymbol{M}_k^* > 0, \; \forall k$. We can conclude that no Turing instability appears also in the cross-diffusion system, under the (biologically reasonable) assumption $D_3 < D_2$.

The introduction of cross-diffusion terms, derived by a time-scale argument presented in the previous Chapter, instead of standard (linear) diffusion terms does not lead to the increase of the set of parameter values in which patterns develop; this is exactly the opposite result obtained in [96, 57] with an another type of cross-diffusion.

7.2 The Beddington-DeAngelis

In this Section we want to study the Turing instability of the cross-diffusion system with the Beddington-DeAngelis-like functional response. We are also interested in the study of the associated linear-diffusion system, that is when linear-diffusion terms are simply added to the reaction part. First of all, we look for the equilibrium states of the ODEs system and then we perform the Turing instability analysis in both cases, and we compare the results.

7.2.1 Homogeneous equilibrium states

In this subsection, we look for the equilibrium states of the ODEs system (that is the reaction part of the whole system (6.10) or equivalently (6.12)):

$$\begin{aligned} \dot{N} &= r\left(1-\frac{N}{\nu}\right)N - \frac{\gamma NP}{B+\sqrt{\Delta}}, \\ \dot{P} &= \frac{\Gamma NP}{B+\sqrt{\Delta}} - \mu P, \end{aligned} \tag{7.2}$$

where A, B and Δ are defined in (6.11).

From the first equation, if $P = 0$, we obtain $N = 0$ or $N = \nu$, corresponding to the total extinction $E_0(0,0)$ and the non-coexistence $E_1(\nu, 0)$ equilibria.

Otherwise, we look for a coexistence equilibrium $E_*(N_*, P_*)$ (by coexistence equilibrium, we mean that $N_*,\ P_* > 0$). From the second equation, we get the identity

$$\frac{\Gamma N_*}{\gamma + N_* + P_* + \sqrt{(\gamma + N_* + P_*)^2 - 4N_*P_*}} - \mu = 0 \tag{7.3}$$

from which, rationalizing the denominator, we can obtain

$$\sqrt{(\gamma + N_* + P_*)^2 - 4N_*P_*} = \gamma + N_* + P_* - \frac{4\mu}{\Gamma}P_*. \tag{7.4}$$

From (7.3), we can also get an expression of P_* in terms of N_*. In fact, we have

$$\Gamma N_* - \mu(\gamma + N_* + P_*) = \mu\sqrt{(\gamma + N_* + P_*)^2 - 4N_*P_*}.$$

We see therefore that the coexistence equilibrium can exist only if

$$\Gamma N_* - \mu(\gamma + N_* + P_*) > 0, \tag{7.5}$$

and then taking the square of both terms we end up with

$$P_* = \frac{\Gamma}{2\mu}\frac{(\Gamma - 2\mu)N_* - 2\gamma\mu}{(\Gamma - 2\mu)} = \frac{\Gamma}{2\mu}N_* - \frac{\Gamma\gamma}{\Gamma - 2\mu}. \tag{7.6}$$

Substituting (7.6) in (7.5), we see that (7.5) is equivalent to

$$\frac{\Gamma - 2\mu}{2}N_* + \gamma\mu\left(\frac{2\mu}{\Gamma - 2\mu}\right) > 0. \tag{7.7}$$

Since we are looking for equilibria with $N_* > 0$. we see that (7.5) or (7.7) can also be rewritten as

$$\Gamma - 2\mu > 0. \tag{7.8}$$

Substituting the expression (7.4) in the equation $\dot{N} = 0$ from the first equation of (7.2) written as

$$\dot{N} = r\left(1 - \frac{N}{\nu}\right)N - \frac{\gamma}{4}(B - \sqrt{\Delta}),$$

we obtain

$$r\left(1 - \frac{N_*}{\nu}\right)N_* - \frac{\gamma\mu}{\Gamma}P_* = 0, \tag{7.9}$$

from which we have another expression of P_* in terms of N_*

$$P_* = \frac{\Gamma}{\gamma\mu}r\left(1 - \frac{N_*}{\nu}\right)N_*. \tag{7.10}$$

Substituting the expression (7.6) in (7.9), we obtain a second order equation in the unknown N_*:

$$\frac{r}{\nu}N_*^2 - \left(r - \frac{\gamma}{2}\right)N_* - \frac{\mu\gamma^2}{\Gamma - 2\mu} = 0. \tag{7.11}$$

We see that, thanks to (7.8),

$$\Delta_N := \left(r - \frac{\gamma}{2}\right)^2 + 4\frac{r}{\nu}\frac{\mu\gamma^2}{\Gamma - 2\mu} > 0, \tag{7.12}$$

so that equation (7.11) has one and only one strictly positive solution given by

$$N_* = \frac{\nu}{2r}\left(r - \frac{\gamma}{2} + \sqrt{\Delta_N}\right). \tag{7.13}$$

Then, the condition $P_* > 0$ is equivalent to

$$\frac{\Gamma}{2\mu}N_* - \frac{\Gamma\gamma}{\Gamma - 2\mu} > 0 \;\Leftrightarrow\; 0 < N_* < \nu, \tag{7.14}$$

depending on the chosen expression for P_*. This condition can be rewritten as

$$\Gamma - 2\mu > \frac{2\gamma\mu}{\nu}, \tag{7.15}$$

by substituting (7.13) in the last term of (7.14). Note that this last necessary condition for the existence of the coexistence equilibrium E_* implies condition (7.8). We

now briefly explain why condition (7.15) is sufficient (and thus both necessary and sufficient) for the existence of E_*. Indeed, (7.15) can be rewritten as

$$\sqrt{\Delta_N} < r + \frac{\gamma}{2},$$

so that N_* (computed from formula (7.13) and (7.12)) is such that $0 < N_* < \nu$. Remembering that this last condition is equivalent to $P_* > 0$ (when P_* is given by (7.10) for example), we see that both N_* and P_* defined in this way are strictly positive. One can easily check that they satisfy $\dot{N} = 0,\ \dot{P} = 0$ in (7.2).

Now we study the stability properties of these equilibrium states. We denote by $J_{i,j},\ i,j = 1,2$ the elements of the Jacobian matrix of the system (7.2):

$$\begin{aligned}
J_{11} &= \frac{\partial}{\partial N}\dot{N} = r - \frac{2r}{\nu}N - \frac{\gamma}{4}\left(1 - \frac{\gamma + N - P}{\sqrt{(\gamma+N+P)^2 - 4NP}}\right),\\
J_{12} &= \frac{\partial}{\partial P}\dot{N} = -\frac{\gamma}{4}\left(1 - \frac{\gamma - N + P}{\sqrt{(\gamma+N+P)^2 - 4NP}}\right),\\
J_{21} &= \frac{\partial}{\partial N}\dot{P} = \frac{\Gamma}{4}\left(1 - \frac{\gamma + N - P}{\sqrt{(\gamma+N+P)^2 - 4NP}}\right),\\
J_{22} &= \frac{\partial}{\partial P}\dot{P} = \frac{\Gamma}{4}\left(1 - \frac{\gamma - N + P}{\sqrt{(\gamma+N+P)^2 - 4NP}}\right) - \mu.
\end{aligned}$$

Evaluating the Jacobian matrix in the equilibrium states, we obtain:

$$J(E_0) = \begin{bmatrix} r & 0 \\ 0 & -\mu \end{bmatrix}, \qquad J(E_1) = \begin{bmatrix} -r & * \\ 0 & J_{22}(E_1) \end{bmatrix},$$

$$J_{22}(E_1) = \frac{\Gamma\nu}{2(\gamma+\nu)} - \mu > 0 \qquad \Leftrightarrow \qquad \Gamma - 2\mu > \frac{2\gamma\mu}{\nu}.$$

Then the equilibrium E_0 is unstable (more precisely a saddle point); the equilibrium E_1 is locally asymptotically stable (more precisely a node) when E_* does not exist, and the equilibrium E_1 is unstable (more precisely a saddle point) otherwise.

The case of E_* is more intricate. First, we compute the quantities

$$Q_* := \gamma + N_* + P_* - \frac{4\mu}{\Gamma}P_* = \frac{\Gamma - 2\mu}{2\mu}N_* + \frac{2\mu\gamma}{\Gamma - 2\mu} > 0 \tag{7.16}$$

and, thank to (7.6) and (7.16),

$$\frac{P_*}{Q_*} = \frac{\Gamma}{\Gamma - 2\mu}\left(1 - \frac{2\mu\gamma\Gamma}{(\Gamma - 2\mu)^2 N_* + 4\mu^2\gamma}\right).$$

Thanks to (7.4) and (7.6), we obtain (remembering the definition of Δ_N in (7.12)) explicit expressions for the elements of the Jacobian matrix evaluated at the equilibrium E_*, denoted by $\boldsymbol{J}$:

$$\begin{aligned}
J_{11}^* := J_{11}(E_*) &= r\left(1 - \frac{2}{\nu}N_*\right) - \frac{\gamma(\Gamma - 2\mu)}{2\Gamma}\frac{P_*}{Q_*} \\
&= -\frac{r}{Q_*}\frac{2\mu\gamma}{\Gamma - 2\mu}\left[\frac{(\Gamma - 2\mu)^2}{4\nu\mu^2\gamma}N_*^2 + \frac{2}{\nu}N_* - 1\right] \\
&= \frac{\mu\gamma^2\Gamma}{(\Gamma - 2\mu)^2 N_* + 4\mu^2\gamma} - \sqrt{\Delta_N},
\end{aligned}$$

$$\begin{aligned}
J_{12}^* := J_{12}(E_*) &= -\frac{\gamma}{4}\left(\frac{\sqrt{(\gamma + N_* + P_*)^2 - 4N_*P_*} - (\gamma + N_* + P_*) + 2N_*}{\sqrt{(\gamma + N_* + P_*)^2 - 4N_*P_*}}\right) \\
&= -\frac{\gamma}{2\Gamma Q_*}(-2\mu P_* + \Gamma N_*) = -\frac{\gamma^2\mu}{Q_*(\Gamma - 2\mu)} < 0,
\end{aligned}$$

$$\begin{aligned}
J_{21}^* := J_{21}(E_*) &= \frac{\Gamma}{4}\left(\frac{\sqrt{(\gamma + N_* + P_*)^2 - 4N_*P_*} - (\gamma + N_* + P_*) + 2P_*}{\sqrt{(\gamma + N_* + P_*)^2 - 4N_*P_*}}\right) \\
&= \frac{1}{2Q_*}(\Gamma - 2\mu)P_* > 0,
\end{aligned}$$

$$\begin{aligned}
J_{22}^* := J_{22}(E_*) &= -\mu + \frac{\Gamma}{4}\left(\frac{\sqrt{(\gamma + N_* + P_*)^2 - 4N_*P_*} - (\gamma + N_* + P_*) + 2N_*}{\sqrt{(\gamma + N_* + P_*)^2 - 4N_*P_*}}\right) \\
&= -\mu + \frac{\Gamma}{2Q_*}\left(N_* - \frac{2\mu}{\Gamma}P_*\right) \\
&= \frac{1}{2Q}\left(-2\mu\left(\gamma + N_* + P_* - \frac{4\mu}{\Gamma}P_*\right) + \Gamma N_* - 2\mu P_*\right) \\
&= \frac{1}{2Q_*}\left((-2\mu\gamma + (\Gamma - 2\mu)N_*) - 4\mu P_* + \frac{8\mu^2}{\Gamma}P_*\right) \\
&= \frac{1}{2Q_*}\left(\frac{2\mu}{\Gamma}(\Gamma - 2\mu)P_* - 4\mu P_* + \frac{8\mu^2}{\Gamma}P_*\right) = -\frac{\mu}{\Gamma Q_*}(\Gamma - 2\mu)P_* < 0.
\end{aligned}$$

Note that the sign of J_{11}^* is not prescribed, while we are able to determine the sign of the others elements ($J_{12}^* < 0,\ J_{21}^* > 0,\ J_{22}^* < 0$). However, we can prove that

$$\det \boldsymbol{J} = J_{11}^* J_{22}^* - J_{12}^* J_{21}^* > 0,$$

(this holds whatever is the sign of J_{11}^*). In fact, substituting in the expression of $\det \boldsymbol{J}(E_*)$ the formulas for $J_{i,j}^*,\ i,j = 1,2$, we have

$$\det \boldsymbol{J} = \frac{r}{Q_*^2}\left(1 - \frac{N_*}{\nu}\right) N_* \left[r\left(\frac{(\Gamma - 2\mu)^2}{2\nu\mu\gamma} N_*^2 + \frac{4\mu}{\nu} N_* - 2\mu \right) + \frac{\Gamma\gamma}{2} \right]$$

and substituting (7.13) in the linear term inside the brackets, we obtain

$$\det \boldsymbol{J} = \frac{r}{Q_*^2}\left(1 - \frac{N_*}{\nu}\right) N_* \left[r\frac{(\Gamma - 2\mu)^2}{2\nu\mu\gamma} N_*^2 + 2\mu\sqrt{\Delta_N} + \frac{\gamma}{2}(\Gamma - 2\mu) \right] > 0.$$

On the contrary, the sign of the trace of the Jacobian matrix evaluated at E_* is not prescribed. When $J_{11}^* < 0$, we have

$$\text{tr } \boldsymbol{J} = J_{11}^* + J_{22}^* < 0,$$

so that E_* is locally asymptotically stable. When $J_{11}^* > 0$, the trace can be nonpositive or nonnegative. We have numerical evidence that both cases can hold, for different values of the parameters of the model.

7.2.2 Turing Instability with linear diffusion terms

We consider the reaction-diffusion system in which linear-diffusion terms are simply added to the reaction part of (6.10) (for given $D_1, D_P > 0$)

$$\begin{aligned} \frac{\partial N}{\partial t} - D_1 \Delta_x N &= r\left(1 - \frac{N}{\nu}\right) N - \frac{\gamma N P}{B + \sqrt{\Delta}}, \\ \frac{\partial P}{\partial t} - D_P \Delta_x P &= \frac{\Gamma N P}{B + \sqrt{\Delta}} - \mu P, \end{aligned} \tag{7.17}$$

where $A,\ B$ and Δ are defined in (6.11), and sets of parameter values such that tr $J(E_*) < 0$ (remember that such parameters indeed exist).

For any wavenumber $k \in \mathbb{R}$, the characteristic matrix evaluated at the equilibrium E_* is defined by

$$\boldsymbol{M} = \begin{bmatrix} J_{11}^* - D_1 k^2 & J_{12}^* \\ J_{21}^* & J_{22}^* - D_P k^2 \end{bmatrix},$$

and has a negative trace. In fact,

$$\text{tr } \boldsymbol{M} = J_{11}^* - D_1 k^2 + J_{22}^* - D_P k^2 = \text{tr } \boldsymbol{J} - D_1 k^2 - D_2 k^2 < 0.$$

Its determinant is

$$\det \boldsymbol{M} = \det \boldsymbol{J} - (D_P J_{11}^* + D_1 J_{22}^*) k^2 + D_1 D_P k^4,$$

so that a necessary condition for the Turing instability is

$$D_1 J_{22}^* + D_P J_{11}^* > 0.$$

If $J_{11}^* < 0$, remembering that $J_{22}^* < 0$, we see that $D_P J_{11}^* + D_1 J_{22}^* < 0$. In this case, the system does not show any Turing instability.

On the opposite, if $J_{11}^* > 0$, for any $k \neq 0$, we can select D_P large enough so that $\det \boldsymbol{J} - D_P J_{11}^* k^2 < 0$. Then, when $D_1 > 0$ is small enough, $\det \boldsymbol{M} < 0$ and Turing instability appears.

7.2.3 Turing Instability with cross-diffusion

If we now consider system (6.10) or the equivalent form (6.12), that is

$$\frac{\partial N}{\partial T} - D_1 \Delta_x N = r \left(1 - \frac{N}{\nu}\right) N - \frac{\gamma}{4} \left(B - \sqrt{B^2 - 4NP}\right),$$

$$\frac{\partial P}{\partial T} - \Delta_x \left(\frac{D_2}{2}(\sqrt{\Delta} - A) + \frac{D_3}{2}(B - \sqrt{\Delta})\right) = \frac{\Gamma}{4} \left(B - \sqrt{B^2 - 4NP}\right) - \mu P,$$

where A, B and Δ are defined by (6.11). Therefore, the characteristic matrix has the form

$$\boldsymbol{M} = \begin{bmatrix} J_{11}^* - J_{\Delta 11}^* k^2 & J_{12}^* - J_{\Delta 12}^* k^2 \\ J_{21}^* - J_{\Delta 21}^* k^2 & J_{22}^* - J_{\Delta 22}^* k^2 \end{bmatrix},$$

where $k \in \mathbb{R}$ is the wavenumber, and the terms $J_{\Delta ij}$, $i, j = 1, 2$ are obtained thanks to a linearization of the diffusion terms around E_*. They are given by the following explicit formulas:

$$
\begin{aligned}
J^*_{\Delta 11} &= D1 > 0,\\
J^*_{\Delta 12} &= 0,\\
J^*_{\Delta 21} &= \frac{D_2 - D_3}{2}\left(\frac{(\gamma + N_* - P_*) - \sqrt{\Delta_*}}{\sqrt{\Delta_*}}\right) = -\frac{D_2 - D_3}{Q_*}\frac{\Gamma - 2\mu}{\Gamma}P_*, \qquad (7.18)\\
J^*_{\Delta 22} &= \frac{D_2}{2}\left(\frac{(\gamma - N_* + P_*) + \sqrt{\Delta_*}}{\sqrt{\Delta_*}}\right) + \frac{D_3}{2}\left(\frac{\sqrt{\Delta_*} - (\gamma - N_* + P_*)}{\sqrt{\Delta_*}}\right)\\
&= \frac{D_2}{Q_*}\left(\gamma + P_*\frac{(\Gamma - 2\mu)}{\Gamma}\right) + \frac{D_3}{Q_*}\frac{2\mu\gamma}{\Gamma - 2\mu} > 0. \qquad (7.19)
\end{aligned}
$$

We notice that only the sign of $J^2_{\Delta 21}$ depends on D_2, D_3. Due to the biological meaning of these parameters, we recall that we systematically assume that $D_2 > D_3$, since searching predators are expected to be "more diffusive" than handling predators. With this assumption, $J^*_{\Delta 21} < 0$.

We still consider sets of parameter values such that $\operatorname{tr} \mathbf{J}(E_*) < 0$. Then the characteristic matrix $\boldsymbol{M}$ has negative trace, because

$$
\operatorname{tr} \boldsymbol{M} = J^*_{11} - D_1 k^2 + J^*_{22} - J^*_{\Delta 22} k^2 = \underbrace{\operatorname{tr} \boldsymbol{J}}_{-} - D_1 k^2 - \underbrace{J^*_{\Delta 22}}_{+} k^2 < 0.
$$

Its determinant is

$$
\det \boldsymbol{M} = \underbrace{\det \boldsymbol{J}}_{+} - (J^*_{11} J^*_{\Delta 22} + J^*_{22} J^*_{\Delta 11} - J^*_{12} J^*_{\Delta 21}) k^2 + \underbrace{(D_1 J^*_{\Delta 22})}_{+} k^4,
$$

so that a necessary condition for the Turing instability is

$$
J^*_{11} J^*_{\Delta 22} + J^*_{22} J^*_{\Delta 11} - J^*_{12} J^*_{\Delta 21} > 0. \qquad (7.20)
$$

If $J^*_{11} < 0$, we have

$$
\underbrace{J^*_{11}}_{-}\underbrace{J^*_{\Delta 22}}_{+} + \underbrace{J^*_{22}}_{-}\underbrace{J^*_{\Delta 11}}_{+} - \underbrace{J^*_{12}}_{-}\underbrace{J^*_{\Delta 21}}_{-},
$$

so that condition (7.20) does not hold and, as in the case of linear diffusion, the system does not show Turing instability. On the opposite, if $J^*_{11} > 0$, we have

$$
\underbrace{J^*_{11}}_{+}\underbrace{J^*_{\Delta 22}}_{+} + \underbrace{J^*_{22}}_{-}\underbrace{J^*_{\Delta 11}}_{+} - \underbrace{J^*_{12}}_{-}\underbrace{J^*_{\Delta 21}}_{-},
$$

so that for any $k \neq 0$, we can select D_2 large enough and $D_3 \sim D_2$ so that $\det \boldsymbol{J} - (J^*_{11} J^*_{\Delta 22} - J^*_{12} J^*_{\Delta 21}) k^2 < 0$. Then, when $D_1 > 0$ is small enough, $\det \boldsymbol{M} < 0$ and Turing instability can appear.

7.2.4 Turing instability regions: linear vs cross diffusion

We recall that the derivation of equations (6.10) (using the mechanistic approach and the "microscopic" model) produces a cross diffusion term in the predator equation, whereas the prey diffusion rate is still a constant. We recall, for reader's convenience, the considered equations

$$\begin{aligned} &\frac{\partial N}{\partial T} - D_1 \Delta_x N = r\left(1 - \frac{N}{\nu}\right) N - \frac{\gamma N P}{B + \sqrt{\Delta}}, \\ &\frac{\partial P}{\partial T} - \Delta_x \left(f(P,N)P\right) = \frac{\Gamma N P}{B + \sqrt{\Delta}} - \mu P, \end{aligned} \tag{7.21}$$

where

$$A = \gamma + N - P, \quad B = \gamma + N + P, \quad \Delta = (\gamma + N + P)^2 - 4NP,$$

$$f(P,N) := D_2 \frac{2\gamma}{A + \sqrt{\Delta}} + D_3 \frac{2N}{B + \sqrt{\Delta}}. \tag{7.22}$$

We want to compare three natural strategies to model the diffusion in systems of ODEs modeling the predator-prey interactions.

1. First, we take the reaction part of (7.21) and we add diffusion terms in such a way that D_2 is a constant rate for predators. This means that we exactly take the diffusion coefficient of searching predators for all predators appearing in the limiting model.
2. Secondly, we take the reaction part of (7.21) and we add diffusion terms in such a way that $D_P = f(P_*, N_*)$, where f is defined in (7.22), is a constant rate of diffusion in the equation for predators. This means that we now take into account the difference (in term of diffusivity) among searching and handling predators, since both diffusion rates D_2 and D_3 are present in equation (7.22).
3. We finally consider the diffusion model (7.21), coming out of the derivation by singular perturbation of a microscopic system, as explained in Section 6.2.

Note first that, thanks to (7.6), it is possible to obtain a simple expression for D_P. Indeed

$$
\begin{aligned}
D_P = f(P_*, N_*) &= D_2 \frac{2\gamma}{A_* + \sqrt{\Delta_*}} + D_3 \frac{2N_*}{B_* + \sqrt{\Delta_*}} \\
&= D_2 \frac{\gamma}{\gamma + N_* - \dfrac{2\mu}{\Gamma} P_*} + D_3 \frac{N_*}{\gamma + N_* + P_* - \dfrac{2\mu}{\Gamma} P_*} \\
&= D_2 \frac{\gamma}{\gamma + \dfrac{2\mu\gamma}{\Gamma - 2\mu}} + D_3 \frac{N_*}{\gamma + \dfrac{\Gamma}{2\mu} N_* - \dfrac{\Gamma\gamma}{\Gamma - 2\mu} + \dfrac{2\mu\gamma}{\Gamma - 2\mu}} \\
&= D_2 \left(1 - \frac{2\mu}{\Gamma}\right) + D_3 \frac{2\mu}{\Gamma}. \qquad (7.23)
\end{aligned}
$$

We note therefore that D_P is a convex combination of the diffusion coefficients D_2, D_3 corresponding to searching and handling predators. Furthermore, assuming that $D_3 < D_2$ (remember that from the modeling point of view, handling predators have a lower diffusion rate than searching predators), we have

$$
D_P = D_2 \left(1 - \frac{2\mu}{\Gamma}\right) + D_3 \frac{2\mu}{\Gamma} = D_2 - \frac{D_2 - D_3}{\Gamma} 2\mu < D_2.
$$

The characteristic matrices of the cases that we consider are finally given by

1. Linear diffusion with D_2:

$$
\boldsymbol{M}_{L2} = \begin{bmatrix} J_{11}^* - D_1 k^2 & J_{12}^* \\ J_{21}^* & J_{22}^* - D_2 k^2 \end{bmatrix}; \qquad (7.24)
$$

2. Linear diffusion with D_P defined in (7.23)

$$
\boldsymbol{M}_{LP} = \begin{bmatrix} J_{11}^* - D_1 k^2 & J_{12}^* \\ J_{21}^* & J_{22}^* - D_P k^2 \end{bmatrix}; \qquad (7.25)
$$

3. Cross diffusion:

$$
\boldsymbol{M}_{C} = \begin{bmatrix} J_{11}^* - D_1 k^2 & J_{12}^* \\ J_{21}^* - J_{\Delta 21}^* k^2 & J_{22}^* - J_{\Delta 22}^* k^2 \end{bmatrix}; \qquad (7.26)
$$

with $J_{\Delta 21}^*$, $J_{\Delta 22}^*$ defined in (7.18) and (7.19).

We first want to compare the Turing instability regions of cases in which we have linear diffusion terms, corresponding to constant diffusion coefficients D_2 and D_P for predators, namely the range for k^2 that gives $\det \boldsymbol{M} < 0$. The characteristic matrices are (7.24) and (7.25), where one should remember that $D_2 > D_P$ (because of the

modeling assumption). Considering the generic matrix of a linear diffusion depending on the parameter $D > 0$:

$$\boldsymbol{M}(D) = \begin{bmatrix} J_{11}^* - D_1 k^2 & J_{12}^* \\ J_{21}^* & J_{22}^* - Dk^2 \end{bmatrix},$$

we can study the Turing instability region with respect to D by computing

$$\begin{aligned} \det \boldsymbol{M}(D) &= \left(J_{11}^* - D_1 k^2\right)\left(J_{22}^* - Dk^2\right) - J_{12}^* J_{21}^* = \\ &= DD_1 k^4 - \left(D_1 J_{22}^* + DJ_{11}^*\right) k^2 + \det \boldsymbol{J}. \end{aligned}$$

The interesting case (Turing instability appearance) is obtained under the necessary condition $D_1 J_{22}^* + DJ_{11}^* > 0$, that is

$$D > \hat{D} := -\frac{D_1 J_{22}^*}{J_{11}^*},$$

where $\hat{D}$ is a threshold. The solutions to the equation $\det \boldsymbol{M}(D) = 0$, which give boundaries of the Turing instability region (when this region exists), can be written as

$$sol_{1,2} = \frac{\left(D_1 J_{22}^* + DJ_{11}^*\right) \pm \sqrt{\left(D_1 J_{22}^* + DJ_{11}^*\right)^2 - 4D_1 D(J_{11}^* J_{22}^* - J_{12}^* J_{21}^*)}}{2D_1 D}. \tag{7.27}$$

The solutions exist if the discriminant in (7.27) is nonnegative, that is

$$\left(D_1 J_{22}^* + DJ_{11}^*\right)^2 - 4D_1 D \det \boldsymbol{J} \geq 0,$$

which leads to an inequality in D:

$$(J_{11}^* D)^2 - 2D_1(J_{11}^* J_{22}^* - 2J_{12}^* J_{21}^*)D + (D_1 J_{22}^*)^2 \geq 0.$$

The associated equation has a nonnegative discriminant, that is

$$(D_1(J_{11}^* J_{22}^* - 2J_{12}^* J_{21}^*))^2 - (D_1 J_{11}^* J_{22}^*)^2 = -4D_1^2 J_{12}^* J_{21}^* \det \mathbf{J}_{E_*} \geq 0,$$

and the equation admits two real roots

$$\begin{aligned} \hat{D}_{1,2} &= \frac{D_1(J_{11}^* J_{22}^* - 2J_{12}^* J_{21}^*) \pm 2D_1 \sqrt{-J_{12}^* J_{21}^* \det \mathbf{J}_{E_*}}}{J_{11}^{*2}} \\ &= \frac{D_1}{J_{11}^{*2}} \left[\sqrt{\det \mathbf{J}_{E_*}} \pm \sqrt{-J_{12}^* J_{21}^*}\right]^2 \geq 0, \end{aligned}$$

which are both nonnegative.

It is also possible to prove that $\hat{D}_1 < \hat{D} < \hat{D}_2$. In fact, it can be easily seen that $\hat{D}_2 > \hat{D}$ is equivalent to

$$\sqrt{-J_{12}^* J_{21}^* \det \boldsymbol{J}} > -\det \boldsymbol{J},$$

while $\hat{D}_1 < \hat{D}$ is equivalent to

$$\sqrt{-J_{12}^* J_{21}^* \det \boldsymbol{J}} > \det \boldsymbol{J}$$

So these conditions are always satisfied. Then the values of D which lead to Turing instability are $D > \hat{D}_2$ (because when $\hat{D} < D < \hat{D}_2$, the quantities $sol_{1,2}$ are not real and for $D < \hat{D}$, no Turing instability can appear).

We now can perform a qualitative study of the behaviour of the roots $sol_{1,2}(D)$, when we vary the parameter $D > \hat{D}_2$. In particular, using from (7.27), we see that

$$sol_{1,2}(D) > 0 \quad \forall D > \hat{D}_2.$$

Moreover, again from formula (7.27), it can be easily seen that

$$sol_1(\hat{D}_2) = sol_2(\hat{D}_2) = \frac{D_1 J_{22}^* + \hat{D}_2 J_{11}^*}{2 D_1 \hat{D}_2} > 0,$$

and also that

$$\lim_{D \to +\infty} sol_2(D) = \frac{J_{11}^*}{D_1} > sol_2(\hat{D}_2),$$

and

$$\lim_{D \to +\infty} sol_1(D) = 0.$$

Furthermore, taking the derivative of (7.27) with respect to D, we obtain

$$\frac{\partial}{\partial D} sol_2(D) = -\frac{J_{22}^*}{2D^2} + \frac{1}{2} \frac{\left(\frac{J_{22}^*}{D} + \frac{J_{11}^*}{D_1}\right)\left(-\frac{J_{22}^*}{D^2}\right) + 2\frac{\det \mathbf{J}}{D_1 D^2}}{\sqrt{\left(\frac{D_1}{D} J_{22}^* + J_{11}^*\right)^2 - 4\frac{D_1}{D} \det \mathbf{J}}},$$

and

$$\frac{\partial}{\partial D} sol_1(D) = -\frac{J_{22}^*}{2D^2} \frac{\sqrt{\left(\frac{D_1}{D} J_{22}^* + J_{11}^*\right)^2 - 4\frac{D_1}{D} \det \mathbf{J}} - \left(\frac{D_1}{D} J_{22}^* + J_{11}^*\right)}{\sqrt{\left(\frac{D_1}{D} J_{22}^* + J_{11}^*\right)^2 - 4\frac{D_1}{D} \det \mathbf{J}}}$$

$$-\frac{\det\mathbf{J}}{D^2\sqrt{\left(\frac{D_1}{D}\,J_{22}^*+J_{11}^*\right)^2-4\frac{D_1}{D}\det\mathbf{J}}}.$$

so that

$$\frac{\partial}{\partial D}sol_1(D)<0 \qquad \frac{\partial}{\partial D}sol_2(D)>0.$$

This means that the value of sol_1 is strictly decreasing with respect to D, while sol_2 is strictly increasing.

Then, we see that the Turing instability region grows when D increases (beyond $\hat{D}_2$). Because of this, choosing a diffusion rate based only on the behaviour of searching predators could lead to inaccurate conclusions about the possibility of pattern formation.

We now wish to compare the Turing instability regions in the case of linear diffusion with constant diffusion rate D_P as defined in (7.23), which has the characteristic matrix

$$\boldsymbol{M}_{LP}=\begin{bmatrix} J_{11}^*-D_1k^2 & J_{12}^* \\ J_{21}^* & J_{22}^*-D_Pk^2 \end{bmatrix},$$

and the case of cross diffusion, that is when the characteristic matrix is

$$\boldsymbol{M}_{C}=\begin{bmatrix} J_{11}^*-D_1k^2 & J_{12}^* \\ J_{21}^*-J_{\Delta 21}^*k^2 & J_{22}^*-J_{\Delta 22}^*k^2 \end{bmatrix}.$$

We observe that

$$\begin{aligned}\det\boldsymbol{M}_{LP}&=D_1D_Pk^4-\left(D_PJ_{11}^*+D_1J_{22}^*\right)k^2+\det\boldsymbol{J},\\ \det\boldsymbol{M}_{C}&=D_1J_{\Delta 22}^*k^4-\left(J_{\Delta 22}^*J_{11}^*+D_1J_{22}^*-J_{12}^*J_{\Delta 21}^*\right)k^2+\det\boldsymbol{J},\end{aligned}$$

and the Turing instability regions can be estimated thanks to the study of those determinants. Both are second order polynomials in k^2 with positive leading coefficients; furthermore, for $k=0$, we see that $\det\boldsymbol{M}_{LP}=\det\boldsymbol{M}_{C}=\det\boldsymbol{J}$. We want to compare the leading coefficients $A_L,\ A_C$ on one hand, and the coefficients of k^2, namely $B_L,\ B_C$, on the other hand. Those coefficients are defined in this way:

$$\begin{aligned}A_L&:=D_1D_P, & B_L&:=D_PJ_{11}^*+D_1J_{22}^*,\\ A_C&:=D_1J_{\Delta 22}^*, & B_C&:=J_{\Delta 22}^*J_{11}^*+D_1J_{22}^*-J_{12}^*J_{\Delta 21}^*.\end{aligned}$$

Substituting the expressions of D_P given in (7.23) and $J^*_{\Delta 22}$ in (7.19) (in terms of D_2 and D_3) in $A_L,\ A_C,\ B_L,\ B_C$, we see that

$$
\begin{aligned}
A_L &= D_1\left[D_2\left(1-\frac{2\mu}{\Gamma}\right)+D_3\frac{2\mu}{\Gamma}\right],\\
A_C &= D_1\left[D_2\left(\frac{\gamma}{Q_*}+\frac{P_*}{Q_*}\left(1-\frac{2\mu}{\Gamma}\right)\right)+D_3\frac{2\mu\gamma}{Q_*(\Gamma-2\mu)}\right],\\
B_L &= \left[D_2\left(1-\frac{2\mu}{\Gamma}\right)+D_3\frac{2\mu}{\Gamma}\right]J^*_{11}+D_1J^*_{22},\\
B_C &= \left[D_2\left(\frac{\gamma}{Q_*}+\frac{P_*}{Q_*}\left(1-\frac{2\mu}{\Gamma}\right)\right)+D_3\frac{2\mu\gamma}{Q_*(\Gamma-2\mu)}\right]J^*_{11}+D_1J^*_{22}+J^*_{12}\frac{D_2-D_3}{Q_*}\left(1-\frac{2\mu}{\Gamma}\right)P_*.
\end{aligned}
$$

We first look at A_L and A_C, coefficients of the leading term of the determinants. Both A_L and A_C are convex combinations of D_2 and D_3, since

$$\left(1-\frac{2\mu}{\Gamma}\right)+\frac{2\mu}{\Gamma}=1,$$

and

$$
\begin{aligned}
\left(\frac{\gamma}{Q_*}+\frac{P_*}{Q_*}\left(1-\frac{2\mu}{\Gamma}\right)\right)+\frac{2\mu\gamma}{Q_*(\Gamma-2\mu)} &= \frac{1}{Q_*}\left[\gamma+P_*\left(1-\frac{2\mu}{\Gamma}\right)+\frac{2\mu\gamma}{(\Gamma-2\mu)}\right]\\
&= \frac{1}{Q_*}\left[\frac{\Gamma-2\mu}{2\mu}N_*+\frac{2\mu\gamma}{(\Gamma-2\mu)}\right]=\frac{Q_*}{Q_*}=1.
\end{aligned}
$$

We now compare the coefficients of D_2 and D_3 in the convex combinations; for D_2, we get

$$\left(\frac{\gamma}{Q_*}+\frac{P_*}{Q_*}\left(1-\frac{2\mu}{\Gamma}\right)\right)>1-\frac{2\mu}{\Gamma}\quad\Leftrightarrow\quad N_*>\frac{2\mu\gamma}{\Gamma-2\mu},$$

and for D_3, we get

$$\frac{2\mu}{\Gamma}>\frac{2\mu\gamma}{Q_*(\Gamma-2\mu)}\quad\Leftrightarrow\quad N_*>\frac{2\mu\gamma}{\Gamma-2\mu},$$

which holds thanks to (7.14). As a consequence, we are able to prove that $D_P<J^*_{\Delta 22}$. Indeed:

$$D_2\left(1-\frac{2\mu}{\Gamma}\right)+D_3\frac{2\mu}{\Gamma}<D_2\left(\frac{\gamma}{Q_*}+\frac{P_*}{Q_*}\left(1-\frac{2\mu}{\Gamma}\right)\right)+D_3\frac{2\mu\gamma}{Q_*(\Gamma-2\mu)}.$$

We now prove that $B_L>B_C$. In fact, we can write

$$B_L = \left[D_2 - (D_2 - D_3)\frac{2\mu}{\Gamma}\right] J_{11}^* + D_1 J_{22}^*,$$
$$B_C = \left[D_2 - (D_2 - D_3)\frac{2\mu\gamma}{Q_*(\Gamma - 2\mu)}\right] J_{11}^* + D_1 J_{22}^* + J_{12}^* \frac{D_2 - D_3}{Q_*}\left(1 - \frac{2\mu}{\Gamma}\right) P_*.$$

Starting from these expressions, we see that $B_L > B_C$ if and only if

$$\left[\cancel{D_2} - (D_2 - D_3)\frac{2\mu}{\Gamma}\right] J_{11}^* + \cancel{D_1 J_{22}^*} >$$
$$\left[\cancel{D_2} - (D_2 - D_3)\frac{2\mu\gamma}{Q_*(\Gamma - 2\mu)}\right] J_{11}^* + \cancel{D_1 J_{22}^*} + J_{12}^* \frac{D_2 - D_3}{Q_*}\left(1 - \frac{2\mu}{\Gamma}\right) P_*.$$

Then we can divide this formula by the common strictly positive factor $D_2 - D_3$ and multiply both sides by Q_*. We obtain

$$\left[-\cancel{(D_2 - D_3)}\frac{2\mu}{\Gamma}\right] J_{11}^* Q_* >$$
$$\left[-\cancel{(D_2 - D_3)}\frac{2\mu\gamma}{\cancel{Q_*}(\Gamma - 2\mu)}\right] J_{11}^* \cancel{Q_*} + J_{12}^* \frac{\cancel{(D_2 - D_3)}}{\cancel{Q_*}}\left(1 - \frac{2\mu}{\Gamma}\right) P_* \cancel{Q_*},$$

and using the expressions of J_{11}^* and J_{12}^*, we end up with

$$-\frac{2\mu}{\Gamma}\left[r\left(1 - \frac{2}{\nu}N_*\right) Q_* - \gamma\frac{\Gamma - 2\mu}{2\Gamma}P_*\right] >$$
$$-\frac{2\mu\gamma}{(\Gamma - 2\mu)Q_*}\left[r\left(1 - \frac{2}{\nu}N_*\right) Q_* - \gamma\frac{\Gamma - 2\mu}{2\Gamma}P_*\right] - \frac{\gamma^2\mu}{Q_*\Gamma}P_*.$$

We can expand the product in the r.h.s.; we obtain

$$-\frac{2\mu}{\Gamma}\left[r\left(1 - \frac{2}{\nu}N_*\right) Q_* - \gamma\frac{\Gamma - 2\mu}{2\Gamma}P_*\right] > -\frac{2\mu\gamma}{(\Gamma - 2\mu)} r\left(1 - \frac{2}{\nu}N_*\right).$$

Now we can divide both sides by 2μ, bring all terms in the l.h.s., and get:

$$\left[\frac{\gamma}{\Gamma - 2\mu} - \frac{Q_*}{\Gamma}\right]\left(r - \frac{2r}{\nu}N_*\right) + \frac{\gamma}{\Gamma}\frac{\Gamma - 2\mu}{2\Gamma}P_* > 0.$$

Using formula (7.16) giving Q_* in terms of N_*, and eliminating the common factor Γ, we obtain

$$\left[\gamma - \frac{\Gamma - 2\mu}{2\mu} N_*\right]\left(r - \frac{2r}{\nu} N_*\right) + \gamma \frac{\Gamma - 2\mu}{2\Gamma} P_* > 0.$$

Using now the expression of P_* in terms of N_* in formula (7.6), we obtain

$$\left[\gamma - \frac{\Gamma - 2\mu}{2\mu} N_*\right]\left(r - \frac{2r}{\nu} N_*\right) + \gamma \frac{\cancel{\Gamma - 2\mu}}{2\cancel{\Gamma}} \frac{\cancel{\Gamma}}{2\mu} \frac{(\Gamma - 2\mu)N_* - 2\gamma\mu}{\cancel{(\Gamma - 2\mu)}} > 0.$$

Using finally the expression of N_* in formula (7.13) (only in the second N_* in the equation above), we end up with the inequality

$$\left[\gamma - \frac{\Gamma - 2\mu}{2\mu} N_*\right]\left(\cancel{r} - \cancel{r} + \frac{\gamma}{2} - \sqrt{\Delta_N}\right) + \frac{\gamma}{4\mu}\Big((\Gamma - 2\mu)N_* - 2\gamma\mu\Big) > 0,$$

which is equivalent to

$$\cancel{\frac{\gamma^2}{2}} - \cancel{\frac{\gamma}{2}\frac{\Gamma - 2\mu}{2\mu} N_*} - \sqrt{\Delta_N}\left[\gamma - \frac{\Gamma - 2\mu}{2\mu} N_*\right] + \cancel{\frac{\gamma}{4\mu}(\Gamma - 2\mu)N_*} - \cancel{\frac{\gamma^2}{2}} > 0,$$

and can be reduced to

$$-\sqrt{\Delta_N}\underbrace{\left[\gamma - \frac{\Gamma - 2\mu}{2\mu} N_*\right]}_{-} > 0,$$

which is always true, since $P_* > 0$.

Finally, we see that the determinants of the characteristic matrices with linear and cross diffusion, respectively

$$\det \boldsymbol{M}_{LP} = A_L k^4 - B_L k^2 + \det \boldsymbol{J}, \quad \text{and} \quad \det \boldsymbol{M}_C = A_C k^4 - B_C k^2 + \det \boldsymbol{J},$$

are such that $A_C > A_L$ and $B_L > B_C$. Looking at the Turing instability regions, that are regions in which the determinant of the characteristic matrix is strictly negative, we see that three cases naturally appear:

1. there are no regions of negative determinant for both linear and cross diffusion (Figure 7.1(a)), then no Turing-patterns appear in both systems;
2. the linear diffusion case has a Turing instability region, but the determinant of the cross diffusion case is positive for all k (Figure 7.1(b)), so that the cross diffusion case does not lead to Turing instability;
3. both cases lead to nonempty Turing instability regions (Figure 7.1(c)). It can be proved that

$$\frac{\sqrt{B_L^2 - 4A_1 \det \boldsymbol{J}}}{2A_L} > \frac{\sqrt{B_C^2 - 4A_C \det \boldsymbol{J}}}{2A_C},$$

which means that the Turing instability region for the cross diffusion case is strictly included in the Turing instability region of the linear diffusion case.

In all cases, we see that the cross-diffusion model leads to a possibility of obtaining nontrivial patterns which is less likely than in the linear diffusion model. Therefore, the use of a model in which standard diffusion terms are directly added to the reaction part may lead to an overestimation of the set of the parameters for which patterns appear, with respect to the cross-diffusion model.

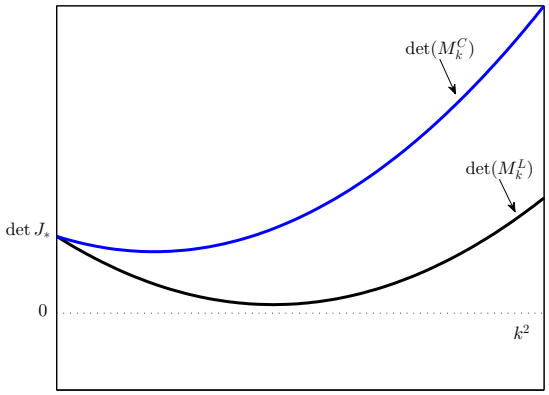

(a)

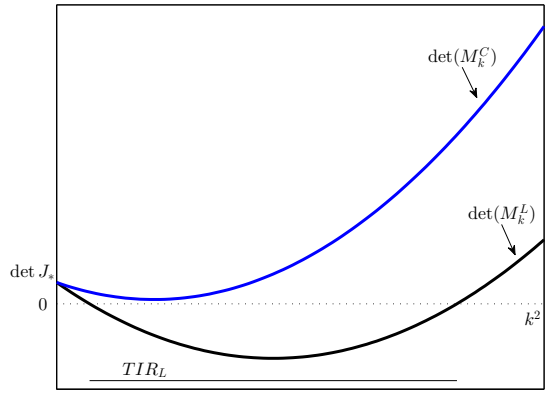

(b)

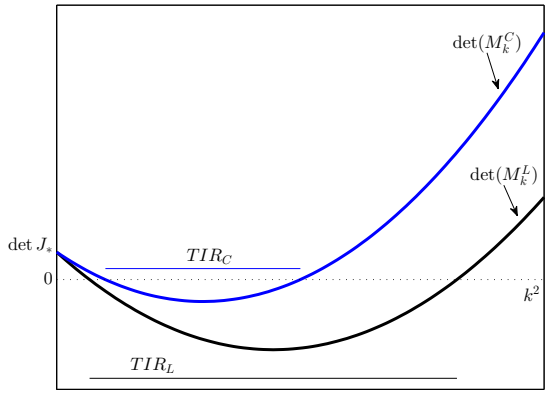

(c)

Fig. 7.1. Turing Instability regions for linear-diffusion and cross-diffusion cases. (a) There are no regions of negative determinant for both linear and cross-diffusion, so that in both cases Turing instability can not appear. (b) The linear-diffusion case has a Turing instability region (TIR_L), but the determinant of the cross-diffusion case is positive for all k, so that the cross-diffusion case does not lead to Turing instability. (c) Both cases lead to nonempty Turing instability regions, but the Turing instability region for the cross-diffusion (TIR_C) case is strictly included in the Turing instability region of the linear-diffusion case (TIR_L).

8

Concluding remarks

This Part focuses on the study of two "microscopic" (in terms of time scales) predator-prey models with diffusion that justify, in a suitable limit, two classical types of functional responses in the reaction part and present a cross-diffusion term. We have also presented rigorous result of convergence of the solutions of these system towards the solution of the reaction-cross diffusion system.

In detail, two trophic levels are considered, prey and predators which are further divided into *searching predators* and *handling predators*. The former are predators active in the predation process, the latter are resting individuals. Then, we start from a system of three partial differential equations, with a standard linear diffusion in terms of Laplacian, and with a Lotka-Volterra reaction term. Through a *quasi steady-state approximation* we end up with a system of two PDEs with prey and total predator densities as unknowns, in which a Holling-type II functional response appears together with a cross-diffusion term in the predator equation. This means that the diffusion term relative to predators is much more complicated than a constant times Laplacian of P (linear diffusive term), which can be simply added to the reaction part [35]. In particular, the diffusion term obtained by the time-scale argument depends on the prey biomass and on both the diffusion coefficient of searching and handling predators d_2 and d_3. Looking at its expression, the cross-diffusion term reduces the predator diffusion when the prey density increases.

Then we modify the starting model inserting a competition among predators. With this change we end up after a *quasi steady-state approximation* with a system of two PDEs for prey and total predator densities, characterized by a Beddington-DeAngelis-like functional response and a cross-diffusion term in the predator equation.

We note that the limiting system presents a functional response close to the Beddington-DeAngelis in the reaction part: in this sense, we have derived this type

of functional response by a time-scale argument from a more complicated model. This type of functional response was derived also by Huisman et al. [56] in the context of ordinary differential equations, starting from a system of four ODEs by a quasi-steady-state approximation. With their approach, also the logistic growth and the predator turnover terms still depend on this complex expression. Thereafter, they have simplified this complicated quadratic expression with a Padé approximation and they recover the standard formula of the Beddington-DeAngelis functional response.

Also in this case, the limiting system presents a cross-diffusion in the predator equation, which depends on both the diffusion coefficients of searching and handling predators d_2 and d_3, while the prey diffusion is still linear.

The Turing instability analysis of the derived models is studied in Chapter 7. For the first one, it is known that predator-prey models with a prey-dependent trophic function in the reaction part and (standard) linear-diffusion can not give rise to Turing instability [10]. Even with the cross-diffusion model, no patterns seem to appear under a (biologically reasonable) assumption on the diffusion coefficients. For the second system, in which the functional response is a Beddington-DeAngelis-like, we look for conditions on the parameter values which lead to Turing instability and we compare these Turing instability regions with the ones obtained when the cross-diffusion term is substituted by a linear diffusion. The main point is the fact that the Turing instability region associated to the cross-diffusion system is always strictly included in the Turing instability region of the linear-diffusion system. As a consequence, the use of reaction-diffusion systems for predator-prey interactions of Beddington-DeAngelis type in which standard diffusion is simply added to the reaction terms may lead to an overestimation of the possibility of appearance of patterns (in the case when the Beddington-DeAngelis functional response is a consequence of the interactions between searching and handling predators).

It is worth to mention that in many instances, the introduction of cross-diffusion terms instead of (standard) linear-diffusion terms leads exactly to the opposite result, that is, the increase of the set of parameter values in which patterns develop [96, 57, 39]. Our study leads then to a rather interesting conclusion: pattern formation originating from Turing instability is counteracted by the cross-diffusion term derived by the QSSA, even though the existing literature seems to suggest that cross-diffusion enhances pattern formation. This raises the question of the sub-classification of cross-diffusion with respect to their properties of enhancing diffusion-driven instability, which could be useful and interesting at this point. Indeed, our approach provides a mechanistic derivation of the cross-diffusion term but often models are based on phenomenological assumptions and then a priori knowledge about the effects can be useful. This issue needs a carefully revision of the literature on this topic. As a first

attempt, the expression on which the Laplacian acts is the key of this difference. The cross-diffusion term, provided by a mechanistic derivation, reduces in a certain sense the diffusion coefficient of predators. However, looking at the Lotka-Volterra model studied in [39], a different type of cross-diffusion is considered, which increases the diffusion of prey and predators. The authors proved that this type of cross-diffusion enhances the Turing instability.

It is worth noting that in the quoted model, a similar cross-diffusion term is considered also in the prey equation. With our approach it is possible to obtain a predator-prey reaction-cross diffusion with a cross-diffusion also in the prey equation, using the mechanistic derivation proposed by Geritz and Gyllenberg [41] in the context of ordinary differential equations. In detail, in addition to the division of the predator population into searchers and handlers, the prey population is divided in active prey (typically foraging and prone to predation) and invulnerable prey (individuals who have found a refuge); then, two different time scales are exploited to reduce the four-dimensional system to a system of two equations with cross-diffusion terms and a Beddington-DeAngelis functional response. The study of the influence of this new cross-diffusion term could be useful to perform the suggested classification, and it is planned as future work.

Appendix

A Very-weak formulation

We clarify here the notion of *very weak solutions* and how the boundary conditions are reflected by the choice of test functions. For this purpose, we consider the following system in the strong formulation:

$$\partial_t N - d_1 \Delta_x N = f(N,P) := rN\left(1-\frac{N}{K}\right) - \frac{\tilde{\gamma}\alpha NP}{\alpha N+\tilde{\gamma}}, \qquad in\ \mathbb{R}^+\times\Omega \tag{8.1}$$

$$\partial_t P - \Delta_x\left(\mu(N)P\right) = g(N,P) := \frac{\Gamma\alpha NP}{\alpha N+\tilde{\gamma}} - \mu P, \qquad in\ \mathbb{R}^+\times\Omega \tag{8.2}$$

$$\nabla_x N\cdot n_{|\partial\Omega} = 0,\ \nabla_x P\cdot n_{|\partial\Omega} = 0, \qquad in\ \mathbb{R}^+\times\partial\Omega \tag{8.3}$$

$$N(0,\cdot) = N_{in},\ P(0,\cdot) = P_{in}, \qquad in\ \Omega. \tag{8.4}$$

where $N = N(t,x) \geq 0,\ P = P(t,x) \geq 0$ are the unknowns, the variable $(t,x) \in \mathbb{R}^+\times\Omega$, with Ω a bounded domain of $\mathbb{R}^d$, $(d = 1,2,3)$, the function $\mu(N)$ in the second equation is

$$\mu(N) := \frac{d_2\tilde{\gamma}+d_3\alpha N}{\alpha N+\tilde{\gamma}},$$

$n = n(x)$ stands for the outward normal at point x of the boundary $\partial\Omega$, N_{in} and P_{in} are nonnegative initial data, and the remaining terms are nonnegative constant parameters.

Remark. Homogeneous Neumann boundary conditions in the flux formulation are equivalent to (8.3); in detail

$$\begin{cases} \nabla_x N \cdot n_{|\partial\Omega} = 0, \\ \nabla_x P \cdot n_{|\partial\Omega} = 0, \end{cases} \quad \Leftrightarrow \quad \begin{cases} \nabla_x N \cdot n_{|\partial\Omega} = 0, \\ \nabla_x \left(\mu(N)P\right) \cdot n_{|\partial\Omega} = 0. \end{cases}$$

Indeed

$$\begin{aligned} \nabla_x \left(\mu(N)P\right) \cdot n_{|\partial\Omega} &= \left[P\nabla_x \mu(N) + \mu(N)\nabla_x P\right] \cdot n_{|\partial\Omega} \\ &= \left[P\mu'(N)\nabla_x N + \mu(N)\nabla_x P\right] \cdot n_{|\partial\Omega} \\ &= P\mu'(N)\nabla_x N \cdot n_{|\partial\Omega} + \mu(N)\nabla_x P \cdot n_{|\partial\Omega}. \end{aligned}$$

Suppose $N,\ P$ smooth. In order to obtain the very-weak formulation of the system (8.1)-(8.4), we consider $\phi,\ \psi$ test functions such that

- $\varphi,\ \psi$ are smooth: $\varphi,\ \psi \in \mathcal{C}^2_C([0,+\infty) \times \bar{\Omega})$.
  We are considering functions that are $\mathcal{C}^2$ in $[0,+\infty) \times \bar{\Omega}$ (up to the boundary) and with a compact support (zero for $t \to +\infty$).
- $\varphi,\ \psi$ satisfy homogeneous Neumann boundary conditions:

$$\nabla_x \varphi \cdot n_{|\partial\Omega} = 0, \quad \nabla_x \psi \cdot n_{|\partial\Omega} = 0. \tag{8.5}$$

We multiply each equation for a test function and we integrate. For the equation (8.1) we obtain

$$\int_0^\infty \int_\Omega \left(\partial_t N - d_1 \Delta_x N\right) \varphi = \int_0^\infty \int_\Omega f(N,P)\varphi, \qquad \forall \varphi.$$

Integrating by pats the l.h.s and remembering that φ has a compact support, we have

$$\begin{aligned} \int_0^\infty \int_\Omega \left(\partial_t N - d_1 \Delta_x N\right) \varphi = &- \int_0^\infty \int_\Omega N \partial_t \varphi - \int_\Omega \varphi(0,\cdot) N_{in} \\ &+ d_1 \int_0^\infty \int_\Omega \nabla_x \varphi \nabla_x N - d_1 \int_0^\infty \int_{\partial\Omega} \varphi \nabla_x N \cdot n, \qquad \forall \varphi. \end{aligned}$$

The last term vanishes due to the homogeneous Neumann boundary conditions; we integrate by parts the third term:

$$\int_0^\infty \int_\Omega \nabla_x \varphi \nabla_x N = - \int_0^\infty \int_\Omega N \Delta_x \varphi + \int_0^\infty \int_{\partial\Omega} N \nabla_x \varphi \cdot n,$$

where the second term again vanishes due to the properties of the test functions. We obtain the very weak formulation of the first equation:

$$-\int_0^\infty \int_\Omega N\partial_t\varphi - \int_\Omega \varphi(0,\cdot)N_{in} - d_1\int_0^\infty \int_\Omega N\Delta_x\varphi = \int_0^\infty \int_\Omega f(N,P)\varphi, \quad \forall\varphi.$$

Analogously for the second equation (8.2), we have

$$\int_0^\infty \int_\Omega (\partial_t P - \Delta_x(\mu(N)P))\,\psi = \int_0^\infty \int_\Omega g(N,P)\psi, \qquad \forall\psi.$$

Integrating by parts the l.h.s and remembering that ψ has a compact support, we have

$$\begin{aligned}\int_0^\infty \int_\Omega (\partial_t P - \Delta_x(\mu(N)P))\,\psi = &-\int_0^\infty \int_\Omega P\partial_t\psi - \int_\Omega \psi(0,\cdot)P_{in} \\ &+\int_0^\infty \int_\Omega \nabla_x\psi\nabla_x(\mu(N)P) - \int_0^\infty \int_{\partial\Omega} \psi\nabla_x(\mu(N)P)\cdot n, \qquad \forall\psi.\end{aligned}$$

The last term vanishes due to the homogeneous Neumann boundary conditions; we integrate by parts the third term:

$$\int_0^\infty \int_\Omega \nabla_x\psi\nabla_x(\mu(N)P) = -\int_0^\infty \int_\Omega \mu(N)P\Delta_x\psi + \int_0^\infty \int_{\partial\Omega} \mu(N)P\nabla_x\psi\cdot n, \qquad \forall\psi,$$

where the second term again vanishes due to the properties of the test functions. We obtain the very-weak formulation of the second equation:

$$-\int_0^\infty \int_\Omega P\partial_t\psi - \int_\Omega \psi(0,\cdot)P_{in} - \int_0^\infty \int_\Omega \mu(N)P\Delta_x\psi = \int_0^\infty \int_\Omega g(N,P)\psi, \quad \forall\psi.$$

Then, the very-weak formulation of system (8.1)-(8.4) is

$$-\int_0^\infty \int_\Omega N\partial_t\varphi - \int_\Omega \varphi(0,\cdot)N_0 - d_1\int_0^\infty \int_\Omega N\Delta_x\varphi = \int_0^\infty \int_\Omega f(N,P)\varphi \tag{8.6}$$

$$-\int_0^\infty \int_\Omega P\partial_t\psi - \int_\Omega \psi(0,\cdot)P_0 - \int_0^\infty \int_\Omega \mu(N)P\Delta_x\psi = \int_0^\infty \int_\Omega g(N,P)\psi \tag{8.7}$$

$$\forall\varphi,\psi \in \mathcal{C}_C^2([0,+\infty)\times\bar{\Omega}), \nabla_x\varphi\cdot n_{|\partial\Omega} = 0,\ \nabla_x\psi\cdot n_{|\partial\Omega} = 0. \tag{8.8}$$

Now, we want to prove the coherence of the very-weak formulation.

First, we keep $\varphi,\ \psi \in \mathcal{C}_C^2(]0,+\infty)\times\Omega)$. We consider the system (8.6)-(8.8) and we integrate backward by parts. We get, for all test functions $\varphi,\ \psi$

$$\int_0^\infty \int_\Omega (\partial_t N - d_1\Delta_x N)\,\varphi = \int_0^\infty \int_\Omega f(N,P)\varphi,$$

$$\int_0^\infty \int_\Omega (\partial_t P - \Delta_x(\mu(N)P))\,\psi = \int_0^\infty \int_\Omega g(N,P)\psi, \quad \forall \varphi, \psi.$$

Standard theorem of distributions leads to the system in the strong formulation (8.1)-(8.2). Now we try to get the initial data (8.4) out of the very weak formulation. We keep $\varphi,\ \psi \in \mathcal{C}_C^2([0,+\infty)\times\Omega)$.From (8.6), that is

$$-\int_0^\infty \int_\Omega N\partial_t\varphi - \int_\Omega \varphi(0,\cdot)N_{in} - d_1\int_0^\infty \int_\Omega N\Delta_x\varphi = \int_0^\infty \int_\Omega f(N,P)\varphi,$$

integrating backward by parts the first and the third terms, we have

$$-\int_0^\infty \int_\Omega N\partial_t\varphi = \int_0^\infty \int_\Omega \varphi\partial_t N + \int_\Omega N(0,\cdot)\varphi(0,\cdot),$$
$$\int_0^\infty \int_\Omega N\Delta_x\varphi = \int_0^\infty \int_\Omega \varphi\Delta_x N,$$

we obtain

$$-\int_0^\infty \int_\Omega N\partial_t\varphi - \int_\Omega (N(0,\cdot)-N_{in})\,\varphi(0,\cdot) - d_1\int_0^\infty \int_\Omega N\Delta_x\varphi = \int_0^\infty \int_\Omega f(N,P)\varphi.$$

But N satisfies the equation (8.1) of the strong formulation, that leads to

$$\int_0^\infty \int_\Omega (\partial_t N - d_1\Delta_x N - f(N,P))\,\varphi = 0,$$

then we have

$$\int_\Omega (N(0,\cdot)-N_{in})\,\varphi(0,\cdot) = 0, \qquad \forall\varphi.$$

We want to prove that the last equation is this equivalent to $N(0,\cdot) = N_{in}$.

If $\Phi \in \mathcal{C}_c^2(\Omega)$ being given, I define $\varphi(t,x) = \Phi(x)\chi(t)$, where $\chi \in \mathcal{C}^\infty(\mathbb{R})$ such that

$$\chi(t) = \begin{cases} 1, 0 \le t \le 1 \\ h(t), 1 < t < 2 \\ 0, t \ge 2, \end{cases}$$

with h is a suitable smooth function which makes $\chi \in \mathcal{C}^\infty(\mathbb{R})$ $(h'(1) = h'(2) = 0)$. Then $\varphi \in \mathcal{C}_c^2([0,+\infty)\times\Omega)$ and $\varphi(0,\cdot) = \Phi$. This implies that

$$\forall\Phi \in \mathcal{C}_c^2(\Omega) \qquad \int_\Omega (N(0,\cdot)-N_{in})\Phi = 0,$$

then $N(0,\cdot) = N_{in}$.

This procedure can be applied also for the equation (8.6), in order to recover $P(0,\cdot) = P_{in}$.

And now we try to get the Neumann boundary conditions out of the very weak formulation. We keep test functions

$$\varphi, \psi \in \mathcal{C}^2_C(]0,+\infty) \times \bar{\Omega}),\ \nabla_x \varphi \cdot n_{|\partial\Omega} = 0,\ \nabla_x \psi \cdot n_{|\partial\Omega} = 0.$$

This implies that $\varphi(0,\cdot) = 0,\ \psi(0,\cdot) = 0$. With this choice, the very weak formulation becomes

$$-\int_0^\infty \int_\Omega N\partial_t\varphi - d_1 \int_0^\infty \int_\Omega N\Delta_x\varphi = \int_0^\infty \int_\Omega f(N,P)\varphi$$
$$-\int_0^\infty \int_\Omega P\partial_t\psi - \int_0^\infty \int_\Omega \mu(N)P\Delta_x\psi = \int_0^\infty \int_\Omega g(N,P)\psi$$

Integrating by part, the first equation:

$$\int_0^\infty \int_\Omega \partial_t N\varphi + d_1 \int_0^\infty \int_\Omega \nabla_x N \nabla_x \varphi - d_1 \int_0^\infty \int_{\partial\Omega} N\nabla_x\varphi \cdot n = \int_0^\infty \int_\Omega f(N,P)\varphi$$

The third term in the l.h.s. vanishes due to the properties of the test functions; integrating the second term by parts, we have

$$\int_0^\infty \int_\Omega \partial_t N\varphi - d_1 \int_0^\infty \int_\Omega \varphi\Delta_x N + d_1 \int_0^\infty \int_{\partial\Omega} \varphi\nabla_x N \cdot n = \int_0^\infty \int_\Omega f(N,P)\varphi$$

which can be rewritten as

$$\int_0^\infty \int_\Omega \left(\partial_t N - d_1\Delta_x N - f(N,P)\right)\varphi + d_1 \int_0^\infty \int_{\partial\Omega} \varphi\nabla_x N \cdot n = 0,$$

and since N is a strong solution, we obtain

$$\int_0^\infty \int_{\partial\Omega} \varphi\nabla_x N \cdot n = 0, \quad \forall\varphi. \tag{8.9}$$

We want to recover that $\nabla_x N \cdot n = 0$.

We consider the simple case $\Omega = \mathbb{R} \times \mathbb{R}^+_*$ and $(x_1, x_2) \in \Omega$. Then $\partial\Omega = \mathbb{R} \times \{0\}$ and $n = (0, \pm 1)$. Equation (8.9) becomes

$$\int_0^\infty \int_{\mathbb{R}} \varphi(t, x_1, 0)\frac{\partial N}{\partial x_2}(t, x_1, 0)dx_1 d_t = 0, \quad \forall\varphi.$$

We want to prove that, if $\Phi(t,x_1)$ being given, $\Phi(t,x_1) \in \mathcal{C}_c^2(]0,+\infty) \times \mathbb{R})$, there exists $\varphi \in \mathcal{C}_c^2(]0,+\infty) \times \mathbb{R} \times \mathbb{R}_*^+)$ such that

$$\Phi(t,x_1) = \varphi(t,x_1,0), \quad \frac{\partial \varphi}{\partial x_2}(t,x_1,0) = 0.$$

We define $\varphi(t,x_1,x_2) := \Phi(t,x_1)\chi(x_2)$, where $\chi \in \mathcal{C}^\infty(\mathbb{R})$ such that

$$\chi(x_2) = \begin{cases} 1, 0 \le x_2 \le 1 \\ h(x_2), 1 < x_2 < 2 \\ 0, x_2 \ge 2, \end{cases}$$

with h is a suitable smooth function (as in the previous case). Then,

$$\frac{\partial \varphi}{\partial x_2}(t,x_1,x_2) = \Phi(t,x_1)\chi'(x_2)$$

so that

$$\frac{\partial \varphi}{\partial x_2}(t,x_1,0) = \Phi(t,x_1)\chi'(0) = 0$$

and

$$\varphi(t,x_1,0) = \Phi(t,x_1)\chi(0) = \Phi(t,x_1).$$

This implies that

$$\frac{\partial N}{\partial x_2} = 0.$$

These arguments can be generalized to a generic domain Ω.

References

1. P. A. Abrams and L. R. Ginzburg, *The nature of predation: prey dependent, ratio dependent or neither?*, Trends in Ecology & Evolution, 15 (2000), pp. 337–341.
2. M. Adamson and A. Y. Morozov, *When can we trust our model predictions? Unearthing structural sensitivity in biological systems*, Proceedings of the Royal Society of London A: Mathematical, Physical and Engineering Sciences, 469 (2012), p. 20120500.
3. ———, *Bifurcation analysis of models with uncertain function specification: How should we proceed?*, Bulletin of Mathematical Biology, 76 (2014), pp. 1218–1240.
4. P. Aguirre, *A general class of predation models with multiplicative Allee effect*, Nonlinear Dynamics, 78 (2014), pp. 629–648.
5. P. Aguirre, J. D. Flores, and E. González-Olivares, *Bifurcations and global dynamics in a predator–prey model with a strong Allee effect on the prey, and a ratio–dependent functional response*, Nonlinear Analysis: Real World Applications, 16 (2014), pp. 235–249.
6. P. Aguirre, E. González-Olivares, and E. Sáez, *Three limit cycles in a Leslie–Gower predator-prey model with additive Allee effect*, SIAM Journal on Applied Mathematics, 69 (2009), pp. 1244–1262.
7. ———, *Two limit cycles in a Leslie–Gower predator–prey model with additive Allee effect*, Nonlinear Analysis: Real World Applications, 10 (2009), pp. 1401–1416.
8. W. C. Allee, *Animal Aggregations: A Study in General Sociology*, University of Chicago Press, Chicago, 1931.
9. W. C. Allee, O. Park, A. E. Emerson, T. Park, K. P. Schmidt, et al., *Principles of Animal Ecology*, WB Saundere Co. Ltd., Philadelphia, 1949.
10. D. Alonso, F. Bartumeus, and J. Catalan, *Mutual interference between predators can give rise to Turing spatial patterns*, Ecology, 83 (2002), pp. 28–34.
11. R. Arditi and L. R. Ginzburg, *Coupling in predator-prey dynamics: ratio-dependence*, Journal of Theoretical Biology, 139 (1989), pp. 311–326.
12. V. I. Arnol'd, *Catastrophe Theory*, Springer-Verlag, Berlin, 1992.
13. A. D. Bazykin, *Nonlinear Dynamics of Interacting Populations*, vol. 11, World Scientific, Singapore, 1998.
14. J. Beddington, *Mutual interference between parasites or predators and its effect on searching efficiency*, The Journal of Animal Ecology, 44 (1975), pp. 331–340.
15. F. Berezovskaya, G. Karev, and R. Arditi, *Parametric analysis of the ratio–dependent predator–prey model*, Journal of Mathematical Biology, 43 (2001), pp. 221–246.
16. A. A. Berryman, *The origins and evolution of predator–prey theory*, Ecology, 73 (1992), pp. 1530–1535.
17. D. Bothe and M. Pierre, *The instantaneous limit for reaction-diffusion systems with a fast irreversible reaction*, Discrete and Continuous Dynamical Systems - Series S, 8 (2011), pp. 49–59.

18. D. Bothe, M. Pierre, and G. Rolland, *Cross-diffusion limit for a reaction-diffusion system with fast reversible reaction*, Communications in Partial Differential Equations, 37 (2012), pp. 1940–1966.
19. D. S. Boukal and L. Berec, *Modelling mate–finding Allee effects and populations dynamics, with applications in pest control*, Population Ecology, 51 (2009), pp. 445–458.
20. D. S. Boukal, M. W. Sabelis, and L. Berec, *How predator functional responses and Allee effects in prey affect the paradox of enrichment and population collapses*, Theoretical Population Biology, 72 (2007), pp. 136–147.
21. M. Breden, L. Desvillettes, and K. Fellner, *Smoothness of moments of the solutions of discrete coagulation equations with diffusion*, arXiv preprint arXiv:1511.05733, (2015).
22. G. Buffoni, M. P. Cassinari, and M. Groppi, *Modelling of predator–prey trophic interactions. Part II: three trophic levels*, Journal of Mathematical Biology, 54 (2007), pp. 623–644.
23. G. Buffoni, M. P. Cassinari, M. Groppi, and M. Serluca, *Modelling of predator–prey trophic interactions. Part I: two trophic levels*, Journal of Mathematical Biology, 50 (2005), pp. 713–732.
24. G. Buffoni and G. Gilioli, *A lumped parameter model for acarine predator–prey population interactions*, Ecological Modelling, 170 (2003), pp. 155–171.
25. G. Buffoni, M. Groppi, and C. Soresina, *Effects of prey over–undercrowding in predator–prey systems with prey–dependent trophic functions*, Nonlinear Analysis: Real World Applications, 12 (2011), pp. 2871–2887.
26. ———, *Dynamics of predator-prey models with a strong Allee effect on the prey and predator-dependent trophic functions*, Nonlinear Analysis: Real World Applications, 30 (2016), pp. 143–169.
27. J. A. Cañizo, L. Desvillettes, and K. Fellner, *Improved duality estimates and applications to reaction-diffusion equations*, Communications in Partial Differential Equations, 39 (2014), pp. 1185–1204.
28. F. Conforto and L. Desvillettes, *Rigorous passage to the limit in a system of reaction-diffusion equations towards a system including cross diffusion*, Communications in Mathematical Sciences, 12 (2014), pp. 457–472.
29. D. L. DeAngelis, R. Goldstein, and R. O'Neill, *A model for trophic interaction*, Ecology, 56 (1975), pp. 881–892.
30. B. Dennis, *Allee effects: population growth, critical density, and the chance of extinction*, Natural Resource Modeling, 3 (1989), pp. 481–538.
31. L. Desvillettes, *About entropy methods for reaction-diffusion equations*, Rivista di Matematica dell'Università di Parma, 7 (2007), pp. 81–123.
32. L. Desvillettes, K. Fellner, M. Pierre, and J. Vovelle, *Global existence for quadratic systems of reaction-diffusion*, Advanced Nonlinear Studies, 7 (2007), pp. 491–511.
33. L. Desvillettes and A. Trescases, *New results for triangular reaction cross diffusion system*, Journal of Mathematical Analysis and Applications, 430 (2015), pp. 32–59.
34. A. Dhooge, W. Govaerts, and Y. A. Kuznetsov, *Matcont: A MATLAB package for numerical bifurcation analysis of ODEs*, ACM Transactions on Mathematical Software, 29 (2003), pp. 141–164, Software available from http://www.matcont.ugent.be/.
35. R. Durrett and S. Levin, *The importance of being discrete (and spatial)*, Theoretical Population Biology, 46 (1994), pp. 363–394.
36. D. Fanelli, C. Cianci, and F. Di Patti, *Turing instabilities in reaction-diffusion systems with cross diffusion*, The European Physical Journal B, 86 (2013), pp. 1–8.
37. J. D. Flores and E. González-Olivares, *Dynamics of a predator–prey model with Allee effect on prey and ratio–dependent functional response*, Ecological Complexity, 18 (2014), pp. 59–66.
38. H. Freedman and J.-H. So, *Global stability and persistence of simple food chains*, Mathematical Biosciences, 76 (1985), pp. 69–86.
39. G. Gambino, M. C. Lombardo, and M. Sammartino, *Turing instability and traveling fronts for a nonlinear reaction–diffusion system with cross-diffusion*, Mathematics and Computers in Simulation, 82 (2012), pp. 1112–1132.

40. Y. Gao and B. Li, *Dynamics of a ratio–dependent predator–prey system with a strong Allee effect*, Discrete & Continuous Dynamical Systems - Series B, 18 (2013), pp. 2283–2313.
41. S. Geritz and M. Gyllenberg, *A mechanistic derivation of the deangelis–beddington functional response*, Journal of theoretical biology, 314 (2012), pp. 106–108.
42. M. E. Gilpin, *A model of the predator–prey relationship*, Theoretical Population Biology, 5 (1974), pp. 333–344.
43. M. E. Gilpin and M. E. Soulé, *Minimum viable populations: processes of species extinction*, In: M. Soulé (Ed.) Conservation Biology: the Science of Scarcity and Diversity, Sinauer Associates, Sunderland, Massachusetts, (1986), pp. 13–34.
44. L. R. Ginzburg and H. R. Akçakaya, *Consequences of ratio–dependent predation for steady–state properties of ecosystems*, Ecology, 73 (1992), pp. 1536–1543.
45. B. Gompertz, *On the nature of the function expressive of the law of human mortality, and on a new mode of determining the value of life contingencies*, Philosophical Transactions of the Royal Society of London, 115 (1825), pp. 513–583.
46. E. González-Olivares, J. Mena-Lorca, A. Rojas-Palma, and J. D. Flores, *Dynamical complexities in the Leslie–Gower predator–prey model as consequences of the Allee effect on prey*, Applied Mathematical Modelling, 35 (2011), pp. 366–381.
47. T. Gross and U. Feudel, *Generalized models as a universal approach to the analysis of nonlinear dynamical systems*, Physical Review E, 73 (2006), p. 016205.
48. J. Guckenheimer and P. Holmes, *Nonlinear Oscillations, Dynamical Systems, and Bifurcations of Vector Fields*, vol. 42, Springer Verlag, New York, 1983.
49. A. Gutierrez, *Physiological basis of ratio–dependent predator–prey theory: the metabolic pool model as a paradigm*, Ecology, 73 (1992), pp. 1552–1563.
50. A. Gutierrez and J. Baumgärtner, *Multitrophic level models of predator-prey energetics: II. a realistic model of plant–herbivore–parasitoid–predator interactions*, The Canadian Entomologist, 116 (1984), pp. 933–949.
51. M. Haque, *Existence of complex patterns in the Beddington–Deangelis predator–prey model*, Mathematical Biosciences, 239 (2012), pp. 179–190.
52. D. Hilhorst, M. Mimura, and H. Ninomiya, *Fast reaction limit of competition-diffusion systems*, Handbook of Differential Equations: Evolutionary Equations, 5 (2009), pp. 105–168.
53. D. Hilhorst, R. Van Der Hout, and L. Peletier, *The fast reaction limit for a reaction-diffusion system*, Journal of Mathematical Analysis and Applications, 199 (1996), pp. 349–373.
54. D. Hilhorst, R. Van Der Hout, and L. A. Peletier, *Nonlinear diffusion in the presence of fast reaction*, Nonlinear Analysis: Theory, Methods & Applications, 41 (2000), pp. 803–823.
55. C. S. Holling, *The functional response of invertebrate predators to prey density*, Memoirs of the Entomological Society of Canada, 98 (1966), pp. 5–86.
56. G. Huisman and R. J. De Boer, *A formal derivation of the Beddington functional response*, Journal of Theoretical Biology, 185 (1997), pp. 389–400.
57. M. Iida, M. Mimura, and H. Ninomiya, *Diffusion, cross-diffusion and competitive interaction*, Journal of Mathematical Biology, 53 (2006), pp. 617–641.
58. V. Ivlev, *Experimental Ecology of the Feeding of Fishes*, vol. 42, Yale University Press, New Haven, CT, 1961.
59. H. Izuhara, M. Mimura, et al., *Reaction-diffusion system approximation to the cross-diffusion competition system*, Hiroshima Mathematical Journal, 38 (2008), pp. 315–347.
60. J. Jacobs, *Cooperation, optimal density and low density thresholds: yet another modification of the logistic model*, Oecologia, 64 (1984), pp. 389–395.
61. A. Kent, C. P. Doncaster, and T. Sluckin, *Consequences for predators of rescue and Allee effects on prey*, Ecological Modelling, 162 (2003), pp. 233–245.
62. A. Kolmogorov, *Sulla teoria di Volterra della lotta per l'esistenza*, Giornale dell'Istituto Italiano degli Attuari, 7 (1936), pp. 74–80.

63. C. Kuehn, S. Siegmund, and T. Gross, *Dynamical analysis of evolution equations in generalized models*, IMA Journal of Applied Mathematics, 78 (2013), pp. 1051–1077.
64. N. Kumar and W. Horsthemke, *Effects of cross diffusion on Turing bifurcations in two-species reaction-transport systems*, Physical Review E, 83 (2011), p. 036105.
65. E. Kuno, *Principles of predator–prey interaction in theoretical, experimental and natural population system*, Advances in Ecological Research, 16 (1987), pp. 249–337.
66. Y. A. Kuznetsov, *Elements of Applied Bifurcation Theory*, vol. 112, Springer Verlag, New York, 1998.
67. Y. A. Kuznetsov and S. Rinaldi, *Remarks on food chain dynamics*, Mathematical Biosciences, 134 (1996), pp. 1–33.
68. J. A. Logan, *Derivation and analysis of composite models for insect populations*, in Estimation and Analysis of Insect Populations, vol. 55 of Lecture Notes in Statistic, Springer, 1989, pp. 278–288.
69. H. Malchow, S. V. Petrovskii, and E. Venturino, *Spatiotemporal patterns in ecology and epidemiology: theory, models, and simulation*, Chapman & Hall/CRC London, 2008.
70. K. McCann and P. Yodzis, *Biological conditions for chaos in a three–species food chain*, Ecology, 75 (1994), pp. 561–564.
71. E. A. McGehee and E. Peacock-López, *Turing patterns in a modified lotka–volterra model*, Physics Letters A, 342 (2005), pp. 90–98.
72. A. B. Medvinsky, S. V. Petrovskii, I. A. Tikhonova, H. Malchow, and B.-L. Li, *Spatiotemporal complexity of plankton and fish dynamics*, SIAM review, 44 (2002), pp. 311–370.
73. Z. Mei, *Numerical Bifurcation Analysis for Reaction-diffusion Equations*, vol. 28, Springer Science & Business Media, 2013.
74. J. A. Metz and O. Diekmann, *The Dynamics of Physiologically Structured Populations*, vol. 68, Springer, 2014.
75. D. G. Miller, *Some comments on multicomponent diffusion: negative main term diffusion coefficients, second law constraints, solvent choices, and reference frame transformations*, The Journal of Physical Chemistry, 90 (1986), pp. 1509–1519.
76. A. Moussa, *Some variants of the classical aubin–lions lemma*, Journal of Evolution Equations, 16 (2016), pp. 65–93.
77. H. Murakawa, *A Relation Between Cross-diffusion and Reaction-diffusion*, Citeseer, 2009.
78. J. D. Murray, *Mathematical Biology. II Spatial Models and Biomedical Applications {Interdisciplinary Applied Mathematics V. 18}*, Springer-Verlag New York Incorporated, 2001.
79. S. Nundloll, L. Mailleret, and F. Grognard, *Influence of intrapredatory interferences on impulsive biological control efficiency*, Bulletin of Mathematical Biology, 72 (2010), pp. 2113–2138.
80. L. Perko, *Differential Equations and Dynamical Systems*, Springer-Verlag, New York, 1991.
81. S. V. Petrovskii and H. Malchow, *A minimal model of pattern formation in a prey-predator system*, Mathematical and Computer Modelling, 29 (1999), pp. 49–63.
82. ———, *Wave of chaos: new mechanism of pattern formation in spatio-temporal population dynamics*, Theoretical population biology, 59 (2001), pp. 157–174.
83. M. Pierre and D. Schmitt, *Blowup in reaction-diffusion systems with dissipation of mass*, SIAM Review, 42 (2000), pp. 93–106.
84. ———, *Blowup in reaction-diffusion systems with dissipation of mass*, SIAM Review, 42 (2000), pp. 93–106.
85. G. Rolland, *Global existence and fast-reaction limit in reaction-diffusion systems with cross effects*, PhD thesis, École normale supérieure de Cachan-ENS Cachan; Technische Universität (Darmstadt, Allemagne), 2012.
86. T. Royama, *A comparative study of models for predation and parasitism*, Researches on Population Ecology, S1 (1971), pp. 1–91.
87. M. Sen, M. Banerjee, and A. Morozov, *Bifurcation analysis of a ratio–dependent prey–predator model with the Allee effect*, Ecological Complexity, 11 (2012), pp. 12–27.

88. G. Seo and D. L. DeAngelis, *A predator–prey model with a Holling type I functional response including a predator mutual interference*, Journal of Nonlinear Science, 21 (2011), pp. 811–833.
89. N. Shigesada, K. Kawasaki, and E. Teramoto, *Spatial segregation of interacting species*, Journal of Theoretical Biology, 79 (1979), pp. 83–99.
90. P. A. Stephens and W. J. Sutherland, *Consequences of the Allee effect for behaviour, ecology and conservation*, Trends in Ecology & Evolution, 14 (1999), pp. 401–405.
91. P. A. Stephens, W. J. Sutherland, and R. P. Freckleton, *What is the Allee effect?*, Oikos, 87 (1999), pp. 185–190.
92. Y. Svirezhev and D. Logofet, *Stability of Biological Communities*, vol. 112, MIR Publishers, Moscow, 1983.
93. J. T. Tanner, *Effects of population density on growth rates of animal populations*, Ecology, 47 (1966), pp. 733–745.
94. C. M. Taylor and A. Hastings, *Allee effects in biological invasions*, Ecology Letters, 8 (2005), pp. 895–908.
95. P. C. Tobin, S. L. Whitmire, D. M. Johnson, O. N. Bjørnstad, and A. M. Liebhold, *Invasion speed is affected by geographical variation in the strength of Allee effects*, Ecology Letters, 10 (2007), pp. 36–43.
96. E. Tulumello, M. C. Lombardo, and M. Sammartino, *Cross-diffusion driven instability in a predator-prey system with cross-diffusion*, Acta Applicandae Mathematicae, 132 (2014), pp. 621–633.
97. L. Van Coller, *Automated techniques for the qualitative analysis of ecological models: continuous models*, Conservation Ecology, 1 (1997), p. 5. Available from http://www.ecologyandsociety.org/vol1/iss1/art5/.
98. G. A. Van Voorn, L. Hemerik, M. P. Boer, and B. W. Kooi, *Heteroclinic orbits indicate overexploitation in predator–prey systems with a strong Allee effect*, Mathematical Biosciences, 209 (2007), pp. 451–469.
99. V. K. Vanag and I. R. Epstein, *Cross-diffusion and pattern formation in reaction–diffusion systems*, Physical Chemistry Chemical Physics, 11 (2009), pp. 897–912.
100. P.-F. Verhulst, *Notice sur la loi que la population suit dans son accroissement. correspondance mathématique et physique publiée par a*, Quetelet, 10 (1838), pp. 113–121.
101. V. Volterra, *Variazioni e Fluttuazioni del Numero di Individui in Specie Animali Conviventi*, vol. 2, Mem. Acad. Lincei, 1926. 31–113.
102. C. P. Winsor, *The Gompertz curve as a growth curve*, Proceedings of the National Academy of Sciences, 18 (1932), pp. 1–8.
103. S. N. Wood, *Partially specified ecological models*, Ecological Monographs, 71 (2001), pp. 1–25.
104. A. Yablokov, *Population Biology: Progress and Problems of Studies on Natural Populations*, MIR Publishers, Moscow, 1986.
105. X.-C. Zhang, G.-Q. Sun, and Z. Jin, *Spatial dynamics in a predator-prey model with Beddington-DeAngelis functional response*, Physical Review E, 85 (2012), p. 021924.
106. S.-R. Zhou, Y.-F. Liu, and G. Wang, *The stability of predator–prey systems subject to the Allee effects*, Theoretical Population Biology, 67 (2005), pp. 23–31.
107. J. Zu, *Global qualitative analysis of a predator–prey system with Allee effect on the prey species*, Mathematics and Computers in Simulation, 94 (2013), pp. 33–54.
108. J. Zu and M. Mimura, *The impact of Allee effect on a predator–prey system with Holling type II functional response*, Applied Mathematics and Computation, 217 (2010), pp. 3542–3556.

Journal publications

Papers relevant to thesis's subject

- G. Buffoni, M. Groppi, C. Soresina, *Dynamics of predator-prey models with a strong Allee effect on the prey and predator-dependent trophic function*, Nonlinear Analysis: Real World Applications 30 (2016): 143-169.

- F. Conforto, L. Desvillettes, C. Soresina, *A justification of Holling-type II and Beddington-DeAngelis functional responses for reaction-diffusion predator-prey models*, in preparation.

Other papers

- G. Buffoni, M. Groppi, C. Soresina, *Effects of prey over-undercrowding in predator-prey systems with prey-dependent trophic functions*, Nonlinear Analysis: Real World Applications 12.5 (2011): 2871-2887.

- E. Bonacini, R. Burioni, M. di Volo, M. Groppi, C. Soresina, A. Vezzani, *How single node dynamics enhances synchronization in neural networks with electrical coupling*, Chaos, Solitons & Fractals, 85 (2016) 32-43.

- E. Bonacini, M. Groppi, R. Monaco, A.J. Soares, C. Soresina, *A network model for landscape evolution: stability analysis and numerical tests*, Communications in Nonlinear Science and Numerical Simulation, 48 (2017) 569?584.

- E. Bonacini, L. Bolzoni, M. Groppi and C. Soresina, *Time-optimal control strategies in SIR epidemic models*, submitted to Mathematical Biosciences.

Communications

- "A network model for landscape evolution: stability analysis and numerical tests", Franco-Italian meeting on kinetic theory and singular parabolic equations, 16 March 2017, Universitè Paris Diderot.
- "A justification of Holling-type II and Beddington-DeAngelis functional responses for reaction-diffusion predator-prey models and Turing instability analysis", 9 March 2017, University of Parma.
- "A justification of Holling-type II and Beddington-DeAngelis functional responses for reaction-diffusion predator-prey models and Turing instability analysis", Particle Systems and PDE's V, 29 November 2016, University of Minho (Portugual).
- "A justification of Holling-type II and Beddington-DeAngelis functional responses for reaction-diffusion predator-prey models and Turing instability analysis", XLI Summer School on Mathematical Physics, 15 September 2015, Ravello (Italy).
- "Dynamics of predator-prey models with a strong Allee effect on the prey and predator dependent trophic function", XL Summer School on Mathematical Physics, 17 September 2015, Ravello (Italy).
- "Synchronization in neural networks: the Master Stability Function approach", XXXIX Summer School on Mathematical Physics, 18 September 2014, Ravello (Italy).
- "Mathematical modeling of neural networks and methods for the study of synchronization", Computational and Theoretical Neuroscience Reading Group Seminar, 12 May 2014, University of Milano.

Posters

- "A network model for landscape evolution: stability analysis and numerical tests" during the poster session of the School *Methods and Models of Kinetic Theory*, June 2016, Porto Ercole (Grosseto) Italy.

- "How single node dynamics enhance synchronization in neural networks with electrical coupling" during the poster session of the *School of Brain Cells & Circuits "Camillo Golgi"*, December 2015, Erice (Trapani) Italy.

- "Time-optimal control strategies in SIR epidemics models" during the poster session of the workshop *Mathematical and Computational Epidemiology*, August 2015, Erice (Trapani) Italy.

- "How single node dynamics enhance synchronization in neural networks with electrical coupling" during the poster session of the School *Methods and Models of Kinetic Theory*, June 2014, Porto Ercole (Grosseto) Italy.

Milano, March 25, 2017